

**The Role of Ly6C<sup>hi</sup> Monocytes  
in Brain Homeostasis and Neurodegeneration**

**Dissertation**

zur Erlangung des akademischen Grades

**doctor rerum naturalium**

**(Dr. rer. nat.)**

genehmigt durch die Fakultät für Naturwissenschaften  
der Otto-von-Guericke-Universität Magdeburg



Von: Dipl.-Biol. Luisa Möhle  
geb. am 27.11.1986 in Stuttgart, Deutschland

Gutachter: PD Dr. rer. nat. Ildiko Rita Dunay  
Prof. Dr. rer. nat. Martin Korte

Eingereicht am: 22.02.2016

Verteidigt am: 16.06.2016

## Acknowledgements

First and foremost, I would like to thank my supervisor PD Dr. Ildiko Rita Dunay for giving me the opportunity to pursue my doctoral studies in her group. I am deeply grateful for your tremendous support, unlimited patience and continuous motivation, which gave me the freedom to develop my personal and scientific abilities over the past years.

Prof. Dr. Dunja Bruder, thank you for accepting to be a member of my thesis committee and for your encouragement.

I also thank the collaborative research center SFB854 for funding my work and the associated research training group MGK854 for offering many opportunities to expand my skills off the bench.

My sincere appreciation goes to all our cooperation partners for many fruitful collaborations. This thesis would not have been feasible without your contributions. In particular, I would like to thank Prof. Jens Pahnke and his group, Dr. Susanne Wolf and Daniele Mattei, Dr. Sabine Pietkiewicz from Prof. Inna N. Lavrik's group, Prof. Andreas Müller, PD Markus Heimesaat, and PD Dirk Montag.

I would like to express my gratitude to my friends and to all my current as well as former colleagues and co-workers who joined me in this fantastic ride. Especially, I would like to thank Alex for always challenging me, Aindrila for being a great lab-sister, Dana for invaluable support and excellent organization of everything "behind the scenes", and Andreas for always having an open ear and a good idea.

To my family, Mama, Papa, Oma, Opa, I cannot thank you enough for guiding me to become who I am today, for always being there for me and for your unconditional love.

What a crazy, demanding, exciting, and wonderful journey it has been!

## Publications

### Part of this work is published under the following title:

**Möhle L\***, Mattei D\*, Heimesaat MM\*, Bereswill S, Fischer A, Alutis M, French T, Hambarzumyan D, Matzinger P, Dunay IR\* and Wolf SA\*. Ly6C<sup>hi</sup> monocytes provide a link between antibiotic-induced changes in gut microbiota and adult hippocampal neurogenesis. *Cell Rep* 15(9):1945-1956.

**Möhle L**, Israel N, Paarmann K, Krohn M, Pietkiewicz S, Müller A, Lavrik IN, Buguliskis JS, Schott BH, Schlüter D, Gundelfinger ED, Montag D, Seifert U, Pahnke J, Dunay IR, 2016. Chronic *Toxoplasma gondii* infection enhances  $\beta$ -amyloid phagocytosis and clearance by recruited monocytes. *Acta Neuropathol Commun* 4(1):25.

### Other publications:

Fu T\*, Znalesniak EB\*, Kalinski T, **Möhle L**, et al., 2015. TFF Peptides Play a Role in the Immune Response Following Oral Infection of Mice with *Toxoplasma Gondii*. *Eur J Microbiol Immunol* 5:221–31.

Heimesaat MM, Dunay IR, Alutis M, Fischer A, **Möhle L**, et al., 2014. Nucleotide-oligomerization-domain-2 affects commensal gut microbiota composition and intracerebral immunopathology in acute *Toxoplasma gondii* induced murine ileitis. *PLoS One* 9:e105120.

Rakhmanov M, Sic H, Kienzler AK, Fischer B, Rizzi M, Seidl M, Melkaoui K, Unger S, **Möhle L**, et al., 2014. High levels of SOX5 decrease proliferative capacity of human B cells, but permit plasmablast differentiation. *PLoS One* 9:e100328.

Bereswill S, Kühl AA, Alutis M, Fischer A, **Möhle L**, et al., 2014. The impact of Toll-like-receptor-9 on intestinal microbiota composition and extra-intestinal sequelae in experimental *Toxoplasma gondii* induced ileitis. *Gut Pathog* 6:19.

Klose CSN\*, Flach M\*, **Möhle L**, et al., 2014. Differentiation of type 1 ILCs from a common progenitor to all helper-like innate lymphoid cell lineages. *Cell* 157:340–56.

**Möhle L\***, Parlog A\*, Pahnke J, Dunay IR., 2014. Spinal cord pathology in chronic experimental *Toxoplasma gondii* infection. *Eur J Microbiol Immunol* 4:65–75.

\*These authors contributed equally.

## Abstract

Ly6C<sup>hi</sup> monocytes are an important myeloid-derived subset of innate immune cells. They are known to contribute to the restriction of infections as well as to immunopathology by phagocytosis, cytokine production and differentiation into specialized subpopulations. Recent groundbreaking studies have suggested that Ly6C<sup>hi</sup> monocytes also play protective roles, e. g. during recovery from spinal cord injury.

The goal of this thesis was to investigate the contribution of Ly6C<sup>hi</sup> monocytes in homeostatic and pathophysiological processes of the central nervous system. In the first part of the results, we found that Ly6C<sup>hi</sup> monocytes link both changes in the intestinal flora upon antibiotic or probiotic treatment and physical exercise to altered neurogenesis levels in a murine model. Moreover, their genetically-induced or antibody-dependent absence reduces neurogenesis and substitution of Ly6C<sup>hi</sup> monocytes can restore reduced neurogenesis levels due to antibiotic-treatment.

In the second part, we provide evidence that Ly6C<sup>hi</sup> monocytes are able to take up  $\beta$ -amyloid in an *ex vivo* phagocytosis assay and that their enhanced presence upon chronic experimental *Toxoplasma gondii* infection leads to reduced plaque disposal in the brain of 5xFAD mice. As soluble  $\beta$ -amyloid levels are also reduced upon monocyte infiltration and Ly6C<sup>hi</sup> monocytes are not located in the direct vicinity of plaques, we conclude that Ly6C<sup>hi</sup> monocytes prevent plaque formation by uptake of biochemical precursors.

Taken together, our results demonstrate that Ly6C<sup>hi</sup> monocytes promote the maintenance of hippocampal neurogenesis as well as clearance of waste products during neurodegenerative diseases. Thus, this study supports a refined and more balanced picture of this essential immune cell population.

# Table of Contents

|   |                    |
|---|--------------------|
| <b><u>ACKNOWLEDGEMENTS</u></b>                      | <b><u>I</u></b>    |
| <b><u>PUBLICATIONS</u></b>                          | <b><u>II</u></b>   |
| <b><u>ABSTRACT</u></b>                              | <b><u>III</u></b>  |
| <b><u>TABLE OF CONTENTS</u></b>                     | <b><u>IV</u></b>   |
| <b><u>LIST OF ABBREVIATIONS</u></b>                 | <b><u>VIII</u></b> |
| <b><u>LIST OF FIGURES AND TABLES</u></b>            | <b><u>XI</u></b>   |
| <b><u>1 INTRODUCTION</u></b>                        | <b><u>1</u></b>    |
| <b>1.1 Immune System</b>                            | <b>1</b>           |
| 1.1.1 Innate Immunity                               | 1                  |
| 1.1.2 Monocytes                                     | 3                  |
| 1.1.3 Phagocytosis                                  | 5                  |
| <b>1.2 Immunity of the central nervous system</b>   | <b>6</b>           |
| 1.2.1 Resident cells: astrocytes                    | 6                  |
| 1.2.2 Resident cells: microglia                     | 7                  |
| 1.2.3 Recruited immune cells in the CNS             | 8                  |
| <b>1.3 Role of monocytes in neurogenesis</b>        | <b>9</b>           |
| 1.3.1 Adult Neurogenesis                            | 9                  |
| 1.3.2 Immune system & neurogenesis                  | 10                 |
| 1.3.3 Gut-Brain-Axis                                | 11                 |
| 1.3.4 Mouse models to study the gut-brain-axis      | 13                 |
| <b>1.4 Role of monocytes in Alzheimer's disease</b> | <b>14</b>          |
| 1.4.1 Alzheimer's disease                           | 14                 |
| 1.4.2 Pathogenesis of Alzheimer's disease           | 15                 |
| 1.4.3 Immune system & Alzheimer's disease           | 18                 |
| 1.4.4 Mouse models for AD                           | 21                 |

---

|   |           |
|---|-----------|
| <b>1.5 Aims of this thesis</b>                                  | <b>22</b> |
| <b>2 MATERIALS AND METHODS</b>                                  | <b>23</b> |
| <b>2.1 Animal models</b>  | <b>23</b> |
| 2.1.1 Wildtype mice (part 1)                                    | 23        |
| 2.1.2 CCR2 <sup>-/-</sup>                                       | 23        |
| 2.1.3 5xFAD   | 23        |
| 2.1.4 <i>T. gondii</i> infection                                | 23        |
| <b>2.2 Experimental design &amp; procedures</b>                 | <b>24</b> |
| 2.2.1 Antibiotic and probiotic treatment                        | 24        |
| 2.2.2 Voluntary exercise  | 24        |
| 2.2.3 Adoptive transfer   | 25        |
| 2.2.4 Monocyte depletion in non-infected wildtype mice          | 25        |
| 2.2.5 Monocyte ablation in <i>T. gondii</i> infected 5xFAD mice | 25        |
| <b>2.3 Organ collection</b>                                     | <b>25</b> |
| <b>2.4 Nucleic acid isolation</b>                               | <b>25</b> |
| <b>2.5 Real Time Polymerase Chain Reaction (RT-PCR)</b>         | <b>26</b> |
| 2.5.1 RT-PCR from whole-brain homogenates                       | 26        |
| 2.5.2 RT-PCR from sorted cell populations                       | 26        |
| <b>2.6 Protein extraction</b>                                   | <b>27</b> |
| 2.6.1 Total $\beta$ -amyloid                                    | 27        |
| 2.6.2 Carbonate buffer and guanidine soluble A $\beta$          | 27        |
| <b>2.7 ELISA</b>  | <b>27</b> |
| <b>2.8 Immunohistology</b>                                      | <b>28</b> |
| 2.8.1 Analysis of BrdU-labeling and co-labeling                 | 28        |
| 2.8.2 Immunohistological analysis                               | 29        |
| 2.8.3 Immunofluorescence analysis                               | 29        |
| 2.8.4 Two-Photon image acquisition and analysis                 | 30        |
| <b>2.9 Primary cell isolation</b>                               | <b>31</b> |
| 2.9.1 Brain   | 31        |
| 2.9.2 Blood, bone marrow  | 31        |
| <b>2.10 Flow cytometry</b>                                      | <b>31</b> |
| 2.10.1 Surface staining   | 31        |

---

## TABLE OF CONTENTS

---

|  |           |
|--|-----------|
| 2.10.2 Conventional flow cytometry   | 32        |
| 2.10.3 Imaging flow cytometry  | 32        |
| <b>2.11 <i>Ex vivo</i> phagocytosis assay</b>  | <b>32</b> |
| <b>2.12 Statistical analysis</b>   | <b>32</b> |
| 2.12.1 Statistical analysis of results for part 1 (Neurogenesis)   | 33        |
| 2.12.2 Statistical analysis of results for part 2 (Alzheimer's disease)  | 33        |
| <b>3 RESULTS</b>   | <b>34</b> |
| <b>3.1 Role of monocytes in neurogenesis</b>   | <b>34</b> |
| 3.1.1 Antibiotic treatment decreases adult hippocampal neurogenesis  | 34        |
| 3.1.2 Running rescues neurogenesis levels despite antibiotics  | 35        |
| 3.1.3 Probiotics fully restore neurogenesis  | 36        |
| 3.1.4 Expression of soluble mediators in the brain remains unaltered upon changes of the intestinal flora                      | 36        |
| 3.1.5 Ly6C <sup>hi</sup> monocytes provide a link between brain, gut and treatment paradigms                                   | 38        |
| 3.1.6 Lack of monocytes decreases neurogenesis   | 42        |
| 3.1.7 Neurogenesis can be rescued by adoptive transfer of Ly6C <sup>hi</sup> monocytes to antibiotic-treated mice              | 45        |
| <b>3.2 Role of monocytes in Alzheimer's disease</b>  | <b>46</b> |
| 3.2.1 <i>T. gondii</i> infection reduces the plaque burden in 5xFAD mice   | 46        |
| 3.2.2 Expression of pro- and anti-inflammatory cytokines is triggered by <i>T. gondii</i> infection in wildtype and 5xFAD mice | 50        |
| 3.2.3 Recruited monocytes express high CCR2, intermediate TREM2 and CD36   | 53        |
| 3.2.4 Myeloid-derived mononuclear cells phagocytose A $\beta$  | 55        |
| 3.2.5 Recruited mononuclear cells increase proteolytic clearance of A $\beta$  | 59        |
| 3.2.6 <i>T. gondii</i> infection reduces A $\beta$ load in older animals   | 63        |
| <b>4 DISCUSSION</b>  | <b>64</b> |
| <b>4.1 Role of monocytes in neurogenesis within the gut-brain-axis</b>   | <b>64</b> |
| <b>4.2 Role of monocytes in Alzheimer's disease</b>  | <b>67</b> |
| <b>4.2.1 Etiologic connection between <i>T. gondii</i> and AD</b>  | <b>67</b> |
| <b>4.2.2 Insights regarding the treatment of AD</b>  | <b>68</b> |
| <b>4.3 Conclusions</b>   | <b>74</b> |

---

TABLE OF CONTENTS

---

|                   |           |
|-------------------|-----------|
| <b>REFERENCES</b> | <b>75</b> |
|-------------------|-----------|

---

|                                    |           |
|------------------------------------|-----------|
| <b>SELBSTSTÄNDIGKEITSERKLÄRUNG</b> | <b>87</b> |
|------------------------------------|-----------|

---

|                         |           |
|-------------------------|-----------|
| <b>CURRICULUM VITAE</b> | <b>88</b> |
|-------------------------|-----------|

---



## List of Abbreviations

|                     |   |
|---------------------|---|
| A $\beta$           | $\beta$ -amyloid                            |
| ABC                 | ATP-binding cassette                        |
| Abx                 | Antibiotics                                 |
| ACTH                | Adrenocorticotrophic hormone                |
| AD                  | Alzheimer's disease                         |
| AICD                | APP intracellular domain                    |
| APP                 | Amyloid precursor protein                   |
| AU                  | Arbitrary units                             |
| BBB                 | Blood-brain-barrier                         |
| BCSFB               | Blood-cerebrospinal-fluid-barrier           |
| BDNF                | Brain derived neurotrophic factor           |
| CCL2                | Chemokine C-C motif ligand 2                |
| CCR2                | Chemokine C-C motif receptor 2              |
| CD                  | Cluster of differentiation                  |
| cDNA                | Complementary DNA                           |
| CNS                 | Central nervous system                      |
| CRF                 | Corticotropin-releasing factor              |
| CTF                 | Carboxy-terminal fragment                   |
| CX <sub>3</sub> CR1 | CX <sub>3</sub> C chemokine receptor 1      |
| DAB                 | 3,3'-Diaminobenzidine                       |
| DC(s)               | Dendritic cell(s)                           |
| Dcx                 | Doublecortin                                |
| DMSO                | Dimethyl sulfoxide                          |
| DNA                 | Deoxyribonucleic acid                       |
| e. g.               | For example (Latin: <i>exempli gratia</i> ) |

## LIST OF ABBREVIATIONS

---

|               |  |
|---------------|--|
| ELISA         | Enzyme-linked immunosorbent assay              |
| Fisher's LSD  | Fisher's Least Significant Difference          |
| GFAP          | Glial fibrillary acid protein                  |
| GuHCl         | Guanidine hydrochloride                        |
| H&E           | Hematoxylin and eosin                          |
| hAPP          | Human APP                                      |
| HPRT          | Hypoxanthine-guanine phosphoribosyltransferase |
| i. p.         | Intraperitoneally                              |
| Iba1          | Ionized calcium-binding adaptor molecule 1     |
| IDE           | Insulin degrading enzyme                       |
| IFN- $\gamma$ | Interferon $\gamma$                            |
| Ig            | Immunoglobulin                                 |
| IL            | Interleukin                                    |
| ILC(s)        | Innate lymphoid cell(s)                        |
| LPS           | Lipopolysaccharide                             |
| MBP           | Myelin basic protein                           |
| M-CSF         | Macrophage colony-stimulating factor           |
| MFI           | Median fluorescence intensity                  |
| MHC           | Major histocompatibility complex class         |
| MMP(s)        | Matrix metalloproteinase(s)                    |
| mRNA          | Messenger RNA                                  |
| NaCl          | Sodium chloride                                |
| NEP           | Nepilysin                                      |
| NFT           | Neurofibrillary tangles                        |
| NGF           | Nerve growth factor                            |
| ns            | Not significant                                |
| NSAIDs        | Nonsteroidal anti-inflammatory drugs           |
| PBS           | Phosphate-buffered saline                      |

---

## LIST OF ABBREVIATIONS

---

|                  |  |
|------------------|--|
| PFA              | Paraformaldehyde                                 |
| RNA              | Ribonucleic acid                                 |
| RT               | Room temperature                                 |
| RT-PCR           | Real time polymerase chain reaction              |
| SCARA1           | Scavenger receptor A1                            |
| SCFA(s)          | Short-chain fatty acid(s)                        |
| SEM              | Standard error of the mean                       |
| SGZ              | Subgranular zone                                 |
| SPF              | Specific pathogen free                           |
| SVZ              | Subventricular zone                              |
| <i>T. gondii</i> | <i>Toxoplasma gondii</i>                         |
| TGF- $\beta$     | Transforming growth factor $\beta$               |
| TLR(s)           | Toll like receptor(s)                            |
| TNF              | Tumor necrosis factor                            |
| TREM2            | Triggering receptor expressed on myeloid cells 2 |
| UPS              | Ubiquitin-proteasome system                      |

## List of Figures and Tables

|  |    |
|--|----|
| Figure 1.1: Monocyte heterogeneity upon defense against protozoan parasites.....   | 3  |
| Figure 1.2: Communication pathways of the gut-brain-axis.....  | 12 |
| Figure 1.3: Proteolytic cleavage of amyloid precursor protein (APP) by $\alpha$ -, $\beta$ - and $\gamma$ -secretases within the anti-amyloidogenic (left) and amyloidogenic (right) pathway. .... | 15 |
| Figure 1.4: Aggregation of A $\beta$ from monomers to plaques. ....  | 16 |
| Figure 3.1: Reduced neurogenesis in antibiotic-treated mice can be partially restored by running. ....   | 35 |
| Figure 3.2: Expression of TNF and BDNF in whole-brain and hippocampus.....   | 37 |
| Figure 3.3: Expression of inflammatory and neurotrophic mediators in the brain .....   | 38 |
| Figure 3.4: The number of Ly6C <sup>hi</sup> monocytes is reduced in the brain of antibiotic-treated mice and is rescued by exercise but not by fecal transplant. ....                             | 40 |
| Figure 3.5: Kinetics of the Ly6C <sup>hi</sup> monocyte populations in bone marrow and blood during gut reconstitution with SPF flora .....  | 41 |
| Figure 3.6: Distribution of the Ly6C <sup>hi</sup> monocyte population in CCR2 <sup>-/-</sup> mice.....  | 42 |
| Figure 3.7: Genetic absence or antibody-induced loss of CCR2 <sup>+</sup> Ly6C <sup>hi</sup> monocytes results in decreased neurogenesis. ....   | 44 |
| Figure 3.8: Transfer of Ly6C <sup>hi</sup> cells into antibiotic-treated animals rescues neurogenesis. ....  | 45 |
| Figure 3.9: <i>T. gondii</i> infection leads to reduced plaque burden in 5xFAD mice. ....  | 47 |
| Figure 3.10: <i>T. gondii</i> infection reduces small and large A $\beta$ aggregates. ....   | 48 |
| Figure 3.11: <i>T. gondii</i> infection induces histopathological changes and activation of microglia. ....  | 49 |
| Figure 3.12: Microglia are activated in wildtype and 5xFAD mice upon <i>T. gondii</i> infection. ....  | 50 |
| Figure 3.13: Expression of pro-inflammatory cytokine mRNA in the brain is triggered in <i>T. gondii</i> infected wildtype and 5xFAD mice. ....   | 51 |
| Figure 3.14: Expression of anti-inflammatory cytokine mRNA in the brain is triggered in <i>T. gondii</i> infected wildtype and 5xFAD mice. ....  | 52 |
| Figure 3.15: mRNA expression of APP in the brain remains unaltered upon infection with <i>T. gondii</i> .....  | 52 |
| Figure 3.16: Myeloid-derived mononuclear cells are recruited to the brain upon <i>T. gondii</i> infection and express phagocytosis related surface molecules. ....                                 | 54 |

---

|   |    |
|---|----|
| Figure 3.17: Recruitment of Ly6C <sup>hi</sup> monocytes, Ly6C <sup>int</sup> mononuclear cells and Ly6C <sup>low</sup> macrophages in wildtype and 5xFAD mice upon <i>T. gondii</i> infection..... | 55 |
| Figure 3.18: Recruited mononuclear cells are potent A $\beta$ phagocytic cells.....   | 56 |
| Figure 3.19: Quantification of uptake of A $\beta$ <sub>42</sub> by imaging flow cytometry.....   | 57 |
| Figure 3.20: Ablation of CCR2 <sup>+</sup> Ly6C <sup>hi</sup> monocytes increases A $\beta$ accumulation in <i>T. gondii</i> infected 5xFAD mice. ....  | 59 |
| Figure 3.21: <i>T. gondii</i> infection enhances mRNA expression of the A $\beta$ degrading enzymes IDE and MMP9. ....  | 60 |
| Figure 3.22: mRNA of A $\beta$ degrading enzymes is expressed in different cell populations.....  | 60 |
| Figure 3.23: Microglia but not Ly6C <sup>hi</sup> monocytes are located in the vicinity of A $\beta$ plaques..  | 61 |
| Figure 3.24: Iba1 but not Ly6C reactivity is increased around A $\beta$ plaques.....  | 62 |
| Figure 3.25: Infection with <i>T. gondii</i> reduces total A $\beta$ burden in older animals. ....  | 63 |
| Figure 4.1: Graphical summary.....  | 74 |
| <br>  |    |
| Table 1.1: Impact of selected immune mediators on neuronal proliferation, survival and differentiation. ....  | 11 |
| Table 3.1: Quantification of A $\beta$ <sub>42</sub> uptake and cell properties by imaging flow cytometry.....  | 58 |

# 1 Introduction

Ly6C<sup>hi</sup> monocytes are a fundamental element of the innate immune response. In the following thesis, I will demonstrate how this cell subset contributes to maintain physiological levels of adult hippocampal neurogenesis in mice and the mechanism of reduction of  $\beta$ -amyloidosis using an experimental model for Alzheimer's disease.

## 1.1 Immune System

With more than  $9 \times 10^{29}$  microbes on our planet and countless other pathogens including viruses, protozoan, and parasites, the integrity of our body is continuously challenged from outside. Moreover, mutated cells loom on the inside and many physiological processes leave behind potentially hazardous residues. Resolving these danger signals requires an elaborate protective system which is guard, soldier and cleaner all at once: the immune system.

Within the vertebrate body, three main levels of protection can be found. First, surface barriers prevent attachment and entrance of pathogens. The second line of defense is provided by innate immune cells, which sense damage or pathogens via pattern recognition receptors. Third, highly specific cells of the adaptive immunity precisely target and fight individual pathogens via recombined high-affinity receptors (Delves & Roitt 2000).

### 1.1.1 Innate Immunity

The innate immune system is evolutionary older than adaptive immunity and can be found not only in vertebrates but also in plants, fungi, insects and primitive multicellular organisms. Recognition and response by the innate immune system are carried out in a generic manner and do not result in long-lasting protection (Delves & Roitt 2000). Both humoral and cellular components are part of the innate immunity (Parkin & Cohen 2001).

The humoral branch consists of complement and contact cascade, naturally occurring antibodies and pentraxins. Through opsonization and activation of phagocytes, these elements facilitate an effective early response to pathogens and cell debris (Shishido et al. 2012).

The cellular compartment of the innate immune system includes a variety of cells with diverse functions. Long-lived mast cells exert their major function during Immunoglobulin E (IgE)-mediated responses e. g. against helminths and are involved in inflammatory responses to allergens along with basophils and eosinophils (Voehringer 2013).

Moreover, there are several types of phagocytic cells: monocytes, macrophages and their respective tissue-specific counterparts, neutrophils, and dendritic cells (DCs).

Monocytes and their function will be described in detail in chapter 1.1.2.

Macrophages are tissue resident phagocytes equipped with many different pattern recognition receptors. Harnessing these receptors, macrophages contribute to tissue homeostasis, effectively remove apoptotic cells, and can also recognize and phagocytose pathogens (Gordon 2002). Depending on their environment, macrophages can secrete different effector molecules including growth factors and cytokines (Arango Duque & Descoteaux 2014). Highly specialized macrophage subsets are specifically located in certain tissues, including Kupffer cells in the liver, microglia in the brain and osteoclasts in the bone (Davies et al. 2013).

Neutrophils are rapidly recruited to sites of inflammation, rendering them crucial contributors to early acute stages of infections and injury. Neutrophil functions cover intra- and extracellular killing of parasites, phagocytosis as well as secretory activity (Kolaczkowska & Kubes 2013).

Classical DCs are short-lived cells with a high phagocytic and migratory potential. After taking up antigens at the site of infection, they travel to lymphoid organs where they activate T cells (Geissmann et al. 2010; Merad et al. 2013). That way, DCs provide a link between innate and adaptive immunity.

Besides the long-known cell types mentioned above, there is another group of innate cells which has been recently reported as innate lymphoid cells (ILCs). ILCs form a family of multifunctional cells including the previously described natural killer cells and are located primarily at barrier surfaces (Diefenbach et al. 2014). Interestingly, the three subpopulations of ILCs display striking similarities with adaptive T helper cell subsets, in particular with respect to their cytokine secretion: ILC1 play a role during immunity against intracellular infections by producing interferon  $\gamma$  (IFN- $\gamma$ ); with interleukin 13 (IL-13), ILC2 contribute substantially to the defense against extracellular multicellular parasites; and ILC3 lead the response to extracellular bacteria and fungi via secretion of IL-22. In addition to their contributions to acute immune responses, ILCs help to eventually resolve inflammation (Sonnenberg & Artis 2015).

### 1.1.2 Monocytes

Monocytes originate in the bone marrow and develop from macrophage/DC precursors. They are subsequently released into the blood stream in a CCR2-dependent manner (Serbina & Pamer 2006). In the blood, monocytes can be divided into two main subsets according to their expression of certain surface molecules: CX3CR1<sup>low</sup> CCR2<sup>+</sup> Ly6C<sup>high</sup> and CX3CR1<sup>high</sup> CCR2<sup>-</sup> Ly6C<sup>-</sup> monocytes (Geissmann et al. 2003).

Monocytes exert a double function: First, they are important immune effector cells. Second, they can develop into macrophages and inflammatory DCs, depending on the inflammatory conditions (Geissmann et al. 2010).

As effector cells, monocytes produce cytokines and take up debris similar to other innate immune effectors (Geissmann et al. 2010). Under steady-state conditions, Ly6C<sup>-</sup> monocytes patrol blood vessels by crawling along the luminal side of the endothelium, ready to extravasate quickly following an infection (Auffray et al. 2007; Auffray et al. 2009). During

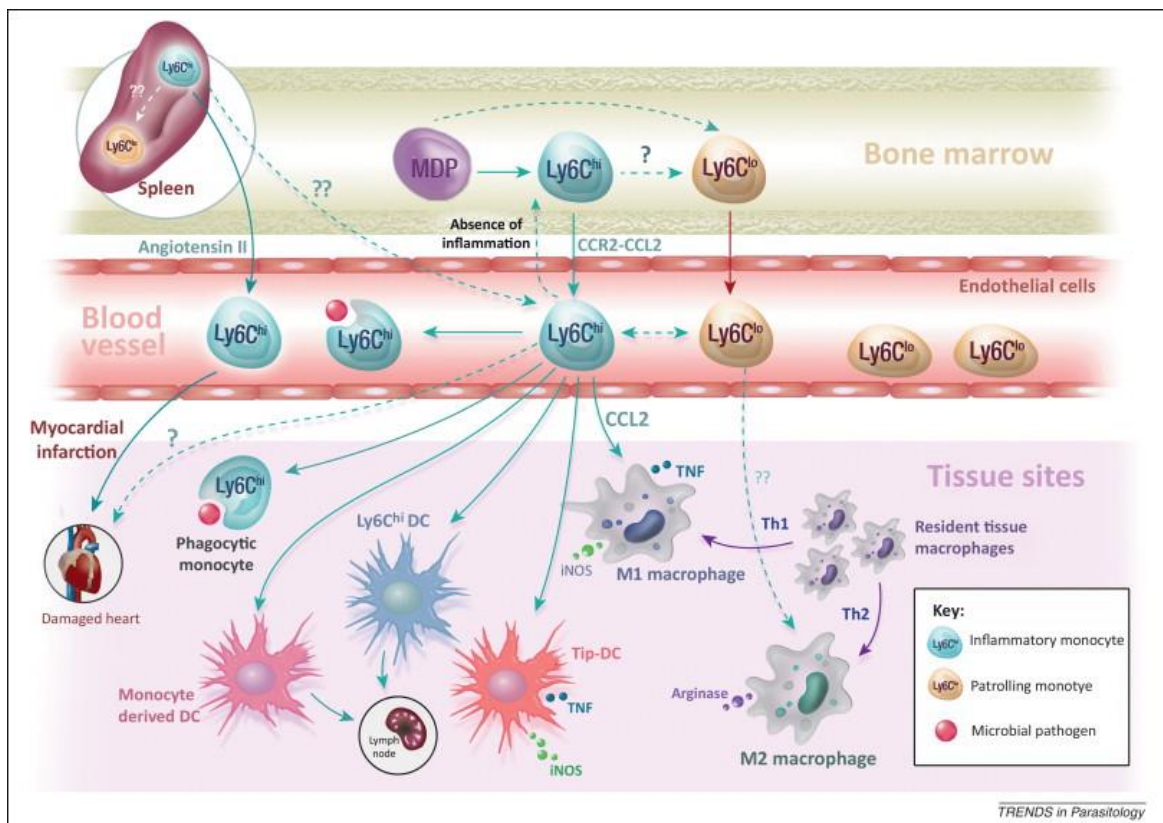


**Figure 1.1: Monocyte heterogeneity upon defense against protozoan parasites.**

This overview over the complex system of mononuclear phagocytes illustrates how Ly6C<sup>hi</sup> and Ly6C<sup>low</sup> monocytes exit from the bone marrow into the blood in a CCR2-dependent manner. After migrating to tissue sites, Ly6C<sup>hi</sup> monocytes can convert into monocyte derived DCs, monocyte derived macrophages and other subtypes. Importantly, Ly6C<sup>hi</sup> monocytes can also directly phagocytose microbial pathogens. (Figure from Sheel & Engwerda 2012).



infection or tissue damage, inflammatory Ly6C<sup>high</sup> monocytes migrate to the site of inflammation and produce high levels of TNF and IL-1 (Karlmark et al. 2012).

As precursors, Ly6C<sup>high</sup> monocytes differentiate into Ly6C<sup>int</sup> DCs and Ly6C<sup>low</sup> macrophages stimulated by the respective microenvironment. This functional monocyte heterogeneity provides a plastic immune response during the different stages of an inflammation and has been described in several experimental models (Gordon & Taylor 2005; Zigmond et al. 2012; Tacke & Zimmermann 2014; Sheel & Engwerda 2012).

The role of monocytes in certain infections including *Toxoplasma (T.) gondii*, *Plasmodium* spp., *Listeria monocytogenes* and Influenza virus has been studied intensively.

During acute infection with the protozoan parasite *T. gondii*, Ly6C<sup>hi</sup> monocytes in the small intestine are vital cells to ensure the survival of mice (Dunay et al. 2008; Dunay et al. 2010). Even at later stages when the infection has reached the brain, Ly6C<sup>hi</sup> monocytes are indispensable for parasite control (Biswas et al. 2015).

*Plasmodium* spp. are close relatives of *T. gondii* and cause malaria in humans and mice. Monocytes and monocyte-derived macrophages contribute to parasite control by phagocytosis, antibody-dependent cell inhibition as well as regulation of cytokine regulation (reviewed in Chua et al. 2013). Concurrently, they are involved in immunopathology including occlusion of small blood vessels in the brain during cerebral malaria (reviewed in Chua et al. 2013).

Ly6C<sup>hi</sup> monocytes are also required for resistance against bacterial infections such as *Listeria monocytogenes* (Serbina et al. 2003). In contrast, monocyte derived cells aggravate the disease by causing severe immunopathology in the central nervous system (CNS) during West Nile Virus encephalitis (Getts et al. 2008).

In addition to their substantial role during infectious diseases, monocytes and their progeny are involved in other inflammatory processes such as liver fibrosis, muscle and spinal cord injury.

Chronic inflammation of the liver caused by alcoholism or infections leads to liver fibrosis. This disease stage is characterized by abundant collagen deposition which inhibits normal liver function. Ablation of CCR2<sup>+</sup> monocytes reduces fibrosis (Karlmark et al. 2009) and increased recruitment enhances it (Karlmark et al. 2010), both pointing out the disease promoting capacity of monocytes. Adding to the diverse functions of monocytes, they also contribute to the resolution of collagen deposition under the same conditions of liver fibrosis

by differentiating into macrophages and producing matrix metalloproteinases (MMPs) (Tacke & Zimmermann 2014).

After muscle injury, monocytes give rise to macrophages supporting muscle regeneration (Arnold et al. 2007). Similarly, infiltrating monocyte-derived macrophages promote tissue repair following spinal cord injury (Shechter et al. 2009).

In conclusion, monocytes can promote as well as resolve inflammation, depending on the context. Therefore the manipulation of monocytes may provide a powerful tool to develop new therapeutic strategies (Shechter & Schwartz 2013).

### **1.1.3 Phagocytosis**

As mentioned above, the innate immune system includes different types of phagocytic cells. The term ‘phagocytosis’ is derived from the Ancient Greek words φαγεῖν (*phagein*; to devour), κύτος (*kytos*; cell), and –osis (process) and describes the active uptake of a particle from the environment by a cell. The uptake of any particle is initiated by binding to cell surface receptors. This specific binding sets phagocytosis apart from macropinocytosis, during which extracellular material is taken up randomly. Recognition of a target particle sets off multiple signaling cascades concomitantly which ultimately lead to the formation of a vesicle containing the particle, a phagosome. While the phagosome undergoes several maturation steps, its contents are eventually degraded (Flannagan et al. 2012; Underhill & Goodridge 2012).

The unlimited range of particles which can be taken up by phagocytes includes small structures such as proteins as well as large ones like pathogens and apoptotic cells. Correspondingly, there are numerous receptors recognizing potential target particles, some of which are sufficient to induce phagocytosis while others require the collaboration with other molecules. Phagocytosis mediating receptors include pattern recognition receptors like toll like receptors (TLRs), antibody binding Fc receptors, Scavenger receptor A (e. g. SCARA1), CD36 and triggering receptor expressed on myeloid cells 2 (TREM2) (Flannagan et al. 2012; Lue et al. 2014).

CD36 is a multiligand class B scavenger receptor which binds different targets like collagen, lipoproteins, fatty acids, and  $\beta$ -amyloid (Nergiz-Unal et al. 2011). At least some of these ligands can promote sterile inflammation by combined signaling of CD36 with a TLR4/TLR6 heterodimer (Stewart et al. 2010). This mechanism provides a possible explanation why CD36

has been linked to diseases like atherosclerosis (Park 2014) and Alzheimer's disease (El Khoury et al. 2003).

TREM2 from the immunoglobulin superfamily is another receptor implicated in the initiation of phagocytosis (Lue et al. 2014). It recently attracted attention because of its possible involvement in Alzheimer's disease (Guerreiro et al. 2013; Jonsson et al. 2013). Consistently,  $\beta$ -amyloid has been identified as a TREM2 ligand (Kleinberger et al. 2014).

Functionally, phagocytosis is an essential part of the developing as well as the mature organism. During embryonic development, high numbers of apoptotic cells have to be removed. In mature organisms, phagocytosis is equally important to maintain tissue homeostasis and to clear the body from any kind of toxic molecules and debris, e. g. protein aggregates and pathogens.

Impaired phagocytosis can lead to autoimmune diseases because apoptotic cells are not cleared appropriately (Poon et al. 2014) and may be, as the example of CD36 shows, involved in the development of multiple other diseases.

## **1.2 Immunity of the central nervous system**

The spinal cord, optic nerve and brain form the CNS. The remaining nerve tracks in the body compose the peripheral, enteric and autonomic nervous systems. Similar to the situation in other tissues, in the CNS there are resident (glia) and recruited immune cells. Glia cells comprise mainly of oligodendrocytes, astrocytes and microglia (Purves et al. 2004). While the primary function of oligodendrocytes is to wrap the neuronal axons in myelin sheaths, astrocytes and microglia have significant immunological functions.

### **1.2.1 Resident cells: astrocytes**

With respect to numbers, astrocytes are the second most prominent glia cell population in the CNS after oligodendrocytes. They are involved in the regulation of blood flow and synaptic activity as well as potassium, glutamate and water balance (Ransohoff & Brown 2012). Moreover, astrocytes express multiple immune receptors including TLRs, scavenger and complement receptors and can secrete cytokines, chemokines and neurotrophic factors. Mediators secreted by astrocytes upon stimulation include IL-6, IL-1 $\beta$ , TNF, TGF- $\beta$ , chemokine C-C motif ligand 2 (CCL2), nerve growth factor (NGF) and brain derived neurotrophic factor (BDNF) (Farina et al. 2007). Equipped with this immunological toolbox, astrocytes can interact with innate and adaptive immunity and contribute to disease control as well as pathogenesis (Ransohoff & Brown 2012). Moreover, they can communicate with

microglia, the third most abundant glia cell and the major tissue resident immune player in the CNS.

### **1.2.2 Resident cells: microglia**

Microglia belong to the myeloid lineage, yet they invade the neuroectoderm (which will later form the CNS) during embryogenesis before definitive hematopoiesis takes place (Ginhoux et al. 2010). In adult rodents microglia represent 5 to 12 % of CNS cells, depending on the region (Lawson et al. 1990). Microglia are phagocytic cells, removing debris as well as pruning synapses (Paolicelli et al. 2011). They express surface markers including CD45 (remnant of their hematopoietic origin), CD11b (part of the complement receptor 3 and expressed on various leukocytes), ionized calcium-binding adaptor molecule 1 (Iba1, expressed exclusively on microglia and macrophages), and F4/80 (traditionally a pan-macrophage marker), pointing towards their considerable immune functions (Saijo & Glass 2011). Beyond that, their extremely broad range of receptors enables microglia to recognize neurotransmitters, neurohormones and -modulators, as well as danger- and pathogen-associated patterns, cytokines and chemokines (Kettenmann et al. 2011).

In the healthy brain, microglia display a ramified, highly plastic morphology. Stimulation of microglia by infection, tissue damage, and modified neuronal activity induces a motile, amoeboid “activated” phenotype (Kettenmann et al. 2011). These “activated microglia” are the source of chemokines and cytokines including IL-1 $\beta$ , IL-6, CCL2, and TNF to activate other cells in the vicinity and recruit further immune cells, but also immunoregulatory cytokines such as IL-10 (Hanisch 2002). Although microglia are more responsive to stimuli like bacterial lipopolysaccharide (LPS), the repertoire of cytokines and receptors shared between astrocytes and microglia can lead to a positive feedback loop and an abundant release of cytokines (Saijo & Glass 2011; Saijo et al. 2009).

In recent years, the simplified portrayal of microglia as either “good” or “bad”, “resting” or “activated”, “friend” or “foe” has been continuously refined (Aguzzi et al. 2013). This will be described in more detail using the example of microglia in Alzheimer’s disease, see chapter 1.4.3.1.

With respect to terminology it is important to note that previously all phagocytic cells in the CNS were described as microglia. Recently, fate mapping studies allowed the discrimination between yolk sac-derived resident phagocytes (microglia) and bone marrow-derived recruited phagocytes (monocytes, macrophages and such) (Ginhoux et al. 2010). Subsequent

differentiation between resident and recruited brain macrophages revealed specific contributions of each subset under several pathological conditions (Schwartz & Baruch 2014).

### **1.2.3 Recruited immune cells in the CNS**

As outlined above, innate immune cells continuously patrol the organism using lymphatic and circulatory vessels and thus, can rapidly detect and react to different kinds of disturbances. Notably, there are particular tissues which are excluded from this surveillance network: the immune privileged regions including the eye, the testis, the pregnant uterus, and the brain. All are vulnerable structures where damage can have devastating consequences like blindness, infertility, abortion, and cognitive impairments. Therefore, the immune privilege increases protection from both pathogen intrusion and collateral damage during immune responses (Arck et al. 2008).

Immune privilege is maintained by a complex network of immunoregulatory and immunosuppressive processes and utilizes membrane-bound molecules such as Fas/FasL, soluble compounds including IL-10 and transforming growth factor  $\beta$  (TGF- $\beta$ ) secretion, and spatial separation (reviewed in Niederkorn 2006).

In the brain, spatial separation is achieved by the combination of different barriers: the meninges, the blood-brain-barrier (BBB), and the blood-cerebrospinal-fluid-barrier (BCSFB). The meninges comprise of three membranes lining the outer surface of the CNS (Ransohoff & Engelhardt 2012). The BBB is established by adjacent endothelial cells which are stimulated mainly by signals from astrocytes and form increased numbers of tight junctions to limit paracellular transport and the transmigration of immune cells from the blood (Abbott et al. 2006). In contrast, the BCSFB comprises of a fenestrated endothelium amended by a tight junction lined epithelium (Shechter et al. 2013).

Under certain inflammatory circumstances, the BBB becomes leaky and foci of infiltrating immune cells from the blood can be found within the CNS. Amongst these infiltrating cells are monocytes, which display a similar functional heterogeneity as found in peripheral tissues. Different experimental paradigms have revealed three main subsets, distinguished by their surface expression of Ly6C: Ly6C<sup>high</sup> monocytes invade the CNS, where they can further develop into Ly6C<sup>int</sup> monocytes resembling DCs and Ly6C<sup>low/-</sup> monocytes with macrophage properties (Biswas et al. 2015; Lin et al. 2009; Zigmond et al. 2012; Mayer-Barber et al. 2011).

In recent years, several interesting publications have added new layers to the concept of how the CNS is integrated into the overall immune system. A new model was promoted suggesting that when leukocytes enter through the BCSFB instead of through the BBB, they are modulated towards a regulatory phenotype beneficial for recovery from spinal cord injury (Shechter et al. 2013; Shechter et al. 2009). And with their remarkable discovery Louveau et al. revised the old dogma that the brain is exempted from lymphatic drainage (Louveau et al. 2015). Finally, there is compelling evidence that immune cell recruitment and contribution is not restricted to inflammation but is instead an essential part of healthy physiology (Kipnis et al. 2004; Ziv et al. 2006; Schwartz et al. 2013).

### **1.3 Role of monocytes in neurogenesis**

Looking at the CNS from an immunological point of view, glia cells often take the center stage. Nevertheless, the functional core of the CNS is formed by neuronal cells which develop from the neuroectoderm during embryogenesis (Liu & Niswander 2005). Neurogenesis, the process of generating functional neurons, was originally considered to occur only during embryogenesis (Ming & Song 2011). However, after the first descriptions of adult neurogenesis in the 1960s and 1980s (Altman & Das 1967; Paton & Nottebohm 1984), numerous studies revealed adult neurogenesis in almost all mammalian species including humans. Today, neurogenesis is acknowledged as a part of adult physiology (Kempermann et al. 1997; Eriksson et al. 1998; Kornack & Rakic 1999; Ming & Song 2011).

#### **1.3.1 Adult Neurogenesis**

Adult neurogenesis has mostly been described within two regions in the adult brain, the subventricular zone (SVZ) of the lateral ventricles and the subgranular zone (SGZ) in the dentate gyrus of the hippocampus. Neuroblasts generated in the SVZ migrate via the rostral migratory stream to the olfactory bulb, where they mature to interneurons. From the SGZ, neuroblasts travel only a short distance and develop into dentate granule neurons in the hippocampus (Ming & Song 2011).

The hippocampus plays a crucial role in memory formation and spatial orientation (Fanselow & Dong 2010). However, the exact functions of adult neurogenesis in the SGZ of the hippocampus have not been elucidated yet. On the one hand, changes in (hippocampal) neurogenesis have been linked to different neurological diseases. These observations cannot give clear answers with respect to functionality, because the influence is most likely bidirectional (Ming & Song 2011). On the other hand, current animal research suggests that in

rodents only some hippocampus-dependent learning and memory tasks rely on the integration of new neurons during adulthood (Deng et al. 2010).

Before their integration into the existing network, neurons undergo maturation. The different maturation stages are characterized by changes in morphology and protein expression, allowing their discrimination in immunohistological stainings. Neural precursors at the least differentiated stage, radial glia-like cells, express Nestin, which is later downregulated and replaced by doublecortin (Dcx) in neuroblasts (Ming & Song 2011). Adult, post-mitotic neurons can be identified by NeuN, a nuclear marker present on almost all neuronal cell types (Mullen et al. 1992).

In adult humans, about 1400 new neurons are integrated into both dentate gyri every day (Spalding et al. 2013). Importantly, these surviving neurons are only a small proportion of the total number of newly generated neurons. Studies in mice have revealed that most of the newborn neurons die by apoptosis (Sierra et al. 2010). It is therefore important to discriminate between production and survival of newborn neurons.

### **1.3.2 Immune system & neurogenesis**

A plethora of different factors have been identified to regulate adult neurogenesis including sex, aging, hormones, neurotransmitters, drugs, stress, diet or physical activity (reviewed in Ming & Song 2005). Both physiological and pathological stimuli influence adult neurogenesis in a complex manner. Multiple studies have shown that physical exercise and hippocampal dependent learning increase adult neurogenesis in the SGZ (van Praag et al. 1999; Ming & Song 2011; Moustroph et al. 2012). Injuries such as seizures and stroke also enhance adult neurogenesis, whereas chronic stress and inflammation both lead to a reduction (Ming & Song 2011).

Accordingly, microglia derived inflammation inhibits neurogenesis after stimulation by irradiation (Monje et al. 2003), LPS or tissue damage (Ekdahl et al. 2003). Later it was found however, that microglia can also support neurogenesis, particularly after stimulation with IL-4 or low levels of IFN- $\gamma$  (Butovsky et al. 2006). Moreover, unchallenged microglia in the SGZ indirectly ensure proper neurogenesis by efficiently removing those newborn neurons which undergo apoptosis (Sierra et al. 2010). Interestingly, T cells have also been found to support neurogenesis (Ziv et al. 2006; Wolf et al. 2009). It is of note that only T cells recognizing the CNS located antigen myelin basic protein (MBP) were able to boost neurogenesis, but not those recognizing ovalbumin. This was reflected also in spatial memory and learning (Ziv et

al. 2006). A subsequent study specified that CD4<sup>+</sup> but not CD8<sup>+</sup> T cells are necessary to maintain neurogenesis levels (Wolf et al. 2009).

The mechanisms by which immune cells influence neurogenesis are largely unknown, even though reduced BDNF levels were reported along with T cell depletion (Wolf et al. 2009). Additionally, the effect of selected immune mediators on neuronal proliferation, survival and differentiation is summarized in Table 1.1, proposing possible links between the immune system and neurogenesis.

**Table 1.1: Impact of selected immune mediators on neuronal proliferation, survival and differentiation.**

(Table adapted from Kohman & Rhodes 2013)

|                               | <b>Proliferation</b> | <b>Survival</b> | <b>Neuronal differentiation</b> |
|-------------------------------|----------------------|-----------------|---------------------------------|
| <b>IL-6</b>                   | -                    | -               | -                               |
| <b>IL-1<math>\beta</math></b> | -                    |                 | -                               |
| <b>TNF</b>                    | -                    |                 | -                               |
| <b>TGF-<math>\beta</math></b> |                      | +               | +                               |
| <b>IL-4</b>                   |                      |                 | +                               |
| <b>IL-10</b>                  | +                    |                 |                                 |

### 1.3.3 Gut-Brain-Axis

The increased recognition of homeostatic immune interactions between periphery and CNS (as described in chapters 1.2 and 1.3.2) brought on more questions: Which events in the periphery do influence the CNS milieu? How is this information from the periphery transmitted to the CNS? Which processes in the CNS are susceptible to immune modulation?

#### 1.3.3.1 Gut flora

One of the factors proposed to influence the CNS milieu is the gut flora. It comprises bacteria, fungi, and viruses populating the luminal surface of the gut (Guarner & Malagelada 2003; Underhill & Iliev 2014; Cadwell 2015). Similarly, all other surfaces including skin, vaginal and upper respiratory tract are covered with microbes. The largest microbial community is located in the gut where it prevents the growth of invasive pathogens and helps with the digestion and uptake of nutrients (Guarner & Malagelada 2003). It has further been revealed that the gut flora is required for proper development of the immune system (Hooper et al. 2012).

Correspondingly, changes in the commensal gut flora have been associated with the susceptibility to diabetes, obesity (Tilg & Kaser 2011), inflammatory bowel disease (Wu et al.



2013), cancer, allergy and other diseases (Round & Mazmanian 2009). Alterations of the gut flora can also limit as well as exacerbate infections (Haag et al. 2012; Dicksved et al. 2014). Further, absence of gut microbiota impairs an effective antiviral response (Ichinohe et al. 2011; Abt et al. 2012).

The gut flora is not only highly diverse, but also differs from individual to individual (Eckburg et al. 2005). Nevertheless, certain trends can be observed, for example the shift from gram-negative Bacteroidetes towards gram-positive Firmicutes in obese mice and humans (Turnbaugh et al. 2006; Ley et al. 2006).

### 1.3.3.2 Consequences for the CNS

In addition to its effects on the immune system, the gut microbiota have been found to influence CNS-related disorders as well. This is reflected in several interesting findings. First, germ-free mice display reduced anxiety (Diaz Heijtz et al. 2011) and do not develop spontaneous autoimmune demyelination in the CNS (Berer et al. 2011). Second, depletion of the gut flora was proposed to alter microglia in the CNS and this altered phenotype can be reverted by short-chain fatty acid (SCFA) treatment (Erny et al. 2015). Third, the neurobehavioral changes accompanying obesity could be induced also by transferring an

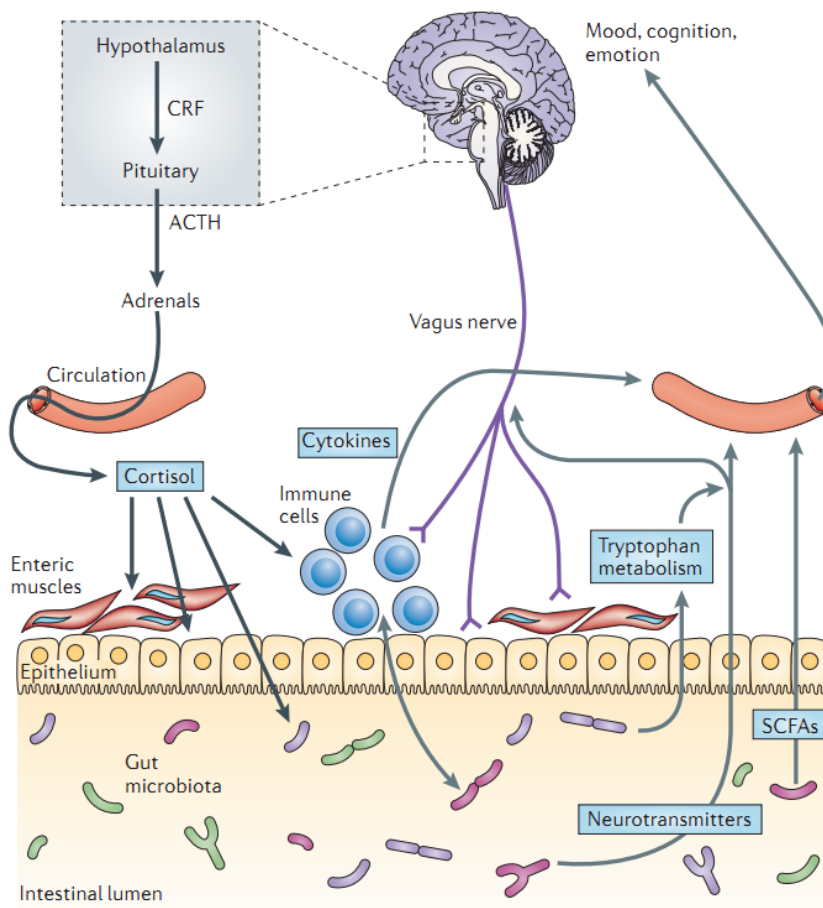


**Figure 1.2: Communication pathways of the gut-brain-axis.**

ACTH, adrenocorticotropic hormone; CRF, corticotropin-releasing factor; SCFAs, short-chain fatty acids (Figure from Cryan & Dinan 2012).

obesity-like gut flora to non-obese mice (Bruce-Keller et al. 2015). Similarly, the visceral pain (or visceral hypersensitivity in animal models) associated with inflammatory bowel disease could be transferred by the gut flora alone (Crouzet et al. 2013).

In line with these experimental results, human studies reported connections between microbial imbalance and psychiatric diseases including depression (Naseribafrouei et al. 2014) and autism (Parracho et al. 2005).

### **1.3.3.3 Transmission of signals between gut and CNS**

There are multiple communication channels used to transmit information between the gut and the CNS, including neural, endocrinal and immune pathways (summarized in Figure 1.2) (Cryan & Dinan 2012). Neural communication can occur via the vagus nerve, providing a direct nervous connection between the enteric nervous system of the gut and the brain. Endocrinal signals include hormones whose release is triggered by the hypothalamus-pituitary-adrenal axis. Classically, the immune system uses cytokines to exchange information, which can also act directly on the CNS (Cryan & Dinan 2012). Immune cells also have receptors for neuro-related molecules, e. g. cannabinoids (Croxford & Yamamura 2005) making it a bidirectional communication. Other neuroactive mediators influenced by gut microbes include SCFAs and neurotransmitters, e. g. via tryptophan metabolism (reviewed in Cryan & Dinan 2012). Lastly, the gut microbes possibly translocate into the blood and form a dormant blood microbiome which could also interfere with immunity (Potgieter et al. 2015).

### **1.3.4 Mouse models to study the gut-brain-axis**

The impact of the gut flora on aspects of physiology and pathology can be studied in different mouse models. Germ-free mice are transferred as embryos into sterile cages and are raised in absence of any microbiological flora. In contrast, gnotobiotic mice are raised under controlled specific pathogen free (SPF) conditions and the gut flora is later eradicated by admission of broad-spectrum antibiotics. The first model suffers from the high maintenance as well as developmental defects of the animals including an immature immune system (Mazmanian et al. 2005; Abt et al. 2012) and behavioral deficits (Diaz Heijtz et al. 2011; Cryan & Dinan 2012). The second model permits mice a normal development and thus, facilitates the study of immunological questions.

## **1.4 Role of monocytes in Alzheimer's disease**

Neurogenesis is, as described above, a physiological homeostatic process. In contrast, Alzheimer's disease (AD) is a pathological condition of the CNS followed by neurodegeneration.

### **1.4.1 Alzheimer's disease**

With an estimated 24 million cases worldwide, dementia is a global health threat. Because the major risk factor for the onset of dementia is old age, patient numbers are predicted to rise, particularly in developed countries where demographics shift towards the elderly. With about 70 %, the leading cause of dementia is AD (Reitz et al. 2011). AD is a neurodegenerative disorder and was first described more than 100 years ago by the German neuropathologist Alois Alzheimer (Alzheimer et al. 1991).

The definite diagnosis of AD requires pathological evidence, in most cases *post mortem*. However, possible or probable AD can be diagnosed according to the gradual onset and aggravation of neuropsychiatric symptoms which cannot be explained by other causes (Reitz et al. 2011).

The first clinical symptoms of AD include disturbances of short-term and episodic memory and loss of the ability to store new information, e. g. noticeable in displacement of every-day items. Subsequent decline in cognitive abilities is characterized by impairment of language, problem-solving, attention, mood, and long-term memory (Weintraub et al. 2012). Advanced and final stages of the disease usually require the patient's hospitalization due to spatial and temporal disorientation, incontinence, and eventually the inability to perform even simple tasks without assistance. The cause of death is commonly not the disease itself but infections, e. g. pneumonia (Förstl & Kurz 1999).

Despite extended and ongoing efforts in research, treatment options of AD are still poor. In the absence of a cure, treatment is carried out symptomatically and targets psychiatric symptoms as well as cognitive impairment. The latter is treated by inhibition of acetylcholinesterase and thereby slowing down the degradation of acetylcholine to antagonize the loss of cholinergic neurons. Additionally, neuronal loss through overstimulation can be fought by inhibiting the glutamatergic system (Lleó et al. 2006).

Unfortunately, already lost cognitive functions cannot be restored. Moreover, the diagnosis of AD and with it the beginning of treatment is preceded by years or decades of "silent" pathogenesis (Saido & Iwata 2006).

The onset of disease usually takes place after 60 to 65 years of age in more than 95 % of AD cases, only in very rare (1-5 %) familial cases due to genetic mutations patients experience an early onset in their late 40s or early 50s (Reitz et al. 2011). Even though there is most likely some genetic contribution in sporadic cases, too, the biggest risk factor for developing AD is old age (Bekris et al. 2010). Additionally, systemic conditions including cerebrovascular disease, hypertension, and diabetes have been speculated to increase the risk for developing AD (Reitz et al. 2011).

### 1.4.2 Pathogenesis of Alzheimer's disease

On the molecular level, the pathogenesis of AD is characterized by intracellular aggregation of hyperphosphorylated tau as neurofibrillary tangles and extracellular accumulation of  $\beta$ -amyloid plaques (Braak & Braak 1991).

Tau is a microtubule associated protein, which is found mostly in neurons. Abundant and abnormal phosphorylation leads to a loss of the microtubule stabilizing function and the

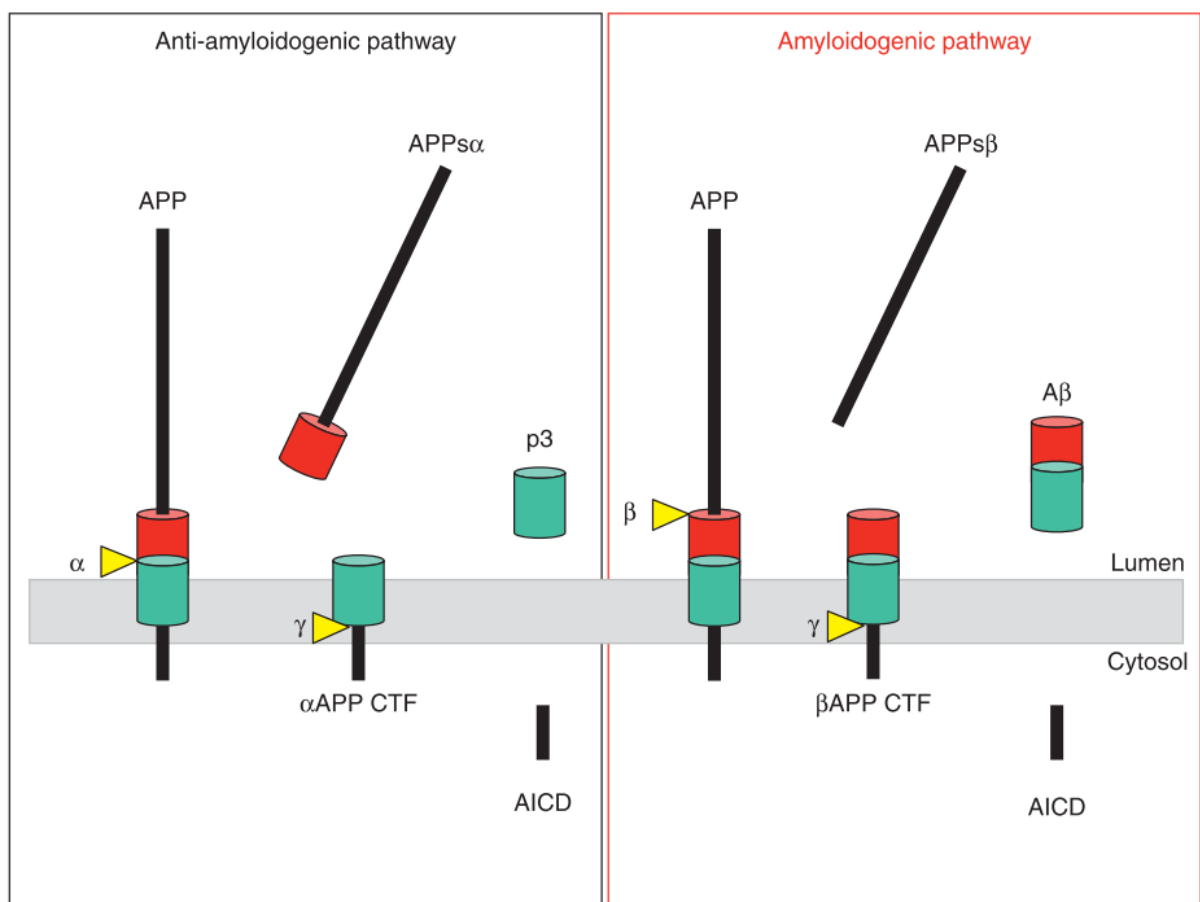


**Figure 1.3: Proteolytic cleavage of amyloid precursor protein (APP) by  $\alpha$ -,  $\beta$ - and  $\gamma$ -secretases within the anti-amyloidogenic (left) and amyloidogenic (right) pathway.**

APP, amyloid precursor protein. CTF, carboxy-terminal fragment. AICD, APP intracellular domain. A $\beta$ ,  $\beta$ -amyloid. (Figure from Haass et al. 2012).

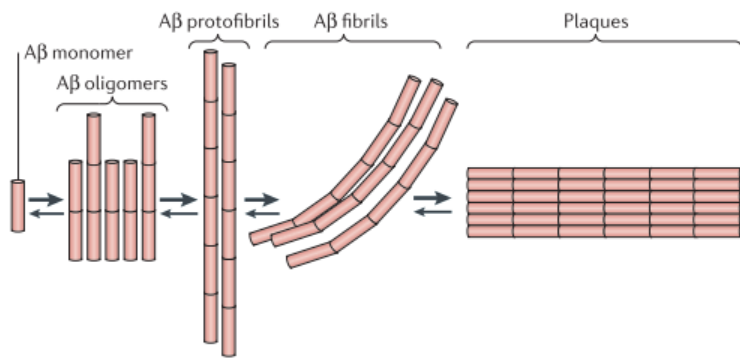


**Figure 1.4: Aggregation of A $\beta$  from monomers to plaques.**

(Figure adapted from Heppner et al. 2015).

aggregation of tau proteins as helical filaments. Intracellularly, these filaments build up and form neurofibrillary tangles (NFT). Even though the amount of hyperphosphorylated tau correlates well with the severity of AD, it is not yet clear whether NFT formation contributes to disease progression or represents rather a neuroprotective mechanism (Wang et al. 2012).

The second hallmark of AD is extracellular plaques, which comprise small peptides of about 4 kDa in size with a varying length of 37 to 43 amino acids,  $\beta$ -amyloid (A $\beta$ ). Monomeric A $\beta$  is generated from amyloid precursor protein (APP). APP is a transmembrane protein and contains cleavage sites for different enzymes including  $\alpha$ -,  $\beta$ - and  $\gamma$ -secretase. In the anti-amyloidogenic pathway (Figure 1.3, left panel), cleavage by  $\alpha$ - and  $\gamma$ -secretase leads to the production of APP $\alpha$  (incorporating the amino-terminal part), p3 (incorporating a large portion of the transmembrane domain) and AICD (APP intracellular domain, incorporating the carboxy-terminal part). The truncated A $\beta$  peptide p3 is pathologically irrelevant. In contrast, the first cleavage of the amyloidogenic pathway (Figure 1.3, right panel) is executed by  $\beta$ -secretase and releases APP $\beta$  (incorporating the amino-terminal part). The remaining  $\beta$ APP carboxy-terminal fragment (CTF) is subsequently processed by  $\gamma$ -secretase, resulting in AICD and A $\beta$  (Haass et al. 2012).

Due to the presence of multiple cleavage sites for  $\gamma$ -secretase activity and a certain imprecision of the execution, there are several different species of A $\beta$ . These differences are biologically relevant, because longer forms like A $\beta_{42}$  are particularly prone to form highly toxic oligomers. Oligomers then assemble as (proto-)fibrils and later aggregate to amyloid plaques (Masters & Selkoe 2012) (Figure 1.4).

Interestingly, certain mutations causing familial AD were found to enhance the amyloidogenic pathway and to alter APP in a way favoring the production of longer A $\beta$  species. Likewise, people born with an additional copy of APP due to trisomy 21 show AD like symptoms early in life. This genetic evidence is the strongest support for the amyloid

cascade hypothesis presenting A $\beta$  as the causative agent of AD (Hardy & Higgins 1992; Hardy & Selkoe 2002).

#### **1.4.2.1 Clearance of A $\beta$**

In general, abnormal accumulation of a substance is due to an imbalance of production and clearance. Interestingly, the level of APP in the cerebrospinal fluid of AD patients was reduced compared to non-demented controls (Van Nostrand et al. 1992; Mawuenyega et al. 2010), suggesting that contrary to the animal models used for research, AD patients do not suffer from an overproduction of APP. Even though familial AD presents with more A $\beta$  due to an enhanced amyloidogenic processing of APP, this is not the case in sporadic AD and thus, brings into focus the mechanisms by which A $\beta$  is removed.

In the CNS, a multi-layered cleaning system comprising general and specific mechanisms is responsible for the clearance of A $\beta$ . General, unspecific elimination of waste including A $\beta$  occurs via the glymphatic system, a general fluid stream guiding substances from the CNS parenchyma towards lymphatic vessels from where they are removed (Nedergaard 2013; Louveau et al. 2015). Specific elimination at the level of the BBB may be supported by ATP-binding cassette (ABC) transporters, which can dispose A $\beta$  into the periphery (Krohn et al. 2011; Pahnke et al. 2014).

In addition to its transport out of the CNS, the *in situ* proteolytic degradation is another way to specifically remove A $\beta$ . There are multiple proteases breaking down A $\beta$ , including the metalloproteases neprilysin (NEP), insulin degrading enzyme (IDE), and matrix-metalloprotease 9 (MMP9) (Saido & Leissring 2012). NEP is one of the major regulators of A $\beta$  and is almost exclusively expressed in neurons (Fukami et al. 2002). IDE is also of great importance for degradation of A $\beta$ , and is expressed in a wide range of tissues (Yfanti et al. 2008). MMP9 is of particular interest, because it is one of the few enzymes that can degrade monomeric as well as oligomeric/fibrillar A $\beta$  (Yan et al. 2006). Despite A $\beta$  being a substrate for many different peptidases and proteases, the lack of only one can have a significant impact on  $\beta$ -amyloidosis (Iwata et al. 2001; Yin et al. 2006). Accordingly, increased expression of IDE or NEP led to reduced levels of A $\beta$  (Leissring et al. 2003).

Notably, most of the proteases can be found in the extracellular space, as well as within the cells, for example in endosomes (Saido & Leissring 2012). This is important, because in immune cells phagocytosing A $\beta$ , the subsequent intracellular degradation is equally important.

### **1.4.3 Immune system & Alzheimer's disease**

The role of immune cells, in particular innate immunity in the pathogenesis of AD is far from being fully understood, despite a high number of published studies. Even though immune cells may influence the course of disease on many layers, two prominent fields of action stand out: First, the secretion of mediators including cytokines and chemokines, and second, the clearance of A $\beta$ . Together, local glia cells and infiltrating immune cells modulate disease progression by engaging in these tasks – or failing to do so.

#### **1.4.3.1 Microglia**

Driving force of the inflammation found in AD are the intrinsic immune cells of the CNS. Indeed, microglia are in intimate proximity to A $\beta$  plaques (Itagaki et al. 1989) and express receptors for A $\beta$  (including CD36 and SCARA-1), inducing activation and stimulating A $\beta$  uptake (Yu & Ye 2015). It is of note that A $\beta$  is continuously present in AD and thus, results in chronic activation and inflammation, which other than in acute injury like stroke cannot be resolved (Wang et al. 2014; Schwartz & Baruch 2014).

Activation of microglia is characterized by morphological changes and secretion of cytokines including IL-6, TNF, and IL-1 $\beta$  (Prokop et al. 2013). There is evidence that the prolonged exposure to pro-inflammatory mediators can cause neuronal damage (Holmes et al. 2003; Holmes 2013). Subsequently, multiple studies have shown that long-term treatment with nonsteroidal anti-inflammatory drugs (NSAIDs) is inversely correlated with the risk for dementia in patients (reviewed in Heneka et al. 2015) and A $\beta$  deposits in mouse models (Lim et al. 2000; Yan et al. 2003). However, the modulation of inflammation is not that simple. Many studies have shown that it strongly depends on which molecule is targeted when and results are not always conclusive (reviewed in Heppner et al. 2015).

In addition to their role in (detrimental) inflammation, microglia also engage in beneficial processes in the course of the disease. As learned from acute axonal injury, microglia can protect neurons (Streit 2005), even though it is unclear whether they can utilize their full potential in AD. Microglia also possess the general tools for A $\beta$  clearance, but they don't seem to make a long-lasting contribution (Grathwohl et al. 2009). Moreover, microglia have been found to be functionally impaired in mouse models of AD compared to age-matched non-transgenic controls (Hickman et al. 2008; Krabbe et al. 2013). Accordingly, Schwartz and Baruch suggest that after microglia fail to fully restore tissue homeostasis (i. e. remove A $\beta$ ), their role as cytokine-producing cells overrides the benefits and leads to long lasting,

unresolved inflammation damaging the surrounding neuronal tissue (Schwartz & Baruch 2014).

Stimulation of microglia with harsh methods such as bacterial LPS could overcome the impairment and thus, was found to reduce  $\beta$ -amyloidosis when examined early after treatment (around one week in different studies). In the long run, however, the amount of plaques increased (reviewed in Prokop et al. 2013).

#### **1.4.3.2 Recruited monocytes**

One idea of dealing with the exhaustion of microglia is to replace or supplement microglia with fresh mononuclear cells from the periphery. While under healthy, physiological circumstances, they do not contribute significantly to the pool of microglia (Ajami et al. 2007; Ginhoux et al. 2010), monocytes/macrophages may represent potential effector cells to be recruited to the CNS. Their potential is underlined by the following four findings:

First, their functional plasticity allows them to react differently to a wide range of stimuli (Gordon & Taylor 2005; Zigmond et al. 2012; Tacke & Zimmermann 2014).

Second, similar to the CNS located microglia, monocytes can engage in phagocytosis and cytokine secretion (Biswas et al. 2015).

Third, perivascular macrophages are monocyte progeny located in the perivascular space around the CNS vasculature. These macrophages are continuously replaced from the bone marrow and contribute to removal of amyloid deposited around blood vessels (Hawkes & McLaurin 2009).

Fourth, in AD patients with comorbid stroke, macrophage recruitment to the CNS was observed and further, A $\beta$  fibrils were detected within lysosomes of the macrophages, pointing out their capacity to take up A $\beta$  (Wisniewski et al. 1991; Akiyama et al. 1996).

Indeed, several studies have directly addressed the role of monocytes in mouse models of AD. It has been shown that the absence of monocytes in CCR2<sup>-/-</sup> mice (where monocytes fail to exit from the bone marrow) worsens the early accumulation of A $\beta$  and increases mortality (El Khoury et al. 2007). Accordingly, the enrichment of monocytes by peripheral injection of macrophage colony-stimulating factor (M-CSF) (Boissonneault et al. 2009), glatiramer acetate treatment or transplantation of CD115<sup>+</sup> monocytes (Koronyo et al. 2015) reduced  $\beta$ -amyloidosis.

In contrast, in a comparative study of microglia, perivascular macrophages and parenchymal monocytes conducted by Mildner and colleagues, the beneficial effects were attributed to

---



perivascular and not to parenchymal macrophages/monocytes (Mildner et al. 2011). Interestingly, the authors also pointed out that CCR2 was necessary for A $\beta$  clearance by perivascular macrophages, but not for their migration to the perivascular space (Mildner et al. 2011).

#### **1.4.3.3 Age & infection**

Increased presence of immune cells including monocytes can be caused by infection. Interestingly, old age (the most important risk factor to develop AD) also comes with an increased susceptibility to infectious diseases. The prevalence of bacterial infections including pneumonia and urinary tract infections is increased by 3- to 20-fold amongst elderly individuals as compared to younger ones (Gavazzi & Krause 2002).

Systemic inflammation can influence the milieu in the CNS via different routes, e. g. vagal-nerve signaling and cytokine or cell signaling at the endothelium or choroid plexus (Perry et al. 2007). Systemic infection was further found to have a negative impact on cognitive functions in AD patients (Holmes et al. 2003).

During life, people go through acute infections as well as acquire chronic infections. In line with this correlation, the seroprevalence of *T. gondii* infection increases with age (Jones et al. 2001). Thus, the interesting question arises, how *T. gondii* influences the pathogenesis of AD.

#### **1.4.3.4 *Toxoplasma gondii***

*T. gondii* is an obligate intracellular protozoan parasite which is able to infect all vertebrates. After oral ingestion of oocysts via contaminated food or water or tissue cysts via contaminated meat, the parasite causes a local acute infection of the small intestine (Dunay et al. 2008; Dunay et al. 2010). Only in the digestive tract of its definitive hosts from the feline family, *T. gondii* completes its life cycle and undergoes sexual replication to be shed as oocysts in the feces. In all other intermediate hosts, *T. gondii* spreads throughout the body via infected migratory cells including dendritic cells (John et al. 2011) and monocytes (Courret et al. 2006) and thus, establishes a systemic chronic infection. Long-term survival of the parasite is possible due to formation of cysts in non-replicating cells like muscle and neuronal cells (Munoz et al. 2011).

As a wide-spread parasite with a strong tropism to the CNS, *T. gondii* has been suspected to contribute to the development of AD. However, results are not conclusive: A small study amongst AD patients confirmed *T. gondii* seropositivity as a possible risk factor for AD (Kusbeci et al. 2011), whereas Jung and colleagues suggested a beneficial effect of chronic

*T. gondii* infection in rodents (Jung et al. 2012). Moreover, a recent study did not find any differences with respect to seropositivity and –intensity between non-demented controls and AD patients (Perry et al. 2015).

#### **1.4.4 Mouse models for AD**

To better study the disease mechanism and possible treatment options, many mouse models have been developed mostly based on those gene mutations causing familial AD (Chin 2011). The models differ essentially with respect to the background mouse strain, the aspect of pathophysiology they mimic (amyloid plaques, neurofibrillary tangles, neurodegeneration, cognitive deficits), and the time the mice take to develop respective symptoms (Chin 2011).

5xFAD mice with C57BL/6SJL background, which have been used for the present study, overexpress human APP (hAPP) under the neuronal murine Thy1 promotor. Five genetic mutations in the hAPP and the PSEN1 gene lead to a rapid and almost exclusive accumulation of A $\beta$ <sub>42</sub>, visible plaque formation as early as 2 months after birth, neuronal loss at the age of 9 months and measurable cognitive impairments starting at 4 to 6 months (Chin 2011; Fröhlich et al. 2013).

## 1.5 Aims of this thesis

### Part 1: Effect of monocytes on neurogenesis

A growing number of studies indicate that the gut microbiome is able to influence immune homeostasis. Moreover, the immune system has been found to affect neurogenesis. Associating these findings with recent studies linking gut flora alterations to neuropsychiatric diseases, we aimed to investigate the following questions:

- I. How does manipulation of the gut flora affect neurogenesis levels in mice?

In addition, if any change occurs, the subsequent aim was:

- II. How does the immune system signal from the gut to the CNS?

### Part 2: Role of monocytes in AD

Given the robust recruitment of monocytes to the CNS upon chronic *T. gondii* infection in mice, we investigated the two following questions:

- III. How is *T. gondii* infection involved in the etiology of AD in mice?
- IV. How does the recruitment of Ly6C<sup>hi</sup> monocytes upon chronic infection influence  $\beta$ -amyloidosis?

## 2 Materials and Methods

### 2.1 Animal models

The animals were handled according to governmental (LaGeSo) and internal (University of Magdeburg/MDC/Charité) rules and regulations. All mice were kept under a 12 hour light/dark cycle with 2-6 mice per cage and had access to food and water ad libitum.

#### 2.1.1 Wildtype mice (part 1)

Female C57BL/6 wildtype mice for each individual experimental were randomly assigned to the different treatment groups and experiments were repeated independently two to three times. We need to emphasize, that not all treatment groups were included in each of the independent experiments. However, necessary control groups were always included.

#### 2.1.2 CCR2<sup>-/-</sup>

CCR2<sup>-/-</sup> mice and their heterozygote and wildtype littermates were housed and treated under SPF conditions in the animal facilities of the Cleveland Clinic, Cleveland Ohio, USA according to the governmental and federal law and recommendation.

#### 2.1.3 5xFAD

Experiments were conducted with 8 weeks old C57BL/6J mice and female and male 5xFAD mice (5xFAD/Tg6799 strain (B6SJL-Tg(APPswF1L<sub>on</sub>, PSEN1\*M146L\*L286V)6799Vas/Mmjax backcrossed for >10 generations to C57BL/6J, JAX stock#006554) (Oakley et al. 2006; Teipel et al. 2011). In this model, A $\beta$  plaques in the brain are detectable from the age of 50 days and their number increases by age (Fröhlich et al. 2013). At least five animals per group in up to two independent experiments were used.

#### 2.1.4 *T. gondii* infection

*T. gondii* cysts of the ME49 type II strain were used for this study. Parasites were harvested from the brains of female NMRI mice strain infected intraperitoneally (i. p.) with 10 *T. gondii* cysts 5 to 10 months earlier. Brains obtained from infected mice were mechanically homogenized in 1 mL sterile phosphate-buffered saline (PBS) and the cysts counted using a light microscope. If not stated otherwise, two cysts were administered i. p. into 8-week-old mice in a total volume of 200  $\mu$ L. This time point was chosen because at the age of 8 weeks,

animals are fertile and are considered adults in this respect. At the chronic stage of infection (8 weeks post infection and 4 weeks post infection for depletion and phagocytosis assays, see below), mice were sampled.

## 2.2 Experimental design & procedures

### 2.2.1 Antibiotic and probiotic treatment

Since commensals are required for normal development especially of the immune and nervous system, we used a model of antibiotic induced dysbiosis according to the protocol published previously (Heimesaat et al. 2006). The antibiotic compounds were applied via the drinking water for 7 weeks and consisted of ampicillin plus sulbactam (1.5 g/L; Pfizer), vancomycin (500 mg/L; Cell Pharm), 0.5 mg/L ciprofloxacin (200 mg/L; Bayer Vital), imipenem plus cilastatin (250 mg/L; MSD), and metronidazol (1 g/L; Fresenius). 72 h before gut flora reconstitution, the antibiotic treatment was discontinued and replaced by sterile tap water. Then antibiotic-treated mice were per orally challenged with a 300µL of fecal transplant by gavage on two consecutive days. The fecal transplant constituted of a mixture from 1 mg feces of 3 different naïve SPF mice dissolved in 15ml PBS. In parallel to the fecal transplants, the Abx plus probiotics group received VSL#3<sup>®</sup> (Sigma-Tau Pharmaceuticals, Inc. Gaithersburg, MD) probiotics orally by gavage on two consecutive days. VLS#3 is a commercially available probiotic mixture consisting of 8 bacterial strains: *Streptococcus thermophilus*, *Bifidobacterium breve*, *Bifidobacterium longum*, *Bifidobacterium infantis*, *Lactobacillus acidophilus*, *Lactobacillus plantarum*, *Lactobacillus paracasei*, *Lactobacillus delbrueckii subsp. Bulgaricus*. We dissolved a total of  $4.5 \times 10^9$  probiotics into 10 mL PBS. By gavaging 300 µl, each mouse received approximately  $1 \times 10^7$  probiotic bacteria.

### 2.2.2 Voluntary exercise

Mice with access to a running wheel were housed in pairs to avoid single housing, which can result in social deprivation that has an impact on neurogenesis per se. We glued a small magnet at the bottom rim of the wheels and monitored the rotations using a cycling computer during the active phase from 6pm – 8am. Knowing the diameter of the wheel (17cm) we were able to calculate the distance the two mice ran per active phase. We monitored the running groups over 10 days and calculated an average distance for each group.

### 2.2.3 Adoptive transfer

Ly6C<sup>hi</sup> monocytes were isolated from the bone marrow of C57BL/6 mice using FACS sorting for adoptive transfer. 10<sup>6</sup> Ly6C<sup>hi</sup> monocytes were injected into the tail vein of adult female C57BL/6 antibiotic-treated mice. The procedure was repeated 48 h later followed by BrdU injections.

### 2.2.4 Monocyte depletion in non-infected wildtype mice

Depletion of monocytes with 75 µg/injection anti-CCR2 monoclonal antibody (MC-21, kindly provided by M. Mack, University of Regensburg) and neutrophil granulocytes with 440 µg/injection anti-Ly6G monoclonal antibody (1A8, BioXCell) was started on d0 by i. p. injection of the respective antibody in 300µL PBS. BrdU was injected on d1 - d3. Antibody injections were continued every third day until d20 and animals were sacrificed on d21. Control animals received 75 µg polyclonal rat IgG (BioXCell).

### 2.2.5 Monocyte ablation in *T. gondii* infected 5xFAD mice

To specifically ablate CCR2<sup>+</sup>Ly6C<sup>hi</sup> monocytes, 66 µg of anti-CCR2 antibody (clone MC-21, kindly provided by M. Mack, University of Regensburg) were administered i. p. on d15, d18, d21, d24 and d27 post infection. Control mice received PBS. On d22 (12-15h post antibody injection), blood was collected retro-orbitally to confirm depletion. Mice were sacrificed and samples were collected on d28.

## 2.3 Organ collection

For organ sampling, mice were deeply anesthetized and if necessary blood was drawn from the inferior vena cava using a 26 G needle and syringe. Subsequently, mice were perfused intracardially with 60 mL sterile ice-cold PBS. The required organs were removed and prepared accordingly for further analysis.

## 2.4 Nucleic acid isolation

After removal, tissue samples from brains were immediately transferred to RNA later (QIAGEN, Germany). They were kept at 4 °C for at least 24 h and then stored at -20 °C until RNA isolation. For total RNA isolation, the tissue was removed from RNA later and homogenized with 1mL of TriFast (peqGOLD, Erlangen, Germany) in BashingBeads tubes (Zymo Research, Freiburg, Germany). PeqGOLD HP Total RNA Kit was used for purification and manufacturer's instructions were followed. On-membrane DNase I digestion

(peqGOLD, Erlangen, Germany) was performed and RNA purity and concentration was determined by absorbance at 230, 260 and 280 nm in a NanoDrop (Fisher Scientific, Germany).

## **2.5 Real Time Polymerase Chain Reaction (RT-PCR)**

### **2.5.1 RT-PCR from whole-brain homogenates**

Relative gene expression was determined similar to previous descriptions (Möhle et al. 2014; Bereswill et al. 2014) using TaqMan<sup>®</sup> RNA-to-C<sub>T</sub><sup>™</sup> 1-Step Kit (life technologies, Germany). Reactions were developed in a LightCycler<sup>®</sup> 480 Instrument II (Roche, Germany). Reverse transcription was performed for 15min at 48°C followed by 10min at 95°C. Subsequently, 45 amplification cycles were run, comprising of denaturation at 95°C for 15sec and annealing/elongation at 60°C for 1min. TaqMan<sup>®</sup> Gene Expression Assays (life technologies, Germany) were used for mRNA amplification of APP (Hs00169098\_m1), BDNF (Mm04230607\_s1), HPRT (Mm01545399\_m1), IDE (Mm00473077\_m1), IFN- $\gamma$  (IFNG, Mm00801778\_m1), IL-1 $\beta$  (IL1B, Mm00434228\_m1), IL-6 (IL6, Mm00446190\_m1), IL-10 (IL10, Mm00439616\_m1), MMP9 (Mm00442991\_m1), NEP (MME, Mm00485028\_m1), NGF (Mm00443039\_m1), TGF- $\beta$  (TGFB1, Mm01178820\_m1) and TNF (Mm00443258\_m1). HPRT mRNA expression was chosen as reference for normalization and target/reference ratios were calculated with the LightCycler<sup>®</sup> 480 Software release 1.5.0 (Roche, Germany). Resulting data were further normalized to values of appropriate control groups.

### **2.5.2 RT-PCR from sorted cell populations**

Isolated brain single cell suspensions were surface stained as described below and sorted on a BD FACSAria<sup>™</sup> III. After sorting, cells were pelleted, any remaining liquid was removed and cells were frozen at -80°C. Total RNA was isolated using the RNeasy<sup>®</sup> Mini Kit (QIAGEN, Germany). cDNA was synthesized with the iScript<sup>™</sup> cDNA Synthesis Kit (BIO-RAD, Germany). Relative gene expression was measured using the TaqMan<sup>®</sup> Universal PCR Master Mix (Applied Biosystems, Germany). TaqMan<sup>®</sup> Gene Expression Assays (life technologies, Germany) and data analysis was the same as for RT-PCR from whole-brain homogenates.

## 2.6 Protein extraction

For protein extraction, freshly harvested brain tissue was snap-frozen in liquid nitrogen and stored at -80 °C until further purification.

### 2.6.1 Total $\beta$ -amyloid

For isolation of total  $\beta$ -amyloid<sub>42</sub> ( $A\beta_{42}$ ), one hemisphere was homogenized in 1.5 mL 5 M guanidine hydrochloride (GuHCl) buffer (5M GuHCl in 50mM Tris/HCl, pH 8.0) using an Ultra-Turrax<sup>®</sup> T8 (IKA, Germany). Afterwards, homogenates were shaken at 150 U/min for 4 h at room temperature (RT) and then stored at -20 °C for analysis. Prior to ELISA analysis, samples were diluted in PBS (without  $Ca^{2+}$  and  $Mg^{2+}$ ) containing 5 % bovine serum albumin, 0.03 % Tween-20 and protease inhibitor (Roche, Germany) and centrifuged at 16000 rpm for 20 min. The supernatant was further used as described in chapter 2.7.

### 2.6.2 Carbonate buffer and guanidine soluble $A\beta$

To discriminate between small (carbonate buffer soluble) and large (guanidine soluble)  $A\beta_{42}$  aggregates, 20mg brain homogenate were homogenized in 400  $\mu$ l carbonate buffer (100 mM  $Na_2CO_3$  in 50 mM NaCl, pH 11.5) including protease inhibitor (Roche, Germany) and centrifuged at 14000 rpm for 20 min. The supernatant was adjusted with 8.2 M GuHCl in 82 mM Tris/HCl (0.6ml GuHCl/1ml carbonate buffer), again centrifuged at 14000 rpm for 20 min and stored at -20 °C until further analysis. The pellet from the first centrifugation step was dissolved in 160  $\mu$ L 5 M GuHCl in 50 mM Tris/HCl, shaken at 1500 rpm for 3 h at RT and also centrifuged at 14000 rpm for 20 min. The supernatant was stored at -20 °C until further analysis as described in chapter 2.7.

## 2.7 ELISA

$A\beta_{42}$  was quantified in whole brain hemispheres by ELISA against human  $A\beta_{42}$  (Thermo Fisher Scientific, Germany). Prior to ELISA analysis, each extract (total, soluble and insoluble) was diluted with BSAT-PBS (5% bovine serum albumin in PBS with 0.03% Tween-20 and protease inhibitor (Roche, Germany)) according to the expected  $A\beta_{42}$  content. ELISA was then performed according to the manufacturer's instructions.



## **2.8 Immunohistology**

### **2.8.1 Analysis of BrdU-labeling and co-labeling**

#### **2.8.1.1 BrdU treatment**

For the analysis of cell proliferation and survival, the animals received i. p. injections of 50 µg BrdU (Sigma-Aldrich)/g body weight at a concentration of 10 mg/mL BrdU in sterile 0.9 % NaCl solution for three consecutive days and were examined four weeks later (if not stated otherwise). Please note that the BrdU injections for our experiments were performed in different labs (University of Magdeburg, Charité Berlin or Cleveland Clinic, Ohio). Despite keeping protocols and substances similar across labs, individual injection techniques and volumes account for differences in baseline BrdU cell numbers. Thus, we always included a matching control group in each individual experiment and one should not compare baseline BrdU numbers across experiments.

#### **2.8.1.2 Immunolabeling**

Brains were cryopreserved in 30 % sucrose overnight, rapidly frozen in dry ice and mounted onto a sliding microtome. 40 µm thick sections were collected into cryoprotecting buffer (25 % glycerol, 25 % ethylenglycol in 0.05 M PBS). Before immunolabeling, sections were washed with PBS and blocked by incubation on a shaker in 0.6 % H<sub>2</sub>O<sub>2</sub> (in PBS) for 30 min at RT. For BrdU labeling, sections were treated with 2 N HCl for 30 min at 37 °C and with 0.1 M borate buffer for 10 min at RT. The sections were again washed and incubated in blocking buffer (3 % donkey serum, 0.1 % TritonX100) for 1 h for permeabilization. The sections were then incubated overnight at 4 °C with the primary antibody (rat BrdU, 1:500, Biozol, Germany; goat Dcx, 1:200, Santa Cruz Biotechnology; mouse NeuN, 1:100, Millipore). Sections were washed and blocked for 30 min. For 3,3'-Diaminobenzidine (DAB)-staining, the slices were incubated for 2 h in the secondary antibody (anti rat Biotin-SP-conjugated, Dianova, at RT). After washing, the third antibody was incubated for 1 h (HRP-conjugated streptavidin, Dianova, at RT), following detection via DAB. The reaction was stopped with water. For immunofluorescence labeling, the slices were labeled by incubation with a fluorophore-labeled antibody (anti goat Alexa488, anti-mouse Cy5, and anti-rat Cy3, all 1:250, Dianova).

### 2.8.1.3 Confocal microscopy

For confocal microscopy we used a Leica SPE microscope (Leica microsystems, Germany) with appropriate gain and black level settings (determined on control tissues stained with secondary antibodies alone). Images were recorded as z-stacks and analyzed using Volocity LE software (PerkinElmer).

### 2.8.1.4 Cell counting and unbiased stereology

Cell counts were determined in an unbiased approach using the optical fractionator procedure of the StereoInvestigator software (MBF Bioscience, USA) for every 6th brain section containing the hippocampus. The obtained cell number was multiplied by the number of slices analyzed, to calculate the number of BrdU<sup>+</sup> cells in the whole hippocampus. Since both hippocampi were counted, we used the total number of BrdU<sup>+</sup> cells per brain as a unit.

## 2.8.2 Immunohistological analysis

Brain hemispheres were removed and immersed in 4% paraformaldehyde (PFA) for several days. Paraffin-embedded, 4 µm thick sections were deparaffinized and conventionally stained with hematoxylin-eosin (H&E) stain. Immunohistochemical analysis was performed according to our previous publications (Fröhlich et al. 2013; Hofrichter et al. 2013; Pahnke et al. 2013; Schumacher et al. 2012; Scheffler et al. 2012; Schmidt & Pahnke 2012; Krohn et al. 2011) using a BOND-MAX (Leica Microsystems GmbH/Menarini, Germany) with antibodies against Aβ (clone 4G8, Chemicon, Germany), ionized calcium-binding adapter molecule 1 (IBA1, Wako 019-19741, Germany) to label microglia, glial fibrillary acid protein (GFAP, DAKO Z033401, Germany) to label astrocytes, NeuN (Millipore MAB377, Germany) to label neurons, and anti-Toxo (Dianova DLN-16734, Germany) to label *T. gondii*. Slides were developed using the Bond<sup>TM</sup> Polymer Refine Detection kit (Menarini/Leica, Germany). For the evaluation whole tissue sections were digitized at 230 nm resolution using a MiraxMidi Slide Scanner (ZeissMicroImaging GmbH, Germany) (Scheffler et al. 2011).

## 2.8.3 Immunofluorescence analysis

For immunofluorescent staining, coronal brain sections (16µm) were prepared with a cryomicrotome (Leica, Germany). Immunolabeling with antibodies against Aβ (4G8, Chemicon, Germany), Iba1 (polyclonal, Wako) and Ly6C (ER-MP20, Acris Antibodies, Germany) were performed overnight at 4°C after 2 min pretreatment with 98% formic acid. Secondary antibodies goat anti-rat (Alexa Fluor 488, 1:200, Invitrogen, Germany), goat anti-

rabbit (Alexa Fluor 488, Invitrogen, Germany) and goat anti-mouse (Alexa Fluor 594, Invitrogen, Germany) were used. Free floating sections were mounted with ProLong Gold with DAPI (life technologies, Germany). A Zeiss (Carl Zeiss, Germany) microscope equipped with an AxioCam HRc 3 digital camera and AxioVision 4 Software were used to analyze staining and obtain images.

Quantification of Iba1 and Ly6C association with plaques was performed using the ImageJ plot profile function (<http://imagej.nih.gov/ij/>). For this purpose, two perpendicular fluorescence profiles spanning 400  $\mu\text{m}$  and centered over the plaques were measured in immunofluorescence stainings. At least 30 plaques from at least four different tissue sections were analyzed.

#### **2.8.4 Two-Photon image acquisition and analysis**

For *in vivo* staining of amyloid plaques, mice were i. p. injected with 10mg kg<sup>-1</sup> methoxy-X04 (Tocris Bioscience) in 5% DMSO/95% NaCl (0.9%) 12 hours before brain harvesting and two-photon image acquisition.

Brains were placed under microscopy coverslips for *ex vivo* microscopy using a Zeiss LSM 710 (Carl Zeiss, Jena, Germany) equipped with a MaiTai DeepSee 2-Photon laser (Spectra-Physics, Darmstadt, Germany) tuned at 800nm. Fluorescence emission was split using a dichroic mirrors and detected using non-descanned detectors. Methoxy-X04 fluorescence was read out at 450-490nm. Fluorescence signal acquired above 520nm was considered autofluorescence. Confocal stacks spanning at least 50 $\mu\text{m}$  were collected with a z-spacing of 4 $\mu\text{m}$  using a W Plan-Apochromat 20x water immersion objective with a numerical aperture of 1.0.

Images were processed and superimposed using the Imaris (Version 7.7., Bitplane, Zürich, Switzerland) software. Methoxy-X04-positive objects co-localizing with blood vessels (identified by different tissue autofluorescence) were manually excluded from the analysis. Plaques were automatically detected and quantified in three dimensions using the measurement package of the Imaris software.

## **2.9 Primary cell isolation**

### **2.9.1 Brain**

For mononuclear cell isolation brains were homogenized in a buffer containing 1 M HEPES pH 7.3 and 45 % Glucose and then sieved through a 70  $\mu$ m strainer as published previously (Möhle et al. 2014). The cell suspension was washed and re-suspended in 10 mL 75 % Percoll (GE Healthcare, Germany) in PBS and overlaid with 10 mL 25 % Percoll in PBS and 5 mL PBS. The gradient was centrifuged for 45 min at 800 g without brake. Cells were recovered from the 25 %/75 % interphase, washed and used immediately for further experiments.

### **2.9.2 Blood, bone marrow**

Blood from the inferior vena cava was diluted in FACS buffer. To obtain the bone marrow, femur and tibia were isolated and surrounding tissue was removed. The proximal and distal ends were removed and a syringe with a 26 G needle attached was inserted to wash out bone marrow cells with FACS buffer.

The cell suspensions were spun down (400 g, 10 min, 4°C) and after carefully discarding the supernatant, lysis of erythrocytes was performed in 1 mL RBC lysis buffer (eBioscience, Germany) for 8 min on ice. After washing with PBS, cells were ready for further analysis.

## **2.10 Flow cytometry**

### **2.10.1 Surface staining**

Single cell suspensions were incubated with an anti-Fc $\gamma$ III/II receptor antibody (clone 93) to block unspecific binding and Zombie Violet<sup>TM</sup> (Biolegend, Germany), a fixable viability dye. Thereafter, cells were stained with fluorochrome conjugated antibodies against cell surface markers: CD45 (1:200, 30-F11, eBioscience, Germany), CD11b (1:333, M1/70, eBioscience, Germany), Ly6G (1:100, 1A8, BD Biosciences, Germany), Ly6C (1:333, HK1.4, eBioscience, Germany), MHC I (1:200, 28-14-8, eBioscience, Germany), MHC II (1:200, M5/114.15.2, eBioscience, Germany), CD11c (1:333, N418, eBioscience, Germany), F4/80 (1:100, BM8, eBioscience, Germany), CCR2 (1:33, 475301, R&D, USA), TREM2 (1:33, 237920, R&D, USA), CD36 (1:100, HM36, Biolegend, Germany), in FACS buffer (PBS containing 2% FCS and 0.1% NaN<sub>3</sub>) for 30 min on ice and then washed and fixed in 4% paraformaldehyde (PFA) for 10 min.

### **2.10.2 Conventional flow cytometry**

Cell acquisition was performed on BD FACS Canto™ II flow cytometer. Data were analyzed using FlowJo software (TreeStar).

### **2.10.3 Imaging flow cytometry**

Data were acquired with FlowSight™ (EMD Millipore, USA) with a 20x objective and analyzed using IDEAS software version 6.0. At least 52,000 (control animals) or 500,000 (*T. gondii* infected animals) cells were acquired for each sample and gated to select images with single cells in good focus (by bright field area/aspect ratio and gradient root mean square of the bright-field image, respectively). To analyze internalization, the erode mask was used on the bright field picture of A $\beta$ <sup>+</sup> cells to remove 2 pixels from the edges of the starting mask and to define the inner part of the cell. Then, the internalization feature was used to define the ratio of intensity of the A $\beta$  signal between the inside of the cells (defined by the erode mask) and the intensity of the total cell. While cells with little internalization have negative scores, cells with high internalization have positive scores. Here, an internalization > 0 was defined as intermediate to high internalization. Compensation matrix generated by single-color compensation controls was used to correct spectral overlap. Representative pictures from cell populations were chosen.

### **2.11 Ex vivo phagocytosis assay**

Animals were sacrificed 4 weeks post infection and single cell suspensions were prepared as described above. Live cells remained unstained by the Zombie Violet™ (Biolegend, Germany) viability dye and were sorted on a BD FACSAria™ III. 150,000 cells were seeded into each well of a 96-well round bottom plate and allowed to settle down for 1 hour in an incubator (37°C, with 5% CO<sub>2</sub> and 70% humidity) before HiLyte Fluor™ 488-labeled, HFIP monomerized A $\beta$ <sub>42</sub> (Eurogentec, Belgium) was added to a final concentration of 500nM. Cells were incubated for 6 hours, washed, surface stained and measured by conventional and imaging flow cytometry.

### **2.12 Statistical analysis**

Statistical analysis was performed with Prism version 6 (GraphPad Software, USA). *p* values of *p* ≤ 0.05 were considered statistically significant.

### **2.12.1 Statistical analysis of results for part 1 (Neurogenesis)**

Before we started statistical analysis, we tested for normality with a normality probability plot. For parametric data we used for all neurogenesis analysis: two-way ANOVA, with Bonferroni post hoc and for the FACS analysis either one-way ANOVA followed by a Fisher's LSD test or unpaired two-tailed Student's t test. When we tested with the F test, similar variances were detected in the groups included in the test. Significances are depicted in the respective figure legends as mean + standard error of the mean (SEM). We performed Dixons Test for single outlier, but did not detected outliers in our data set. When we sacrificed the animals, we prepared a list with animal IDs. We prepared the specimens for further analysis and coded the samples in order to do a blind analysis afterwards. The investigator who analyzed the samples was blind to the animal's treatment group.

### **2.12.2 Statistical analysis of results for part 2 (Alzheimer's disease)**

Results are presented as mean + SEM. Different tests were used to compare values, namely Mann-Whitney U test (plaque numbers and volume), Fisher's LSD test (results with multiple comparisons) and unpaired two-tailed Student's t test (results with one comparison).  $p$  values of  $p \leq 0.05$  were considered statistically significant.

## 3 Results

### 3.1 Role of monocytes in neurogenesis

The work presented in the first part of the results has been performed in collaboration with the research group of Dr. Susanne Wolf (MDC Berlin), where neurogenesis levels were determined by BrdU immunolabeling and analyses.

#### 3.1.1 Antibiotic treatment decreases adult hippocampal neurogenesis

Adult C57BL/6 mice were treated with broad-spectrum antibiotics (Abx) for seven weeks, which has been shown previously to eliminate the intestinal microbiota (Heimesaat et al. 2006). In these antibiotic-treated mice, we labeled proliferating cells by injection of BrdU, a thymidine analog that is incorporated into the DNA during cell replication. Analysis of the hippocampi was performed four weeks after BrdU injections (Kempermann & Gage 2000), to analyze the survival of generated neurons (i. e. net neurogenesis). Proliferated cells were further characterized based on their expression of the phenotypical markers Dcx and NeuN. Dcx labels the majority of proliferating mitotic neuronal progenitor cells and marks the time point of commitment to the neuronal lineage, while NeuN is expressed by mature neurons. In this thesis, I will present the basic quantification of BrdU<sup>+</sup> cells, the full phenotyping will be available in the publication.

In immunofluorescence labeled brain sections including the hippocampus we detected that the number of BrdU<sup>+</sup> cells in the SGZ of the DG was significantly lower in the brains of antibiotic-treated (Figure 3.1A and B, light blue bars) compared to naïve SPF mice (Figure 3.1A and B, light grey bars). These first data suggest that antibiotic treatment has a long lasting effect on neurogenesis.

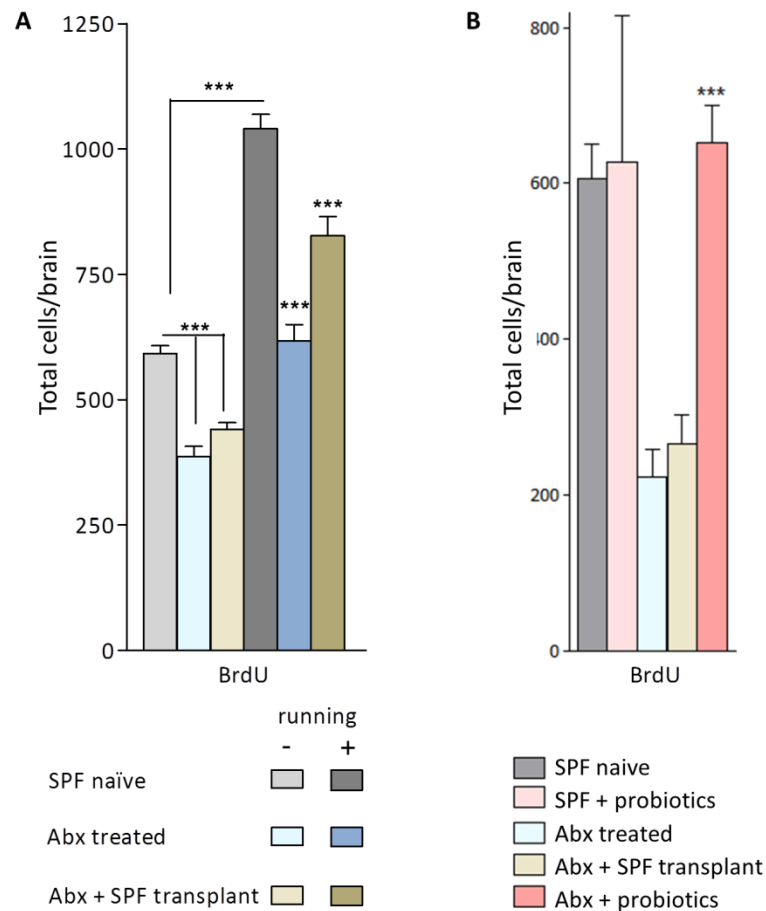


**Figure 3.1: Reduced neurogenesis in antibiotic-treated mice can be partially restored by running.**

(A) The total number of BrdU<sup>+</sup> cells was quantified from naïve SPF mice or SPF mice treated with antibiotics (Abx treated). One group of mice received a fecal transplant (Abx + SPF transplant), and half the mice in each group were given access to a running wheel (darker bars, running +). Two-way ANOVA with Bonferroni post hoc test. \*\*\*p<0.001.

(B) The total number of BrdU<sup>+</sup> cells normalized after probiotic treatment. Two-way ANOVA with Bonferroni post hoc test. \*\*\*p<0.001.

### 3.1.2 Running rescues neurogenesis levels despite antibiotic

Many factors have been shown to influence neurogenesis, such as sex, drugs, stress, diet and physical activity (reviewed in Ming & Song 2005). Amongst these, we were particularly interested in the effect of physical activity, because exercise is easily available for patients, e. g. antibiotic-treated individuals. To test if physical exercise affects neurogenesis, especially in antibiotic-treated mice, we supplied mice with running wheels for ten days during the treatment, injected BrdU for the last three days of exercise and assessed neurogenesis four weeks later. Exercise duration was similar across all groups, covering a distance of 0.28±0.05 km/day. Access to running wheels significantly increased neurogenesis by 44 % in naïve SPF mice (Figure 3.1A, dark grey bar). In antibiotic-treated mice, the beneficial effect



of exercise was less pronounced and neurogenesis was only increased by 28 % (Figure 3.1A, dark blue bar). After reconstitution of the intestinal flora with a fecal transplant, exercise increased neurogenesis levels again by 47 % (Figure 3.1A, dark brown bar) similar to its effect on naïve SPF mice.

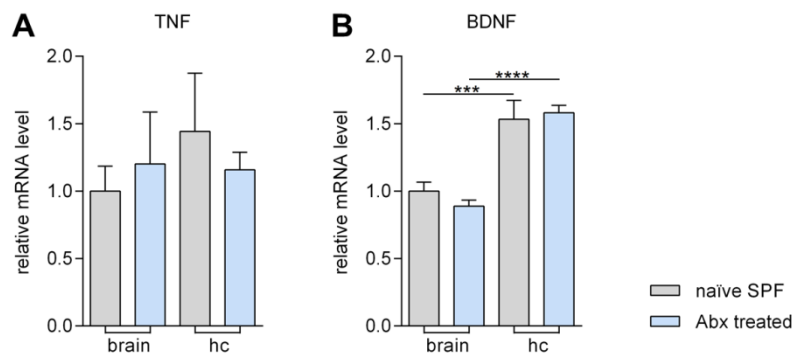
### **3.1.3 Probiotics fully restore neurogenesis**

After observing the significant reduction of neurogenesis accompanying gut microbiota depletion, we were interested if reconstitution with a complex gut flora rescues neurogenesis. To this end, mice received a fecal transplant from naïve SPF mice two days after discontinuation of the antibiotic treatment. After allowing the flora to settle for seven days, we injected BrdU and analyzed neurogenesis levels four weeks later. Even though the intestinal flora was restored in mice by the SPF transplant (data not included in this thesis), this recovery had little effect on the hippocampal neurogenesis (Figure 3.1A and B, light brown bars). Another group of antibiotic-treated mice received VSL#3 probiotics instead of an SPF transplant. In these probiotic-treated mice, the number of proliferated cells was back to naïve SPF levels (Figure 3.1B, dark red bar). Control treatment of naïve SPF mice with probiotics did not increase neurogenesis (Figure 3.1B, light red bar). These results indicate that the impairment of neurogenesis by antibiotic treatment can only be restored by treatment with probiotics and not with conventional SPF flora.

### **3.1.4 Expression of soluble mediators in the brain remains unaltered upon changes of the intestinal flora**

Soluble mediators contribute to brain homeostasis including neurogenesis. Among others, TNF (Iosif et al. 2006) and BDNF (Scharfman et al. 2005; Rossi et al. 2006) were reported to directly influence neurogenesis.

*TNF* mRNA expression as measured by RT-PCR was the same in whole-brain and hippocampus extracts and remained unchanged upon treatment with antibiotics (Figure 3.2A; brain: naïve SPF  $1.0 \pm 0.1$ , Abx treated  $0.9 \pm 0.05$ ; hippocampus: naïve SPF  $1.6 \pm 0.05$ , Abx treated  $1.5 \pm 0.1$ ). While *BDNF* mRNA expression was significantly higher in the hippocampus than in the rest of the brain, antibiotic treatment did not influence its expression in the whole brain or in the hippocampus alone (Figure 3.2B; brain: naïve SPF  $1.0 \pm 0.2$ , Abx treated  $1.2 \pm 0.4$ ; hippocampus: naïve SPF  $1.2 \pm 0.1$ , Abx treated  $1.4 \pm 0.4$ ).

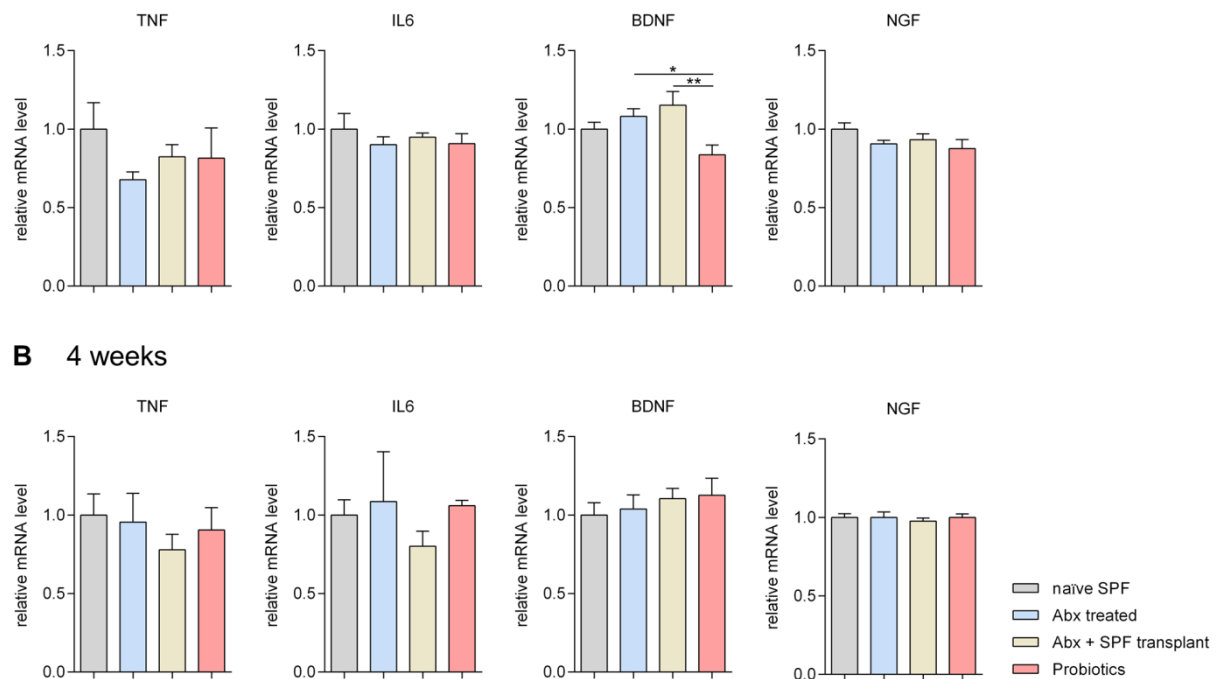


**Figure 3.2: Expression of TNF and BDNF in whole-brain and hippocampus**

Four weeks after antibiotic treatment, total RNA was isolated from either one whole hemisphere (brain) or from the hippocampus only (hc). Relative expression of *TNF* and *BDNF* mRNA was measured by RT-PCR. Data are normalized on the naïve SPF group (brain) and presented as mean + SEM. Statistical analysis was performed using Fisher's LSD test. \*\*\* $p < 0.001$ , \*\*\*\* $p < 0.0001$ .

Extending the investigation of soluble factors, we measured the expression of *TNF*, *IL-6*, *BDNF* and *NGF* mRNA at two time points after reconstitution of the intestinal flora. Since we had not seen differences restricted to the hippocampus in our previous analysis, we conducted the experiment with whole-hemisphere extracts.

We did not detect differences regarding the expression of the immune mediators *TNF* and *IL-6* both one and four weeks after reconstitution in any of the treatment groups (Figure 3.3A and B; *TNF* one week – SPF naïve  $1.0 \pm 0.2$ , Abx treated  $0.7 \pm 0.05$ , Abx + SPF transplant  $0.8 \pm 0.1$ , probiotics  $0.8 \pm 0.2$ ; *TNF* four weeks – SPF naïve  $1.0 \pm 0.1$ , Abx treated  $1.0 \pm 0.2$ , Abx + SPF transplant  $0.8 \pm 0.1$ , probiotics  $0.9 \pm 0.1$ ; *IL-6* one week – SPF naïve  $1.0 \pm 0.1$ , Abx treated  $0.9 \pm 0.05$ , Abx + SPF transplant  $0.9 \pm 0.03$ , probiotics  $0.9 \pm 0.06$ ; *IL-6* four weeks – SPF naïve  $1.0 \pm 0.1$ , Abx treated  $1.1 \pm 0.3$ , Abx + SPF transplant  $0.8 \pm 0.1$ , probiotics  $1.1 \pm 0.03$ ). Similar results were obtained for the expression of *BDNF* and *NGF* (Figure 3.3A and B; *BDNF* one week – SPF naïve  $1.0 \pm 0.04$ , Abx treated  $1.1 \pm 0.05$ , Abx + SPF transplant  $1.2 \pm 0.09$ , probiotics  $0.8 \pm 0.06$ ; *BDNF* four weeks – SPF naïve  $1.0 \pm 0.08$ , Abx treated  $1.0 \pm 0.09$ , Abx + SPF transplant  $1.1 \pm 0.07$ , probiotics  $1.1 \pm 0.1$ ; *NGF* one week – SPF naïve  $1.0 \pm 0.04$ , Abx treated  $0.9 \pm 0.02$ , Abx + SPF transplant  $0.9 \pm 0.04$ , probiotics  $0.9 \pm 0.06$ ; *NGF* four weeks – SPF naïve  $1.0 \pm 0.02$ , Abx treated  $1.0 \pm 0.03$ , Abx + SPF transplant  $1.0 \pm 0.02$ , probiotics  $1.0 \pm 0.02$ ). Even though *BDNF* expression was significantly reduced in mice receiving probiotic treatment (compared to the Abx treated and Abx + SPF transplant groups) at one week after reconstitution, this returned to normal after four weeks of antibiotic-free time. Reduced *BDNF* expression would point towards lower neurogenesis levels, whereas we had observed higher levels in mice receiving probiotic treatment.

**A 1 week****Figure 3.3: Expression of inflammatory and neurotrophic mediators in the brain**

(A) One or (B) four weeks after reconstitution with an SPF transplant or probiotics, total RNA was isolated from whole-hemisphere homogenates. Relative expression of *TNF*, *IL-6*, *BDNF* and *NGF* mRNA was measured by RT-PCR. Data are normalized on the naïve SPF group and presented as mean + SEM. Statistical analysis was performed using Fisher's LSD test. \*p>0.05, \*\*p<0.01.

Taken together, none of the quantified soluble mediators explained the previously described changes in neurogenesis, as they all remained largely unaltered upon treatment with anti- or probiotics.

**3.1.5 Ly6C<sup>hi</sup> monocytes provide a link between brain, gut and treatment paradigms**

The neuronal associations between the gut and the brain are well known (Mayer 2011) and recent evidence suggests that both structures may be further linked by the immune system. Previous studies indicate that immune cells help to maintain neurogenesis levels (Wolf et al. 2009; Ziv et al. 2006). Interestingly, immune cells can be influenced by antibiotics (Morgun et al. 2015) as well as exercise (Shantsila et al. 2012). Therefore, we explored if mononuclear innate immune cells in the brain may act as a link between brain, gut and exercise.

We analyzed the immune cell subpopulations infiltrating the brain by flow cytometry. Mononuclear cells isolated from whole-hemisphere homogenates were stained for CD45, CD11b, Ly6G and Ly6C. Figure 3.4A illustrates the gating strategy for Ly6C<sup>hi</sup> monocytes in the brain: CD45<sup>int</sup> CD11b<sup>+</sup> microglia were discriminated from CD45<sup>hi</sup> CD11b<sup>+</sup> infiltrating

---

myeloid cells. Within the myeloid population we further separated Ly6G<sup>+</sup> neutrophils from Ly6C<sup>hi</sup> monocytes.

We detected that the percentage of Ly6C<sup>hi</sup> monocytes had dropped almost by half in antibiotic-treated mice compared to naïve SPF mice (Figure 3.4C, light grey and light blue bars; naïve SPF: 0.26±0.1%; Abx: 0.16±0.05 %). This decrease was also evident in bone marrow and blood, even one week after discontinuation of antibiotic treatment and transplantation of SPF flora (Figure 3.5B and E). Four weeks after transplantation of SPF flora, the number of Ly6C<sup>hi</sup> monocytes was back to the naïve SPF level in bone marrow and blood (Figure 3.5C and F).

Reconstitution of the intestinal flora with an SPF transplant did not rescue the Ly6C<sup>hi</sup> monocyte population in the brain (Figure 3.4C, light brown bar; 0.14±0.02 %). Reconstitution with probiotics on the other hand significantly increased the number of Ly6C<sup>hi</sup> monocytes in the brain (Figure 3.4C, dark red bar; 0.46±0.15 %). Similarly, exercise in the form of access to a running wheel increased the number of Ly6C<sup>hi</sup> monocytes in the brain of antibiotic-treated mice (Figure 3.4C, dark blue bar; 0.27±0.06 %). Of note, only exercise and not probiotic treatment could raise Ly6C<sup>hi</sup> monocyte numbers in naïve SPF mice.

We detected similar trends for the myeloid population, which in addition to Ly6C<sup>hi</sup> monocytes contains also Ly6G<sup>+</sup> neutrophils as well as the Ly6C<sup>int</sup> and Ly6C<sup>low</sup> populations (Figure 3.4B). The number of intrinsic microglia remained unaltered upon all experimental groups (Figure 3.4D).

Interestingly, the measured alterations in the Ly6C<sup>hi</sup> monocyte population matched the pattern we had previously observed for hippocampal neurogenesis levels. We found reduced Ly6C<sup>hi</sup> monocyte numbers as well as decreased neurogenesis levels in antibiotic-treated compared to naïve SPF mice. Correspondingly, the neurogenesis rescue by running or probiotic treatment (Figure 3.1) was paralleled by an increase in the Ly6C<sup>hi</sup> monocyte population found in the brain.

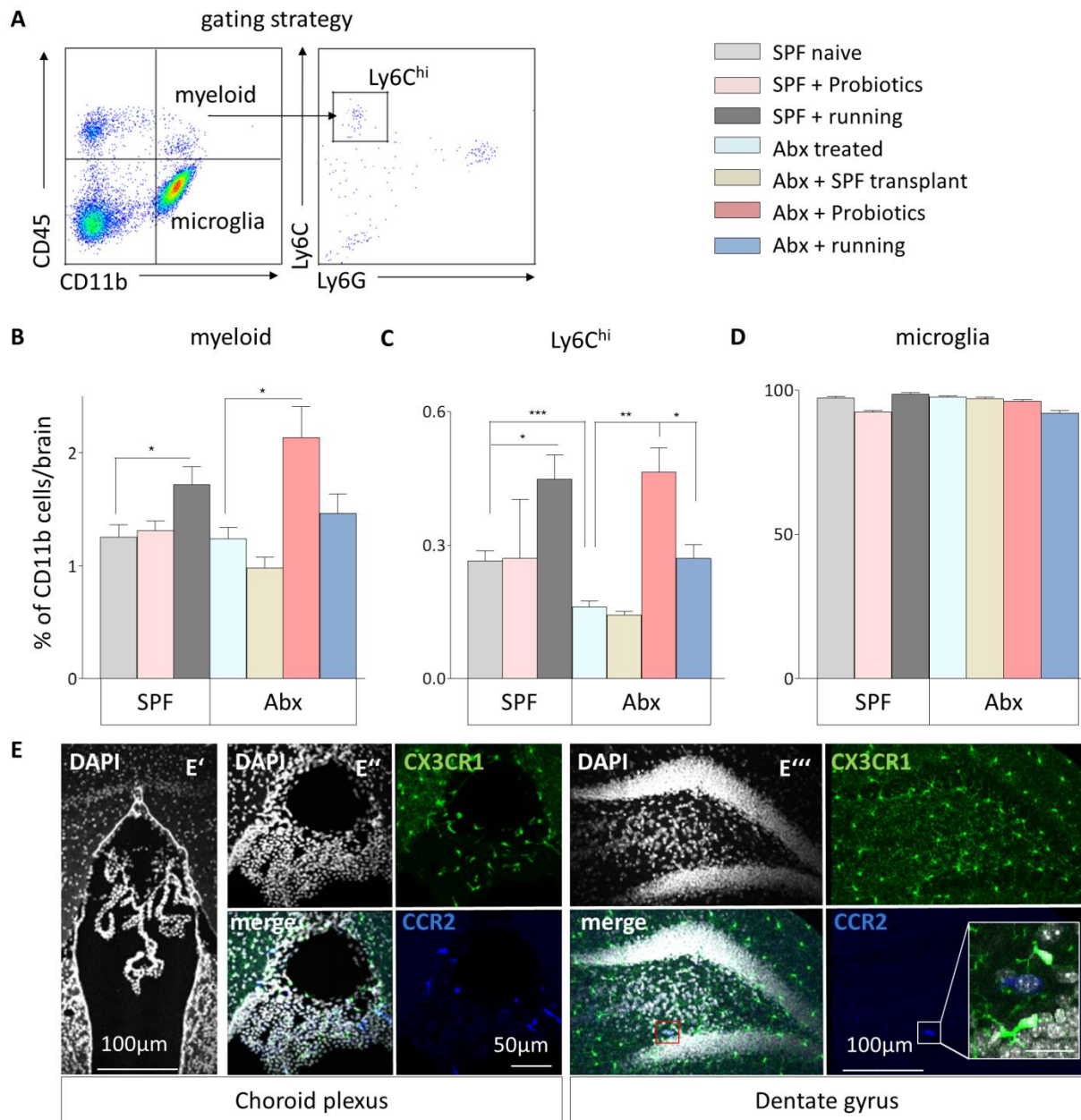


**Figure 3.4: The number of Ly6C<sup>hi</sup> monocytes is reduced in the brain of antibiotic-treated mice and is rescued by exercise but not by fecal transplant.**

(A) Cells isolated from brains were stained for CD45, CD11b, Ly6G and Ly6C for flow cytometric analysis. Representative pseudocolor plots demonstrate the gating strategy used to identify resident CD11b<sup>+</sup> CD45<sup>int</sup> microglia (lower right quadrant) and recruited CD11b<sup>+</sup> CD45<sup>hi</sup> myeloid cells (upper right quadrant). The right-hand plot displays how we separated Ly6G<sup>+</sup> neutrophils from Ly6C<sup>hi</sup> monocytes within the myeloid population.

(B-D) Bar graphs display the number of (B) total myeloid cells, (C) Ly6C<sup>hi</sup> monocytes, and (D) microglia in brain homogenates as percentage of CD11b<sup>+</sup> cells. Fisher's LSD test. \*p<0.05, \*\*p<0.01, \*\*\*p<0.001.

(E) To visualize the location of the Ly6C<sup>hi</sup> monocytes, we utilized a reporter for CCR2 (RFP) and CX3CR1 (EGFP). (E') Localization of the choroid plexus within the 3<sup>rd</sup> ventricle, cell nuclei stained with DAPI (white), 10x objective. (E'') Representative images of CCR2<sup>+</sup> cells (blue) in the choroid plexus (DAPI white) that are distinct from CX3CR1 expressing cells (green), 20x objective. (E''') Representative picture of a CCR2<sup>+</sup> cell (blue) in the hippocampus (DAPI white, CX3CR1 green), 20x objective. In the insert within the CCR2 single channel image we zoomed on the single CCR2 expressing cell with a 63x objective (merge of DAPI in white, CCR2 in blue and CX3CR1 in green).

## RESULTS

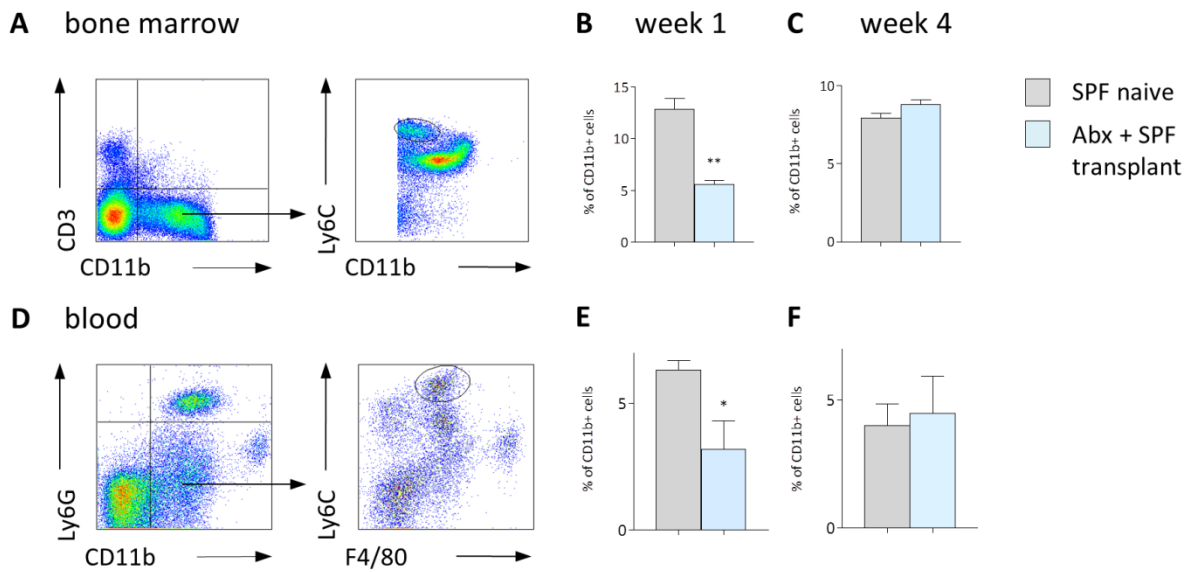


**Figure 3.5: Kinetics of the Ly6C<sup>hi</sup> monocyte populations in bone marrow and blood during gut reconstitution with SPF flora**

(A, D) Cells isolated from peripheral organs were stained against specific surface markers for flow cytometric analysis. Representative pseudocolor plots demonstrate the gating strategies used to identify Ly6C<sup>hi</sup> monocytes from (A) bone marrow and (D) blood. In (A) we gated for the CD3<sup>neg</sup>CD11<sup>pos</sup> population. In (D) we gated for the Ly6G<sup>neg</sup>CD11b<sup>pos</sup> population. The Ly6C<sup>hi</sup> population is gated in the right hand plots and quantified as a percentage of CD11b<sup>+</sup> cells.

(B) In the bone marrow, we found a lower proportion of Ly6C<sup>hi</sup> monocytes in Abx treated animals reconstituted with SPF flora compared to SPF naïve one week after discontinuation of Abx treatment.

(C) Four weeks after discontinuation of the Abx treatment and start of SPF fecal transplant, no differences in the proportion of Ly6C<sup>hi</sup> monocytes in the bone marrow were measured between the groups.

(E) In the blood, there were fewer Ly6C<sup>hi</sup> monocytes in Abx treated than in SPF naïve mice one week after discontinuation.

(F) Four weeks after discontinuation of the Abx treatment and start of SPF fecal transplant, the differences were no longer present and the same proportion of Ly6C<sup>hi</sup> monocytes was found in all experimental groups.

Unpaired two-tailed Student's t test. \*p<0.05, \*\*p<0.01.

Because the total number of Ly6C<sup>hi</sup> monocytes is very low in the non-inflamed, non-infected brain parenchyma, the previous analyses were performed with single cell solutions prepared from whole-hemisphere homogenates. In addition to the quantitative approach, we were interested in the location of Ly6C<sup>hi</sup> monocytes in the brain. Therefore, we used CCR2-RFP CX3CR1-eGFP reporter mice to visualize Ly6C<sup>hi</sup> monocytes and resident microglia. CCR2 has a substantial overlap with the Ly6C<sup>hi</sup> population and labels infiltrating monocytes, while in the brain, CX3CR1 is expressed exclusively by (brain-)resident microglia. We detected the majority of CCR2<sup>+</sup> cells in the choroid plexus (Figure 3.4E'), which has previously been described as an entrance gate for immune cells to the brain (Schwartz & Baruch 2014). Figure 3.4E'' shows representative images of CCR2<sup>+</sup> cells (blue) in the choroid plexus (DAPI-labeled

nuclei in white) that are distinct from CX3CR1 expressing cells (green). While CCR2<sup>+</sup> Ly6C<sup>hi</sup> monocytes are abundant in the brain parenchyma of infected mice (Möhle et al. 2014), we rarely detected them here in non-infected brains. Figure 3.4''' shows the hippocampus with a representative CCR2<sup>+</sup> cell (CCR2 blue, DAPI white, CX3CR1 green).

### 3.1.6 Lack of monocytes decreases neurogenesis

To determine whether altered Ly6C<sup>hi</sup> monocyte numbers were cause, effect or simply coincided with the rate of hippocampal neurogenesis, we used three different strategies to alter monocyte numbers: genetic depletion, antibody-induced depletion and adoptive transfer.

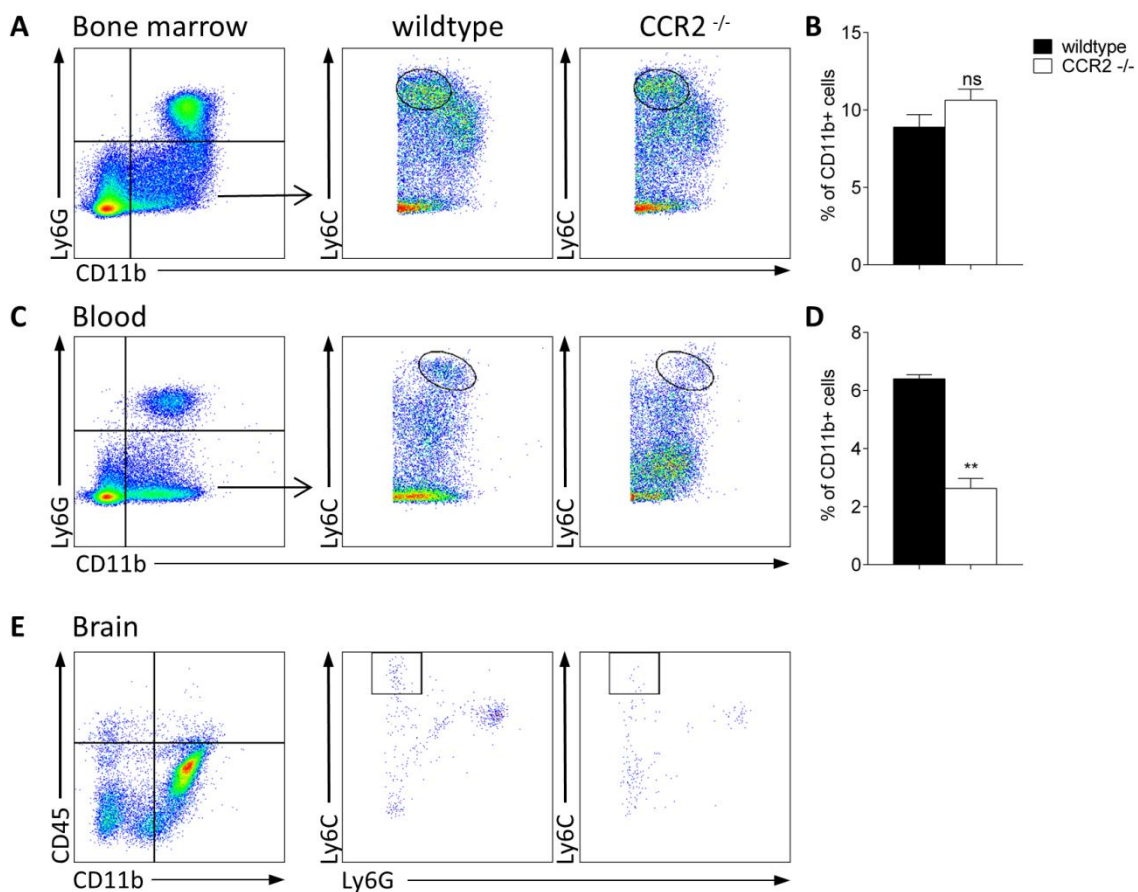


**Figure 3.6: Distribution of the Ly6C<sup>hi</sup> monocyte population in CCR2<sup>-/-</sup> mice.**

(A, C) Cells isolated from bone marrow and blood were stained against specific surface markers for flow cytometric analysis. Representative pseudocolor plots demonstrate the gating strategies used to identify Ly6C<sup>hi</sup> monocytes from (A) bone marrow and (C) blood of wildtype (middle plots) and CCR2<sup>-/-</sup> mice (right plots). First, CD11b<sup>+</sup> Ly6G<sup>-</sup> cells were gated (left plots), amongst which the Ly6C<sup>hi</sup> monocytes were then identified (middle and right plots).

(B, D) The number of Ly6C<sup>hi</sup> monocytes in all three tissues was quantified as percentage of CD11b<sup>+</sup> cells and is displayed as mean + SEM. n=2, unpaired two-tailed Student's t test. ns, not significant, \*\*p<0.01.

(E) Ly6C<sup>hi</sup> monocytes in the brain were identified as the CD45<sup>hi</sup> CD11b<sup>+</sup> Ly6G<sup>-</sup> population.

Genetic depletion was achieved by knocking out CCR2. Lack of this chemokine receptor prevents CCR2<sup>+</sup> Ly6C<sup>hi</sup> monocytes from exiting the bone marrow and consequently reduces their number in the periphery (Serbina & Pamer 2006). We confirmed the general presence of Ly6C<sup>hi</sup> monocytes in the bone marrow and their significantly decreased number in the periphery (Figure 3.6A-D).

We found significantly less Ly6C<sup>hi</sup> monocytes in the brains of CCR2<sup>-/-</sup> compared to wildtype mice (Figure 3.6E and Figure 3.7B). Likewise, CCR2<sup>-/-</sup> mice exhibited significantly decreased levels of adult hippocampal neurogenesis (Figure 3.7A). A direct effect of CCR2 on neurogenesis is unlikely, because neurogenesis remained unaltered in heterozygous CCR2<sup>+/-</sup> mice (Figure 3.7A).

Since it is unclear how the continuous absence of CCR2 may affect the development of brain and immune system, we utilized a second model in which we targeted Ly6C<sup>hi</sup> monocytes in adult mice. Injection of an anti-CCR2 monoclonal antibody (MC-21) specifically reduced the number of Ly6C<sup>hi</sup> monocytes in the brain (Figure 3.7B). In contrast to macrophages, monocytes have a relatively short life span of maximum three to five days in the blood (Whitelaw 1966; Yona et al. 2013). One day after the first antibody treatment, we injected BrdU and evaluated the effect of the depletion on neurogenesis levels three weeks later. Here we found that the treatment of naïve SPF mice with MC-21 led to a 25 % decrease in total BrdU<sup>+</sup> cells compared to IgG-treated controls (Figure 3.7A). The depletion of another subset of myeloid cells, namely Ly6G<sup>+</sup> neutrophils (Figure 3.7E), did not have any effect on neurogenesis levels and Ly6C<sup>hi</sup> monocyte numbers. Despite some alterations we have seen in the total myeloid population (Figure 3.4B), we can exclude a contribution of Ly6G<sup>+</sup> neutrophils in this case.

Together, these two depletion studies suggest that CCR2<sup>+</sup> Ly6C<sup>hi</sup> monocytes are necessary to maintain neurogenesis levels in the adult brain.



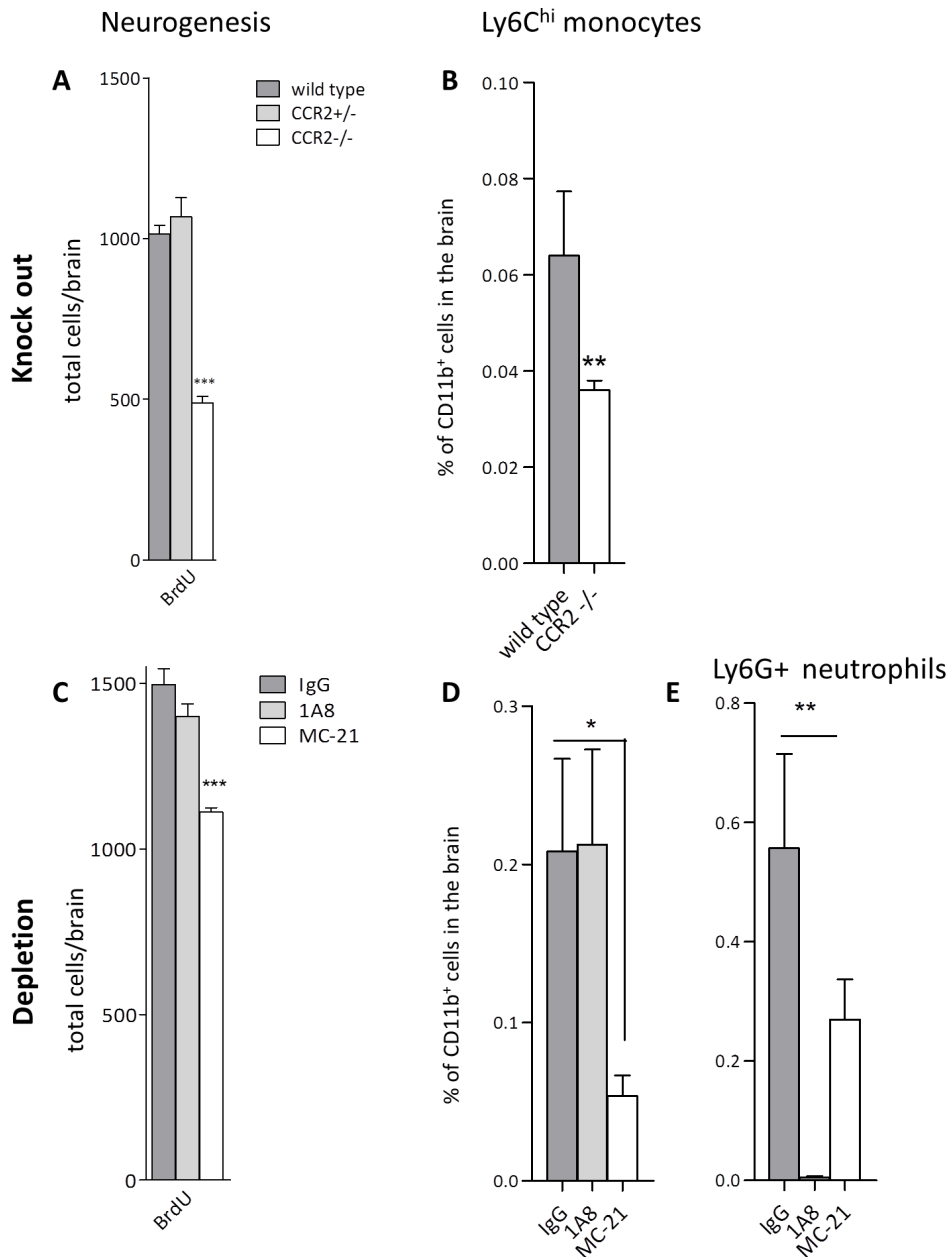


**Figure 3.7: Genetic absence or antibody-induced loss of CCR2<sup>+</sup>Ly6C<sup>hi</sup> monocytes results in decreased neurogenesis.**

(A, B) Adult female CCR2<sup>-/-</sup>, CCR2<sup>+/-</sup> and wildtype littermates were analyzed four weeks after BrdU injections.

(A) Neurogenesis was evaluated by counting BrdU<sup>+</sup> cells in the hippocampus. Two-way ANOVA, Bonferroni post hoc test. \*\*\*p<0.001.

(B) The decrease of Ly6C<sup>hi</sup> cells as a proportion of CD11b<sup>+</sup> cells in the brains of CCR2<sup>-/-</sup> animals compared to wildtype littermates was measured using a gating strategy as in Figure 3.6E. Unpaired two-tailed Student's t test. \*\*p<0.01.

(C, D) SPF naïve mice were injected with an anti-CCR2 antibody (MC-21) to deplete CCR2<sup>+</sup> Ly6C<sup>hi</sup> monocytes or an anti-Ly6G antibody (1A8) to deplete Ly6G<sup>+</sup> neutrophils.

(C) Neurogenesis was evaluated after three weeks of depletion by counting BrdU<sup>+</sup> cells in the hippocampus. Unpaired two-tailed Student's t test. \*\*\*p<0.001.

(D, E) The proportion of (D) Ly6C<sup>hi</sup> monocytes and (E) Ly6G<sup>+</sup> neutrophils in the brain was measured as a percentage of CD11b<sup>+</sup> cells using the gating strategy shown in Figure 3.6E. Unpaired two-tailed Student's t test. \*p<0.05, \*\*p<0.01.

### 3.1.7 Neurogenesis can be rescued by adoptive transfer of Ly6C<sup>hi</sup> monocytes to antibiotic-treated mice

To resolve whether the transfer of Ly6C<sup>hi</sup> monocytes can rescue neurogenesis in antibiotic-treated mice, we intravenously injected  $10^6$  Ly6C<sup>hi</sup> monocytes sorted from the bone marrow into antibiotic-treated mice, two and seven days after discontinuation of antibiotic treatment. 24 h after the first cell transfer, we started BrdU injections and analyzed the numbers of Ly6C<sup>hi</sup> monocytes as well as proliferating neurons three weeks later. Adoptive transfer of isolated bone marrow-derived Ly6C<sup>hi</sup> monocytes into antibiotic-treated mice significantly increased the number of Ly6C<sup>hi</sup> monocytes in the brain (Figure 3.8B). This rescue was paralleled by restored neurogenesis levels in antibiotic-treated mice which received a Ly6C<sup>hi</sup> monocyte transfer (Figure 3.8A). However, naïve SPF mice did not benefit from the adoptive transfer with respect to the Ly6C<sup>hi</sup> monocyte population in the brain and hippocampal neurogenesis levels. In conclusion, these results confirm that Ly6C<sup>hi</sup> monocytes are involved in the signaling between the periphery and the brain to restore neurogenesis.

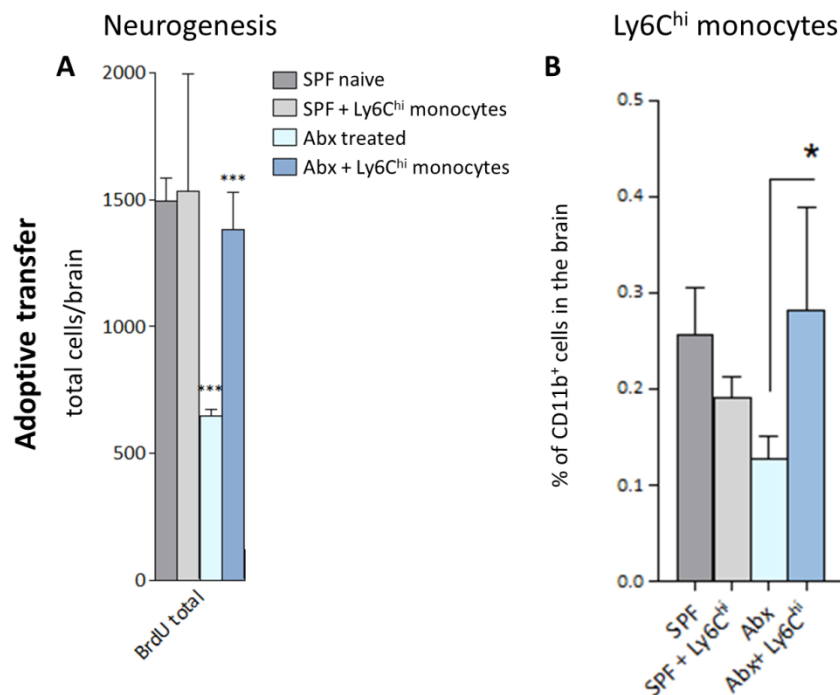


**Figure 3.8: Transfer of Ly6C<sup>hi</sup> cells into antibiotic-treated animals rescues neurogenesis.**

(A, B) Naïve SPF and antibiotic-treated mice were injected twice with freshly isolated FACS sorted Ly6C<sup>hi</sup> monocytes from the bone marrow. Proliferating cells were labeled with BrdU one day after the first adoptive transfer.

(A) BrdU<sup>+</sup> cells in the hippocampus were counted. Two-way ANOVA, Bonferroni post hoc test. \*\*\* $p < 0.001$ .

(B) Adoptive transfer of Ly6C<sup>hi</sup> monocytes increased the number of Ly6C<sup>hi</sup> monocytes in the brain of Abx treated mice, but not in naïve SPF mice. Unpaired two-tailed Student's t test. \* $p < 0.05$ , \*\* $p < 0.01$ .

## 3.2 Role of monocytes in Alzheimer's disease

To investigate the influence of *T. gondii* induced microglia activation and cell recruitment on neurodegenerative diseases, in particular the effect of monocytes and their progeny, we used the 5xFAD murine model of AD. After infecting mice with *T. gondii*, we first analyzed cerebral A $\beta$  content, followed by the general immune response and individual cell properties at the chronic stage of infection, which is after four to eight weeks of infection.

### 3.2.1 *T. gondii* infection reduces the plaque burden in 5xFAD mice

We detected that the infection with *T. gondii* led to reduced plaque burden as determined by immunohistological staining of A $\beta$  plaques in 5xFAD mice (Figure 3.9A and A'). Quantification revealed significantly lower plaque numbers in the cortex of mice infected with *T. gondii* as compared to transgenic control mice (control 21.9 plaques/mm<sup>2</sup>, *T. gondii* 5.9 plaques/mm<sup>2</sup>,  $p < 0.006$ , Figure 3.9B). This observation was further confirmed by *in situ* two-photon microscopy, which was technically restricted to the observation of cortical layers I and II (Figure 3.9C and C'). Here, volumes of the remaining methoxy-X04 stained amyloid plaques were significantly reduced in *T. gondii* infected animals (controls 1548 $\pm$ 205 $\mu$ m<sup>3</sup>, *T. gondii* 466 $\pm$ 92 $\mu$ m<sup>3</sup>,  $p < 0.002$ , Figure 3.9D).

While immunohistological methods can only identify A $\beta$  plaques, ELISA measurement allows the quantification of total A $\beta$ . Using a sequential protocol, we separated monomeric and small oligomeric A $\beta$  (carbonate-soluble) from larger aggregates (guanidine-soluble) in whole-brain homogenates. This separation is based on the different solubility of smaller and larger aggregates. Smaller aggregates can be dissolved in a rather mild carbonate buffer, whereas larger aggregates require a harsh guanidine buffer to be fully dissolved. We quantified the amount of A $\beta$ <sub>42</sub> and found that it was significantly reduced in both fractions (carbonate soluble: control 109.3 $\pm$ 21.6 ng/ml, *T. gondii* 31.1 $\pm$ 12.5 ng/ml,  $p < 0.05$ ; guanidine fraction: control 406.9 $\pm$ 79.9 ng/ml, *T. gondii* 132.3 $\pm$ 35.2 ng/ml,  $p < 0.05$ , Figure 3.10).

Using morphological methods, we detected substantial changes in the cortex and subcortical regions of infected mice such as inflammatory lesions (Figure 3.11A'), extensive Iba1-reactivity (Figure 3.11B') due to the activation of microglia and myeloid cell infiltration, as well as GFAP-positive astrogliosis (Figure 3.11C'). Non-infected 5xFAD mice presented with known brain histology (Figure 3.11A) and only minor activation of resident glia cells (Iba1 and GFAP staining, Figure 3.11B, C) (Oakley et al. 2006).

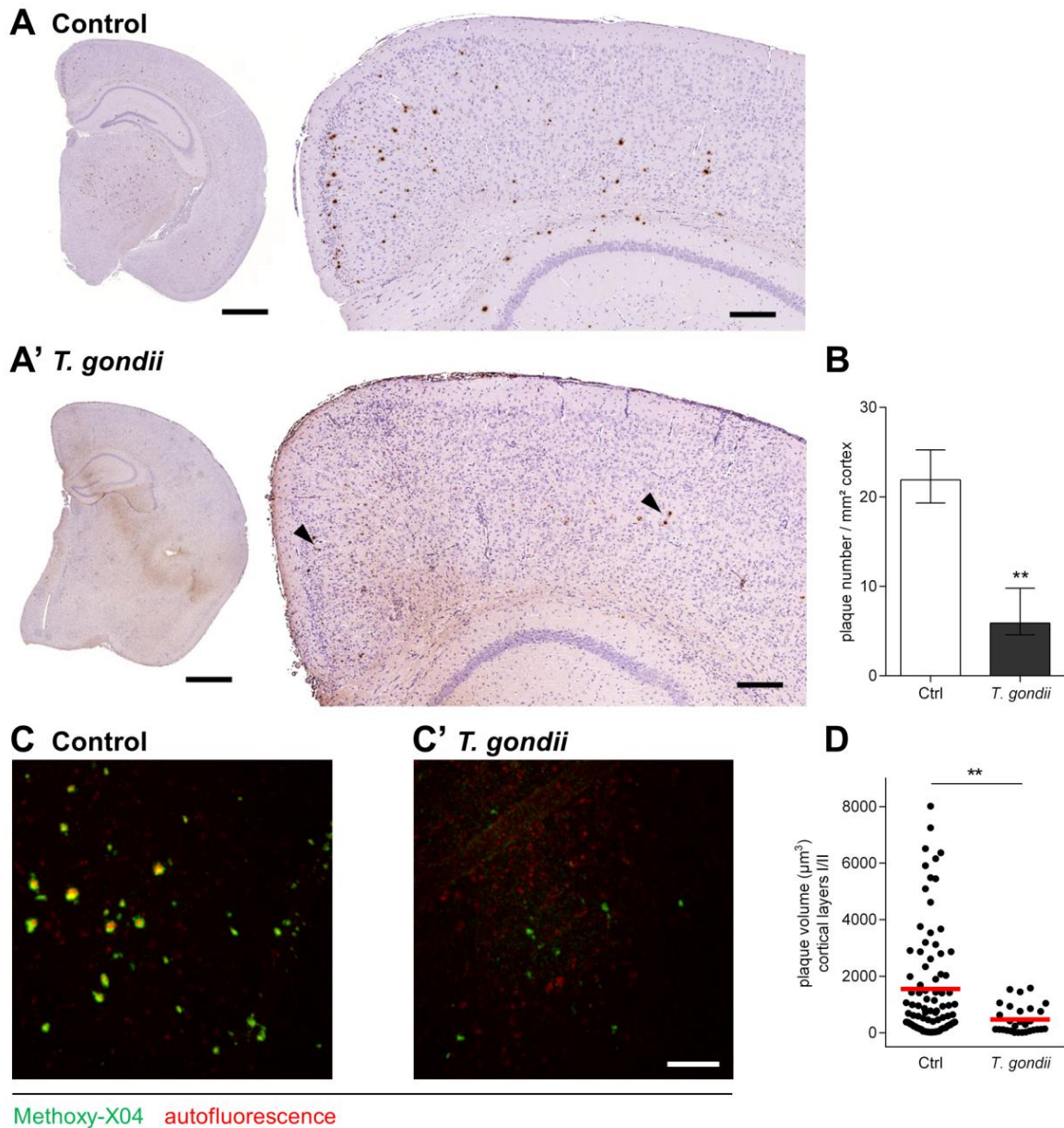


**Figure 3.9: *T. gondii* infection leads to reduced plaque burden in 5xFAD mice.**

(A, A') show representative cortex regions with immunohistochemical labeling against A $\beta$  from (A) non-infected and (A') *T. gondii* infected 5xFAD mice. Arrow heads point towards remaining plaques in infected animals. Scale bars represent 1000  $\mu$ m (left) and 200  $\mu$ m (right).

(B) Quantification of cortical A $\beta$  plaques. Data are displayed as mean  $\pm$  SEM. Significance as determined by unpaired t test with Welch's correction is indicated. \*\*p $\leq$ 0.01.

(C, C') *Ex vivo* two-photon micrographs of the cerebral cortex layers I and II of (C) control and (C') *T. gondii* infected 5xFAD mice injected with methoxy-X04. Amyloid plaques stained with methoxy-X04 are represented in green, autofluorescence is shown in red. One representative z-stack projection spanning at least 50  $\mu$ m depth is shown for each condition. Scale bar, 100  $\mu$ m.

(D) Plaque volume in cortical layers I and II determined from at least five *ex vivo* two-photon micrographs shown in (C, C'). Each symbol represents one plaque and bars represent the mean, statistical significance is denoted by asterisks. \*\*p $\leq$ 0.01.

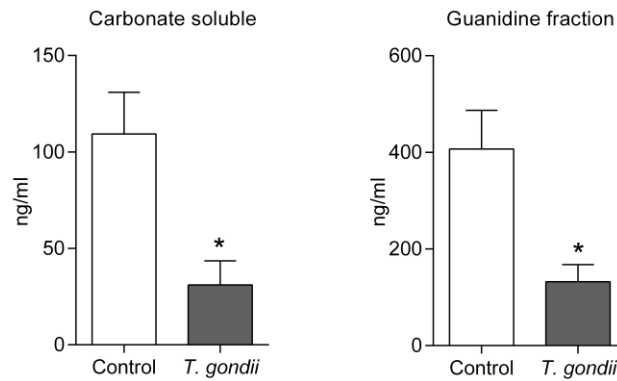


**Figure 3.10: *T. gondii* infection reduces small and large A $\beta$  aggregates.**

A $\beta$ <sub>42</sub> in the carbonate soluble (monomeric and small oligomeric A $\beta$ <sub>42</sub> aggregates) and guanidine soluble fractions (large A $\beta$ <sub>42</sub> aggregates) of whole-brain homogenates was measured by ELISA. Data are presented as mean + SEM. Significance levels ( $p$  values) determined by unpaired Student's  $t$  test are indicated. \* $p \leq 0.05$ .

Activation of microglia can be recognized by an increased expression of certain surface molecules including major histocompatibility complex class (MHC) I and MHC II, CD11c and CD45. Flowcytometric analysis revealed a significantly increased expression of these markers by brain microglia in *T. gondii* infected wildtype and 5xFAD mice compared to respective non-infected controls (Figure 3.12). For MHC II, CD11c and CD45, genotype did not influence expression levels in neither non-infected nor *T. gondii* infected animals. Mild baseline activation of microglia was observed for MHC I, which resulted in an increased expression of MHC I by microglia in *T. gondii* infected 5xFAD animals compared to *T. gondii* infected wildtype mice (Figure 3.12).

Specific immunodetection for neurons (NeuN labeling) revealed no alterations in the number of neurons in the cortex of infected versus control mice (Figure 3.11D, D'). The slightly darker shading in the infected brain is due to increased background staining as previously seen in this infection model in wildtype C57BL/6J mice (Möhle et al. 2014). Occasionally, *T. gondii* cysts were detectable (Figure 3.11A inset).

Noting the vast activation of microglia and astrocytes as well as a strong recruitment of myeloid cells in the infected animals, we have to potentially take into account additional specific and unspecific immunological responses as further factors for the reduction of A $\beta$  (Rubio-Perez & Morillas-Ruiz 2012; Perry et al. 2010).

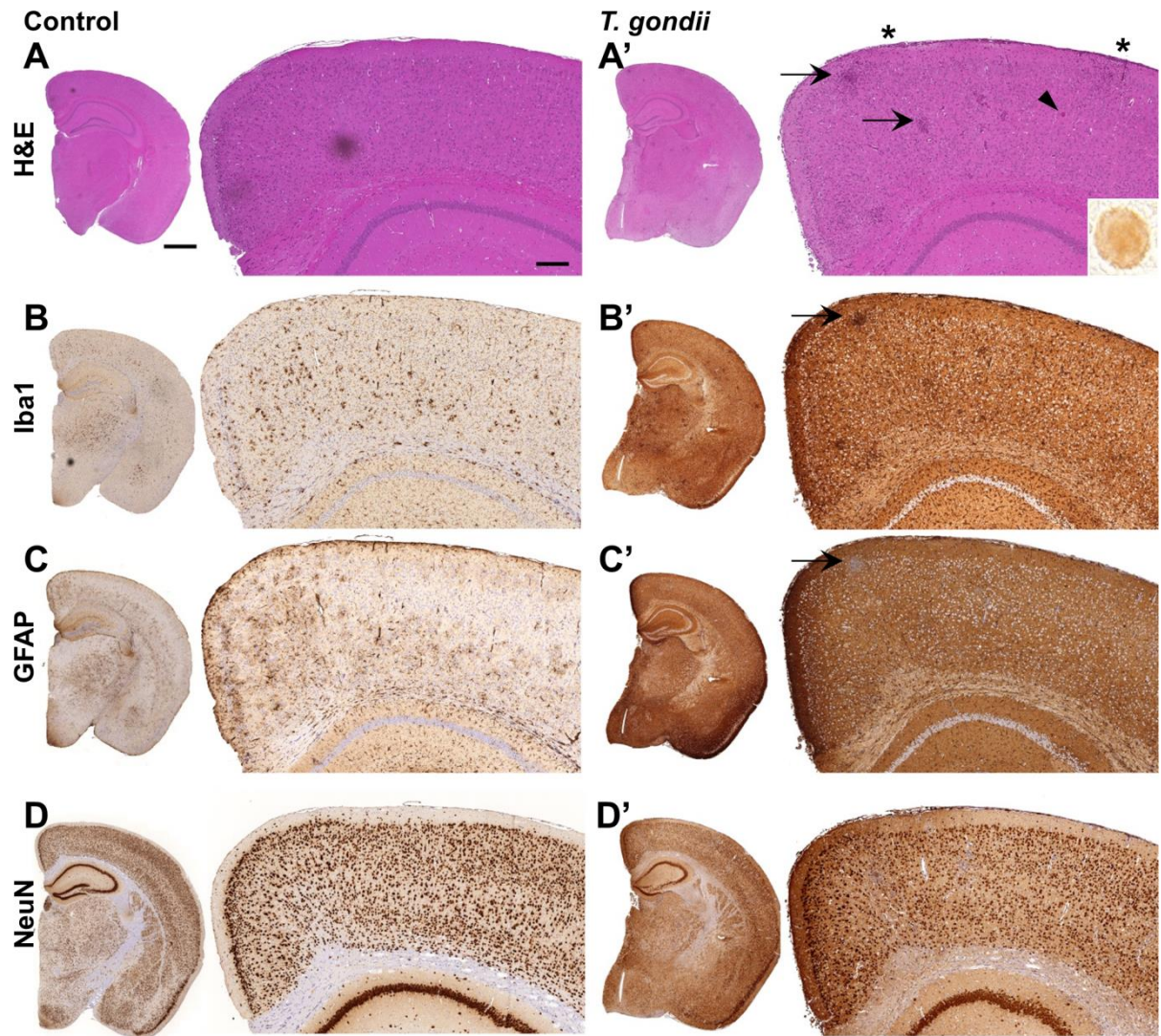


**Figure 3.11: *T. gondii* infection induces histopathological changes and activation of microglia.**

(A, A') Hematoxylin and eosin (H&E) stained coronal sections from (A) non-infected and (A') *T. gondii* infected 5xFAD mice. \* denotes meningeal infiltrates, arrows show inflammatory foci, the arrow head highlights a *T. gondii* cyst. The inset shows a cyst stained with an antibody against *T. gondii*.

(B-D') Representative pictures of immunohistochemical stainings against (B, B') Iba1, (C, C') GFAP, and (D, D') NeuN of coronal brain sections from (B, C, D) non-infected and (B', C', D') *T. gondii* infected 5xFAD mice.

Scale bars represent 1000  $\mu\text{m}$  (left column) and 200  $\mu\text{m}$  (right column).

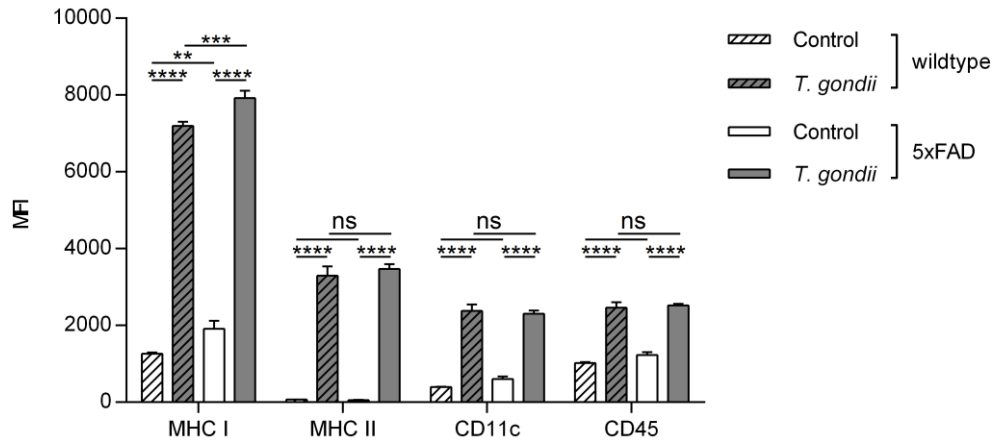


**Figure 3.12: Microglia are activated in wildtype and 5xFAD mice upon *T. gondii* infection.**

Mononuclear cells were isolated from wildtype and 5xFAD mouse brains and subjected to flowcytometric analysis. Microglia were gated as shown in Figure 3.16 and the surface expression of major histocompatibility complex class (MHC) I, MHC II, CD11c and CD45 was quantified using the median fluorescence intensity (MFI) of the respective channel. Bars represent mean + SEM. Significance levels ( $p$  values) are indicated as determined by Fisher's LSD test. ns, not significant, \*\* $p \leq 0.01$ , \*\*\* $p \leq 0.001$ , \*\*\*\* $p \leq 0.0001$ .

### 3.2.2 Expression of pro- and anti-inflammatory cytokines is triggered by *T. gondii* infection in wildtype and 5xFAD mice

Collectively, resident and recruited cells form a robust immune response to control *T. gondii* infection by producing pro-inflammatory cytokines, chemokines and anti-parasitic effector molecules (Möhle et al. 2014). To characterize this component of the immune response, particularly comparing wildtype and 5xFAD *T. gondii* infected mice, we measured the expression of certain cytokines in the brain by semi-quantitative RT-PCR.

The infection triggered a strongly enhanced mRNA expression of pro-inflammatory cytokines, including *IFN- $\gamma$*  (wildtype control:  $0.23 \pm 0.04$ ; wildtype *T. gondii*:  $2011 \pm 384$ ; 5xFAD *T. gondii*:  $2279 \pm 95$ ; all values are fold-change over 5xFAD controls), *TNF* (wildtype control:  $0.35 \pm 0.05$ ; wildtype *T. gondii*:  $201 \pm 33$ ; 5xFAD *T. gondii*:  $238 \pm 13$ ; all values are fold-change over 5xFAD controls), *IL-1 $\beta$*  (wildtype control:  $0.37 \pm 0.03$ ; wildtype *T. gondii*:  $183 \pm 52$ ; 5xFAD *T. gondii*:  $211 \pm 14$ ; all values are fold-change over 5xFAD controls), and *IL-6* (wildtype control:  $0.7 \pm 0.09$ ; wildtype *T. gondii*:  $22 \pm 6$ ; 5xFAD *T. gondii*:  $26 \pm 1$ ; all values are fold-change over 5xFAD controls) (Figure 3.13). Notably, no differences were detected due to the genotype.

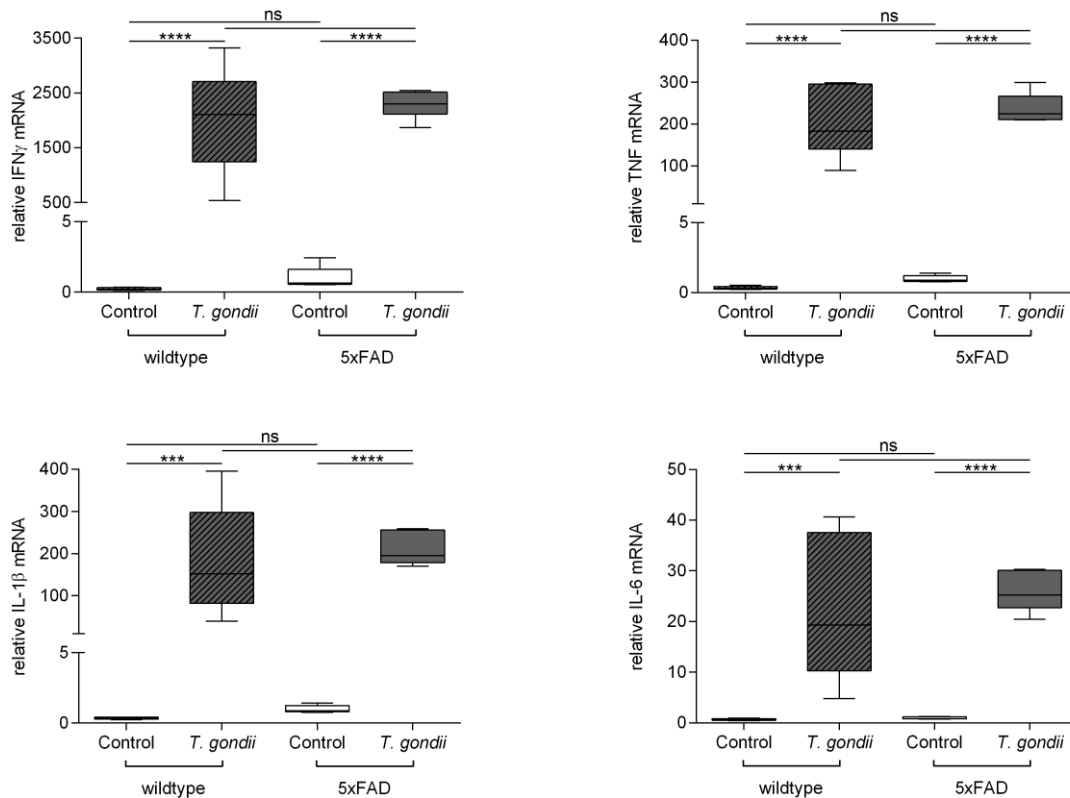


**Figure 3.13: Expression of pro-inflammatory cytokine mRNA in the brain is triggered in *T. gondii* infected wildtype and 5xFAD mice.**

Total RNA was isolated from brains collected from chronically *T. gondii* infected (n=7) and non-infected control (n=5) wildtype and 5xFAD mice. Semi-quantitative RT-PCR was performed for *IFN- $\gamma$* , *TNF*, *IL-1 $\beta$* , and *IL-6* and relative mRNA levels were normalized on housekeeping gene expression. Data are presented as fold change over 5xFAD controls in box and whisker graphs. Significance levels (p values) are indicated as determined by unpaired Student's t test. ns, not significant, \*\*\*p $\leq$ 0.001, \*\*\*\*p $\leq$ 0.0001.

During chronic *T. gondii* infection, the pro-inflammatory immune response is followed by the production of cytokines associated with anti-inflammatory functions (Gaddi & Yap 2007). In this context, we detected increased mRNA expression of *IL-10* (wildtype control: 0.85 $\pm$ 0.09; wildtype *T. gondii*: 125 $\pm$ 19; 5xFAD *T. gondii*: 148 $\pm$ 9; all values are fold-change over 5xFAD controls) and *TGF- $\beta$*  (wildtype control: 0.52 $\pm$ 0.06; wildtype *T. gondii*: 3.7 $\pm$ 0.4; 5xFAD *T. gondii*: 5.1 $\pm$ 0.4; all values are fold-change over 5xFAD controls) in *T. gondii* infected mice (Figure 3.14). While *IL-10* mRNA expression was independent of the genotype, *TGF- $\beta$*  mRNA expression was higher in 5xFAD *T. gondii* infected compared to wildtype *T. gondii* infected mice.



## RESULTS

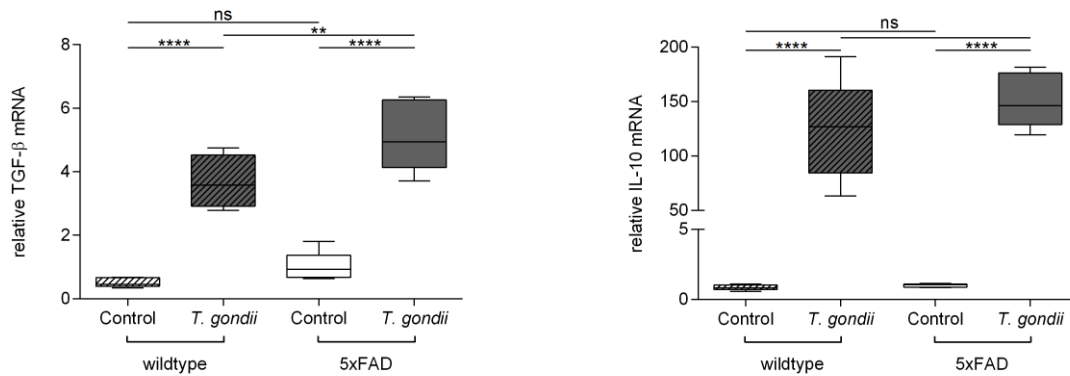


**Figure 3.14: Expression of anti-inflammatory cytokine mRNA in the brain is triggered in *T. gondii* infected wildtype and 5xFAD mice.**

Total RNA was isolated from brains collected from chronically *T. gondii* infected (n=7) and non-infected control (n=5) wildtype and 5xFAD mice. Semi-quantitative RT-PCR was performed for *TGF-β* and *IL-10* and relative mRNA levels were normalized on housekeeping gene expression. Data are presented as fold change over 5xFAD controls in box and whisker graphs. Significance levels (*p* values) are indicated as determined by unpaired Student's *t* test. ns, not significant, \*\**p*<0.01, \*\*\*\**p*<0.0001.

It is apparent that the immune response triggered by *T. gondii* causes tremendous changes in gene expression profiles. Thus, we wanted to exclude that the reduction of Aβ plaques was due to a downregulation of APP which might lead to a diminished production of Aβ<sub>42</sub>. We measured mRNA expression of *hAPP* in the brains of 5xFAD mice and did not detect significant changes compared to non-infected 5xFAD mice (5xFAD *T. gondii*: 0.64±0.06 fold-change over 5xFAD controls, *p*>0.05; Figure 3.15).

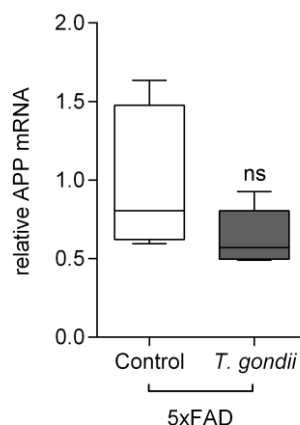


**Figure 3.15: mRNA expression of APP in the brain remains unaltered upon infection with *T. gondii*.**

Total RNA was isolated from brains collected from non-infected control (n=5) and chronically *T. gondii* infected (n=7) 5xFAD mice. Semi-quantitative RT-PCR was performed for *hAPP* and the relative mRNA level was normalized on housekeeping gene expression. Data are presented as fold change over 5xFAD controls in box and whisker graphs. Significance levels (*p* values) are indicated as determined by unpaired Student's *t* test. ns, not significant.

### 3.2.3 Recruited monocytes express high CCR2, intermediate TREM2 and CD36

Local activation of glia cells upon *T. gondii* infection is accompanied by recruitment of immune cells from the periphery to the brain. Among recruited immune cells, the CD45<sup>hi</sup> CD11b<sup>hi</sup> myeloid compartment plays an important role in cerebral toxoplasmosis (Fischer et al. 2000; Clark et al. 2011; Schlüter et al. 1995). Myeloid cells comprise of Ly6G<sup>+</sup> neutrophils, Ly6G<sup>neg</sup> Ly6C<sup>hi</sup> monocytes, Ly6G<sup>neg</sup> Ly6C<sup>int</sup> monocyte-derived DCs and Ly6G<sup>neg</sup> Ly6C<sup>low</sup> monocyte-derived macrophages. In the following, we focused our analysis on these three subsets of myeloid-derived CD45<sup>hi</sup> CD11b<sup>hi</sup> Ly6G<sup>neg</sup> CCR2<sup>+</sup> mononuclear cells (gating strategy depicted in Figure 3.16A, A'). These subsets of myeloid cells were chosen because age-related defects in the Ly6C<sup>hi</sup> monocyte population have been linked to cognitive decline in a murine AD model (Naert & Rivest 2012a).

To validate that cell recruitment in 5xFAD mice resembles the cell recruitment observed in wildtype mice, we analyzed the relative proportions of Ly6G<sup>neg</sup> mononuclear cell subsets amongst recruited cells by flow cytometry. In both *T. gondii* infected groups, the presence of Ly6C<sup>hi</sup>, Ly6C<sup>int</sup> and Ly6C<sup>low</sup> cells was greatly enhanced compared to respective non-infected mice (Figure 3.16A, A', Figure 3.17). Quantitative analysis revealed no genotype-related differences with respect to Ly6C<sup>hi</sup>, Ly6C<sup>int</sup> and Ly6C<sup>low</sup> mononuclear cells (Figure 3.17).

Similar to the activation of microglia, these cells can be phenotypically characterized by expression of different surface molecules. We were especially interested in phagocytosis-related molecules, such as TREM2, CD36, and SCARA1.

To this end, we quantified the MFI by flow cytometry and compared the surface expression on resident and myeloid-derived mononuclear cells. The expression pattern was similar for all three markers: We found the highest expression of TREM2, CD36 and SCARA1 on Ly6C<sup>low</sup> F4/80<sup>hi</sup> macrophages and activated microglia and a lower expression on Ly6C<sup>hi</sup> CCR2<sup>hi</sup> monocytes and resting microglia. Ly6C<sup>int</sup> mononuclear cells expressed intermediate amounts of TREM2, CD36 and SCARA1 on their surface (TREM2: microglia 688±25, activated microglia 2191±179, Ly6C<sup>hi</sup> 595±48, Ly6C<sup>int</sup> 1298±13, Ly6C<sup>low</sup> 3222±511, Figure 3.16D; CD36: microglia 152±8, activated microglia 1616±281, Ly6C<sup>hi</sup> 749±37, Ly6C<sup>int</sup> 1175±92, Ly6C<sup>low</sup> 1879±208, Figure 3.16E; SCARA1: activated microglia 15977±3220, Ly6C<sup>hi</sup> 6319±1395, Ly6C<sup>int</sup> 10805±2221, Ly6C<sup>low</sup> 14964±3088, Figure 3.16F).

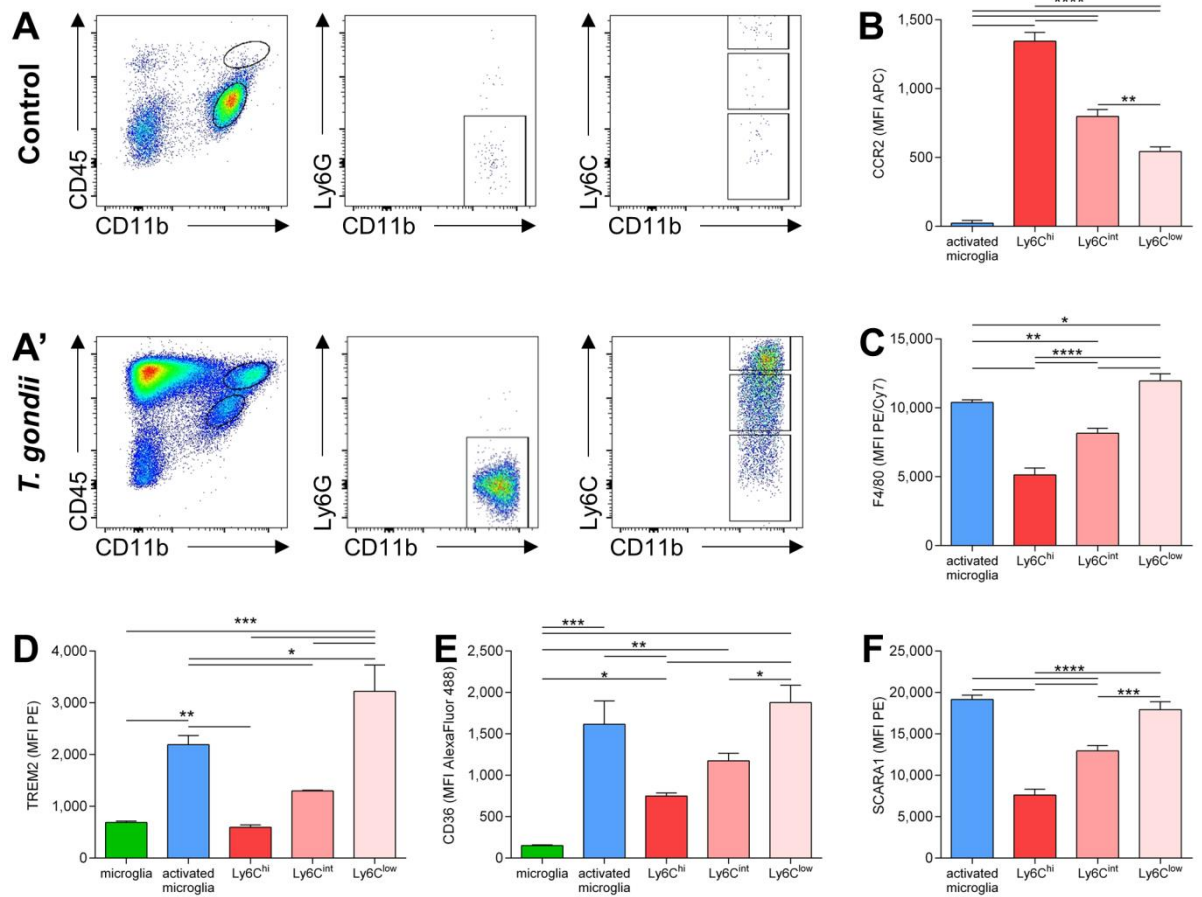


**Figure 3.16: Myeloid-derived mononuclear cells are recruited to the brain upon *T. gondii* infection and express phagocytosis related surface molecules.**

Mononuclear cells were isolated from 5xFAD mouse brains and subjected to flowcytometric analysis.

(A, A') Representative pseudocolor plots are shown for (A) non-infected and (A') infected 5xFAD animals and demonstrate the recruitment of CD45<sup>hi</sup>CD11b<sup>hi</sup>Ly6G<sup>neg</sup>Ly6C<sup>+</sup> cells to the brain upon *T. gondii* infection. After gating cells by their forward and side scatter properties, excluding doublets and dead cells (not shown), we used CD45 and CD11b expression to discriminate between resting microglia (A, bottom elliptic gate) or activated microglia (A', bottom elliptic gate), respectively, and myeloid cells (A', top elliptic gate). From myeloid cells, Ly6G<sup>+</sup> neutrophils were excluded and the Ly6C expression of the remaining CD11b<sup>hi</sup>Ly6G<sup>-</sup> cells was used to gate Ly6C<sup>hi</sup>, Ly6C<sup>int</sup> and Ly6C<sup>low</sup> mononuclear cells.

(B-E) We compared the surface expression of CCR2, F4/80, TREM2, CD36, and SCARA1 between resting microglia, activated microglia and myeloid-derived mononuclear cell subsets. The median fluorescence intensity (MFI) for each marker and population is displayed as mean + SEM. Significance levels (*p* values) determined by Fisher's LSD test are indicated. \**p*≤0.05, \*\**p*≤0.01, \*\*\**p*≤0.001, \*\*\*\**p*≤0.0001.

Our data indicate that the recruitment of different myeloid-derived mononuclear cell subsets to the CNS induced by cerebral toxoplasmosis may contribute to the removal of Aβ by activated microglia.

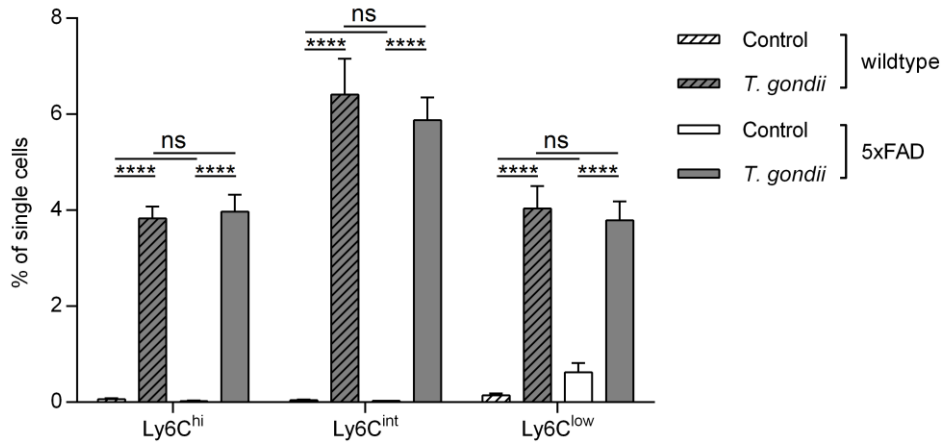


**Figure 3.17: Recruitment of Ly6C<sup>hi</sup> monocytes, Ly6C<sup>int</sup> mononuclear cells and Ly6C<sup>low</sup> macrophages in wildtype and 5xFAD mice upon *T. gondii* infection.**

Mononuclear cells were isolated from wildtype and 5xFAD mouse brains and subjected to flowcytometric analysis. CD45<sup>hi</sup> CD11b<sup>hi</sup> Ly6G<sup>-</sup> Ly6C<sup>hi</sup>, Ly6C<sup>int</sup> and Ly6C<sup>low</sup> mononuclear cell populations were gated as shown in Figure 3.16. Bars represent the percentage of single cells of each population displayed as mean + SEM. Significance levels (*p* values) are indicated as determined by Fisher's LSD test. ns, not significant, \*\*\*\**p*≤0.0001.

### 3.2.4 Myeloid-derived mononuclear cells phagocytose A $\beta$

Previous examination of resident and recruited immune cell subpopulations in chronic *T. gondii* infection revealed that these cell subsets display different phagocytic capacity (Biswas et al. 2015). Here we compared mononuclear cell subpopulations with respect to their ability to specifically phagocytose A $\beta$ <sub>42</sub> in an *ex vivo* phagocytosis assay. To this end, we freshly isolated brain mononuclear cells and exposed them to fluorophore-conjugated A $\beta$ <sub>42</sub> *ex vivo*. Resident surveilling microglia (CD45<sup>int</sup> CD11b<sup>+</sup>), activated microglia (CD45<sup>+</sup> CD11b<sup>+</sup>) as well as Ly6C<sup>hi</sup> monocytes, Ly6C<sup>int</sup> and Ly6C<sup>low</sup> cells (CD45<sup>hi</sup> CD11b<sup>hi</sup> Ly6G<sup>-</sup> Ly6C<sup>hi/int/low</sup>) were distinguished by flow cytometric analysis. The low ability of resident microglia to take up A $\beta$ <sub>42</sub> was reflected in their low MFI for A $\beta$ <sub>42</sub>-HiLyte Fluor 488 (1749±88, Figure 3.18B, green bar). Upon *T. gondii* infection, microglia cells became activated, but their A $\beta$ <sub>42</sub> uptake remained low (1564±119, Figure 3.18B, blue bar). Notably, Ly6C<sup>hi</sup> monocytes exhibited the highest MFI (5238±239, Figure 3.18B, dark red bar) suggesting greater phagocytic capacity. Similarly, also Ly6C<sup>int</sup> and Ly6C<sup>low</sup> cells were found to exhibit significantly higher MFI compared to microglia or activated microglia (Ly6C<sup>int</sup> 4396±204, Ly6C<sup>low</sup> 3890±387, Figure 3.18B, medium and light red bars, *p*<0.0001). Relative MFIs measured in cells isolated from wildtype mice showed a similar pattern, confirming that A $\beta$ <sub>42</sub> uptake was not restricted to 5xFAD cells (Figure 3.19). Differences in the absolute values can be – at least in part – attributed to the different quantification methods used for both analyses, i. e. conventional versus imaging flow cytometry.

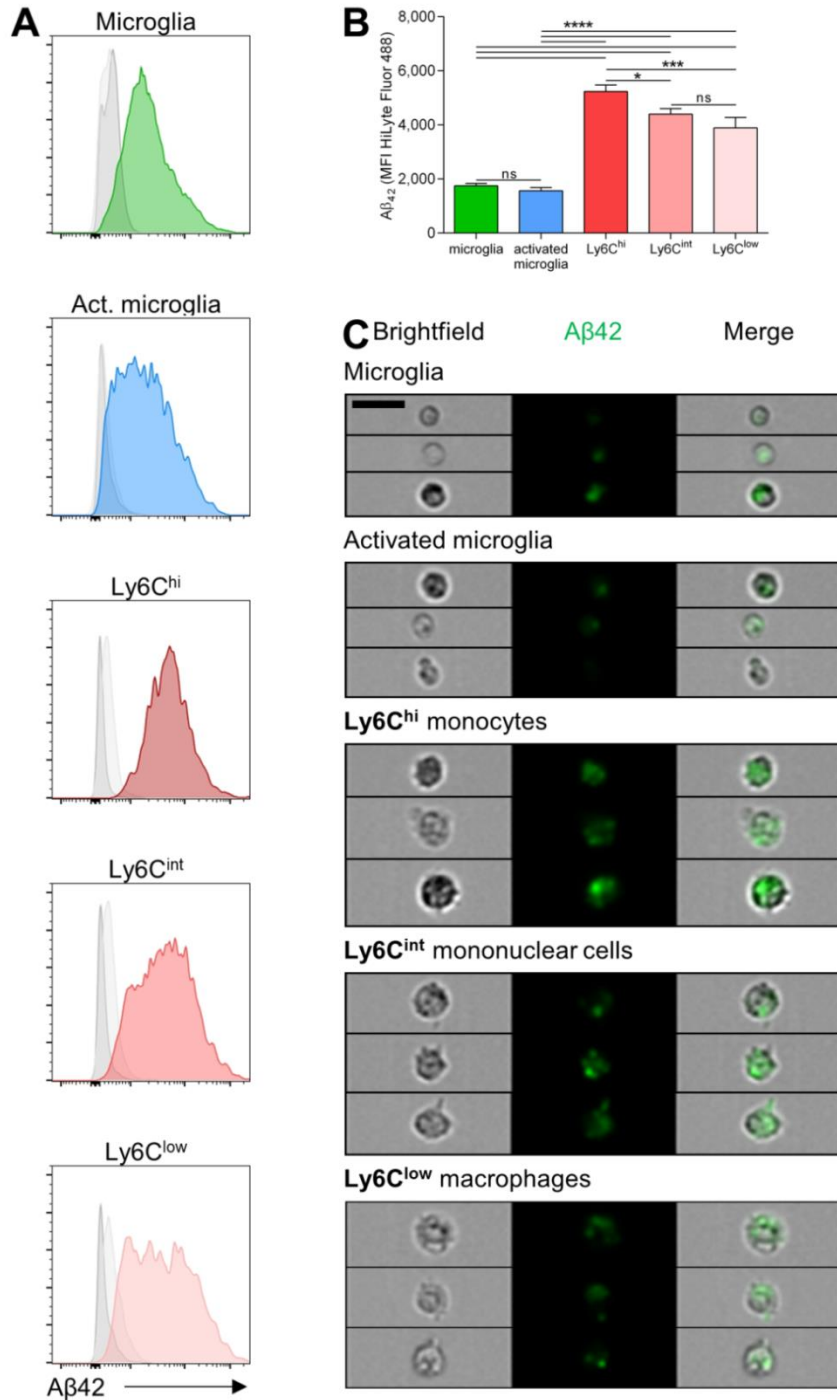


**Figure 3.18: Recruited mononuclear cells are potent Aβ phagocytic cells.**

(A-C) *Ex vivo* phagocytosis assay was performed with mononuclear cells isolated from 5xFAD and C57BL/6 mouse brains and cleared from dead cells by sorting via flow cytometer.

(A) Populations were gated as described in Figure 3.16. Representative histograms show the uptake of fluorescence labeled Aβ<sub>42</sub> peptide by different cell populations. Gray curves show the 4°C control (dark gray) and the Aβ<sub>42</sub><sup>-</sup> control (light gray) for each population.

(B) Bars indicate the median fluorescence intensity (MFI) of each population to express differences in the amount of Aβ<sub>42</sub> taken up. Data are displayed as mean + SEM (n=4-5).

(C) Representative images obtained with FlowSight™ are shown for each population. Scale bar, 20 μm.

Significance levels (*p* values) determined by Fisher's LSD test are indicated. ns, not significant, \**p*≤0.05, \*\*\**p*≤0.001, \*\*\*\**p*≤0.0001.

We further verified that the detected fluorescence resulted from internalized  $A\beta_{42}$  rather than from unspecific surface-bound signals. Therefore, we analyzed the cells using imaging flow cytometry that allows obtaining images of individual cells. Gating was performed as described in Figure 3.16A and representative pictures for each population are shown in Figure 3.18C. Microglia and activated microglia populations contained lower numbers of  $A\beta^+$  cells (Table 3.1, first column). Consistent with the previous measurements by conventional flow cytometry, fluorescence was low or absent in resting and activated microglia, but all monocyte populations showed an intense signal (Figure 3.18C and Figure 3.19). Fluorescence was distributed equally across the cells, sometimes with several additional bright spots inside individual cells. This further indicated the uptake of  $A\beta_{42}$  by recruited mononuclear cells ( $CD45^{hi} CD11b^{hi} Ly6G^- Ly6C^{hi/int/low}$ ) upon *T. gondii* infection. Morphologically, monocytes and the other two monocyte-derived cell subsets were more granular than (activated) microglia, represented by higher side scatter intensities (Figure 3.18C and Table 3.1, last column). We quantified the internalization of  $A\beta_{42}$  by calculating the ratio of the fluorescence intensity within the cell to the intensity of the entire cell. Ratios higher than 0 indicate intermediate to high internalization and were found in more than 97% of all  $A\beta^+$  cells regardless of the population (Table 3.1, second column). The mean internalization varied between populations with activated microglia being the lowest and  $Ly6C^{hi}$  monocytes being the highest (Table 3.1, third column).

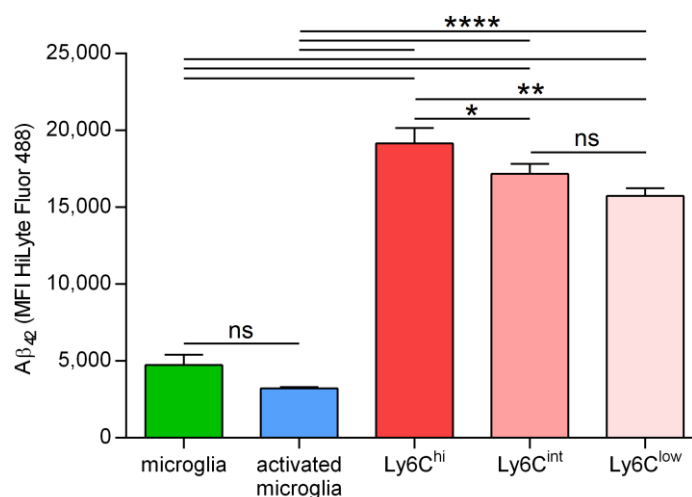


**Figure 3.19: Quantification of uptake of  $A\beta_{42}$  by imaging flow cytometry.**

The uptake of  $A\beta_{42}$  by different mononuclear cell populations isolated from C57BL/6 wildtype was quantified in an *ex vivo* phagocytosis assay using imaging flow cytometry. Populations were gated as described in Figure 3.16. Bars represent the mean fluorescence intensity of each population. Data are displayed as mean + SEM (n=4-5). Significance levels ( $p$  values) determined by Fisher's LSD test are indicated. ns, not significant, \* $p \leq 0.05$ , \*\* $p \leq 0.01$ , \*\*\*\* $p \leq 0.0001$ .

RESULTS

**Table 3.1: Quantification of A $\beta$ <sub>42</sub> uptake and cell properties by imaging flow cytometry.**

| Population                 | A $\beta$ <sup>+</sup> cells | ratio > 0   | Mean ratio | Mean side scatter intensity |
|----------------------------|------------------------------|-------------|------------|-----------------------------|
| <b>Microglia</b>           | 77.8±2.5 %                   | 99.3±0.2 %  | 5.0±0.1    | 1916±85                     |
| <b>Activated microglia</b> | 71.8±2.3 %                   | 97.1±0.2 %  | 3.0±0.02   | 1161±35                     |
| <b>Ly6C<sup>hi</sup></b>   | 99.4±0.09 %                  | 99.8±0.02 % | 5.4±0.06   | 3574±143                    |
| <b>Ly6C<sup>int</sup></b>  | 96.1±0.5 %                   | 99.4±0.1 %  | 5.0±0.1    | 3376±130                    |
| <b>Ly6C<sup>low</sup></b>  | 92.8±0.8 %                   | 99.0±0.05 % | 4.8±0.08   | 3107±93                     |

To confirm that it is indeed the recruited monocytes and their progeny contributing to plaque removal, we ablated Ly6C<sup>hi</sup> monocytes using a monoclonal anti-CCR2 antibody. We chose a lower antibody concentration to only reduce monocyte numbers, because the complete elimination would highly increase the susceptibility of infected mice as recently described by our research group (Biswas et al. 2015). One week after initiating the ablation, we detected significantly reduced Ly6C<sup>hi</sup> monocyte levels in the blood (Figure 3.20A, B, C). After two weeks of anti-CCR2 antibody administration (28 days after infection), Ly6C<sup>hi</sup> monocyte numbers were still significantly reduced in the blood (Figure 3.20B, C). This peripheral depletion led to a trending reduction of Ly6C<sup>hi</sup> monocytes and Ly6C<sup>low</sup> monocyte-derived macrophages in the brain on day 28 after *T. gondii* infection (Figure 3.20D). From the isolated brains, we quantified A $\beta$ <sub>42</sub> by ELISA. Importantly, diminished Ly6C<sup>hi</sup> monocyte numbers were associated with an increased total amount of A $\beta$ <sub>42</sub> in the brain of *T. gondii* infected 5xFAD mice (*T. gondii* 148±30ng/ml, *T. gondii* + anti-CCR2 414±75ng/ml, Figure 3.20E).

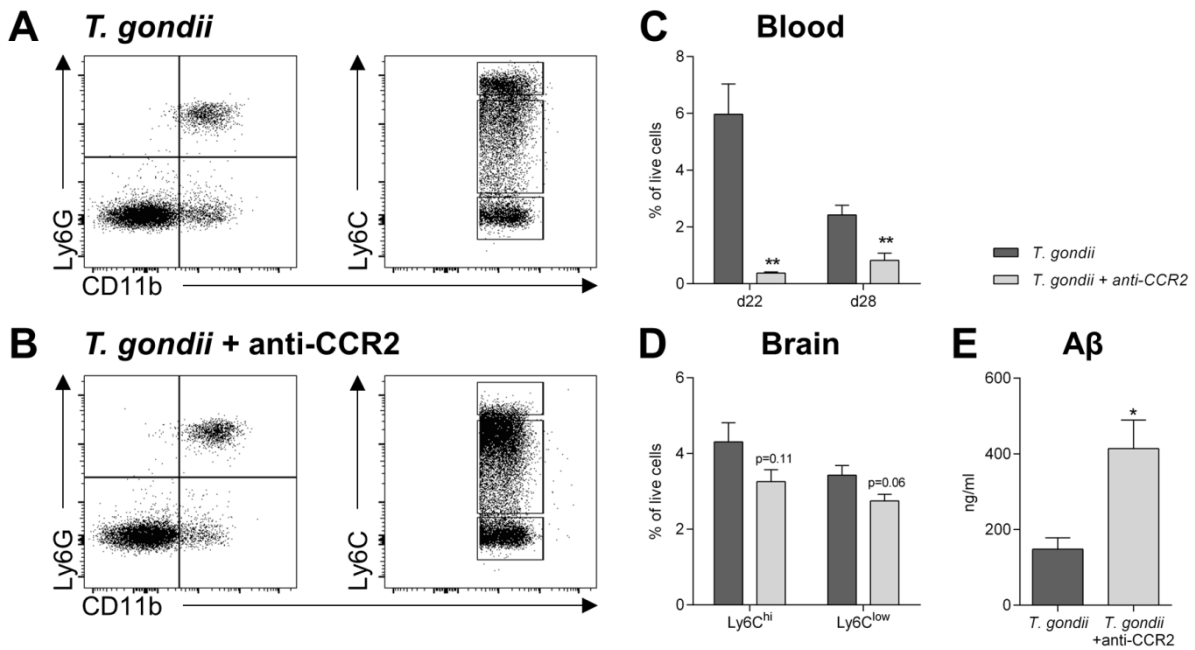


**Figure 3.20: Ablation of CCR2<sup>+</sup>Ly6C<sup>hi</sup> monocytes increases A $\beta$  accumulation in *T. gondii* infected 5xFAD mice.**

*T. gondii* infected 5xFAD mice were treated with the anti-CCR2 monoclonal antibody MC-21 to specifically ablate CCR2<sup>+</sup>Ly6C<sup>hi</sup> monocytes.

(A, B) Ly6C<sup>hi</sup> monocytes in the blood were measured 28 days post infection and after 13 days of anti-CCR2 administration. Representative dot plots picture the gating strategy and the specific ablation of Ly6C<sup>hi</sup> monocytes in (B) anti-CCR2 treated animals compared to (A) PBS treated animals.

(C, D) Ly6C<sup>hi</sup> monocytes in the blood on d22 and d28 as well as in the brain on d28 were analyzed and their percentage of live cells is displayed.

(E) The amount of A $\beta$ <sub>42</sub> in the brains of 5xFAD mice after *T. gondii* infection with and without monocyte ablation was measured by ELISA.

Data (n=4 per group) are presented as mean + SEM. Significance levels (*p* values) determined by unpaired Student's *t* test are indicated. \**p* ≤ 0.05, \*\**p* ≤ 0.01.

### 3.2.5 Recruited mononuclear cells increase proteolytic clearance of A $\beta$

Along with uptake of A $\beta$ , its proteolytic processing is also very important. Therefore, we measured the expression of three A $\beta$ -degrading enzymes in the brain, namely insulin-degrading enzyme (*IDE*), neprilysin (*NEP*), and matrix metalloproteinase 9 (*MMP9*), using RT-PCR, and we observed a significant increase in the expression of *MMP9* and *IDE* mRNA following infection with *T. gondii* (*MMP9*: 1.3±0.1 fold-change over 5xFAD controls, *p*<0.01, Figure 3.21; *IDE*: 1.7±0.1 fold-change over 5xFAD controls, *p*<0.01, Figure 3.21). The expression of *NEP* remained unaltered (Figure 3.21, 0.94±0.1 fold-change over 5xFAD controls, *p*>0.6).



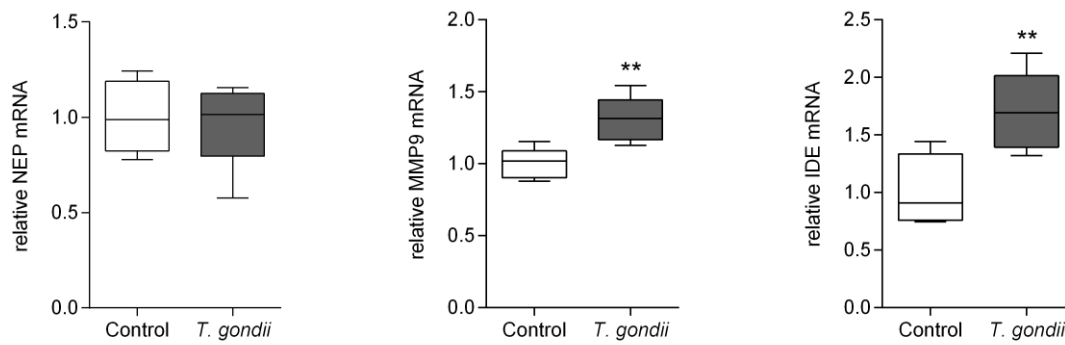


**Figure 3.21: *T. gondii* infection enhances mRNA expression of the A $\beta$  degrading enzymes IDE and MMP9.**

Expression of neprilysin (NEP), matrix metalloproteinase 9 (MMP9) and insulysin (IDE) in the brain was measured by RT-PCR in non-infected (n=5) and *T. gondii* infected (n=7) 5xFAD mice. Data are presented as fold-change over non-infected 5xFAD mice in box and whisker graphs. Significance levels ( $p$  values) determined by unpaired Student's t test are indicated. \*\* $p \leq 0.01$ .

We further performed a detailed investigation of brain resident as well as recruited immune cells in *T. gondii* infected mice. Of note, in the chronic stage of infection the intracellular parasites form cysts within neurons hiding from the immune system, thus the analyzed cells were not directly infected with tachyzoites. We found that *MMP9* mRNA was upregulated nearly three-fold in activated compared to surveilling microglia, but almost undetectable in recruited mononuclear cells (Figure 3.22). *IDE* mRNA was similarly expressed across all innate immune cell populations we investigated (Figure 3.22).

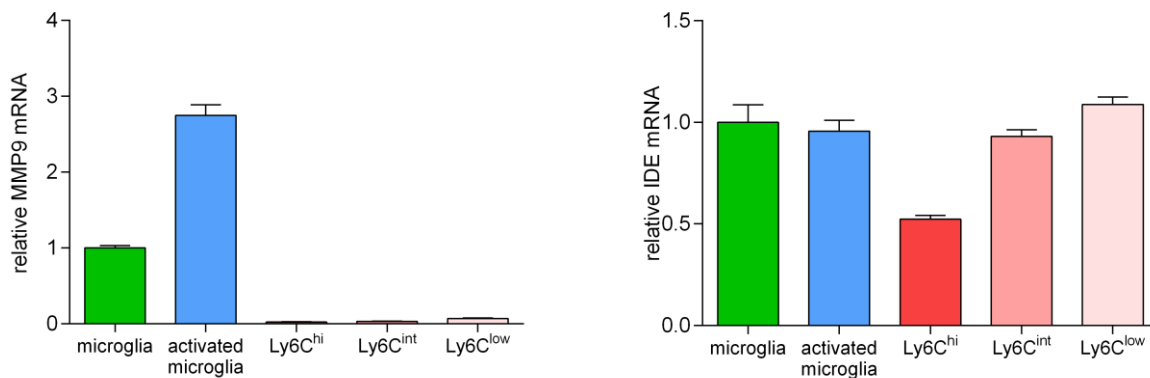


**Figure 3.22: mRNA of A $\beta$  degrading enzymes is expressed in different cell populations.**

Expression of MMP9 and IDE by innate immune cells isolated and sorted from the brains of non-infected and *T. gondii* infected C57BL/6 mice was measured by RT-PCR. Each sample consists of pooled cells from 6 animals and was measured in triplicates.

Furthermore, we investigated which cell types are located around the A $\beta$  plaques in the cortex of *T. gondii* infected 5xFAD mice by performing immunofluorescence stainings against Iba1, Ly6C, and A $\beta$ . Due to their general distribution in the parenchyma, Iba1<sup>+</sup> microglia and monocyte-derived macrophages were closely associated with A $\beta$  plaques (Figure 3.23A, B). Interestingly, Ly6C<sup>+</sup> cells were not located directly in the vicinity of A $\beta$  plaques (Figure

3.23C, D). As to that, it is important not to confuse Ly6C<sup>+</sup> monocytes with Ly6C expressing endothelial cells (Jutilla et al. 1988), which can be recognized by their elongated shape. This qualitative finding was confirmed by quantification of fluorescence intensity around plaques (Figure 3.24A, B).

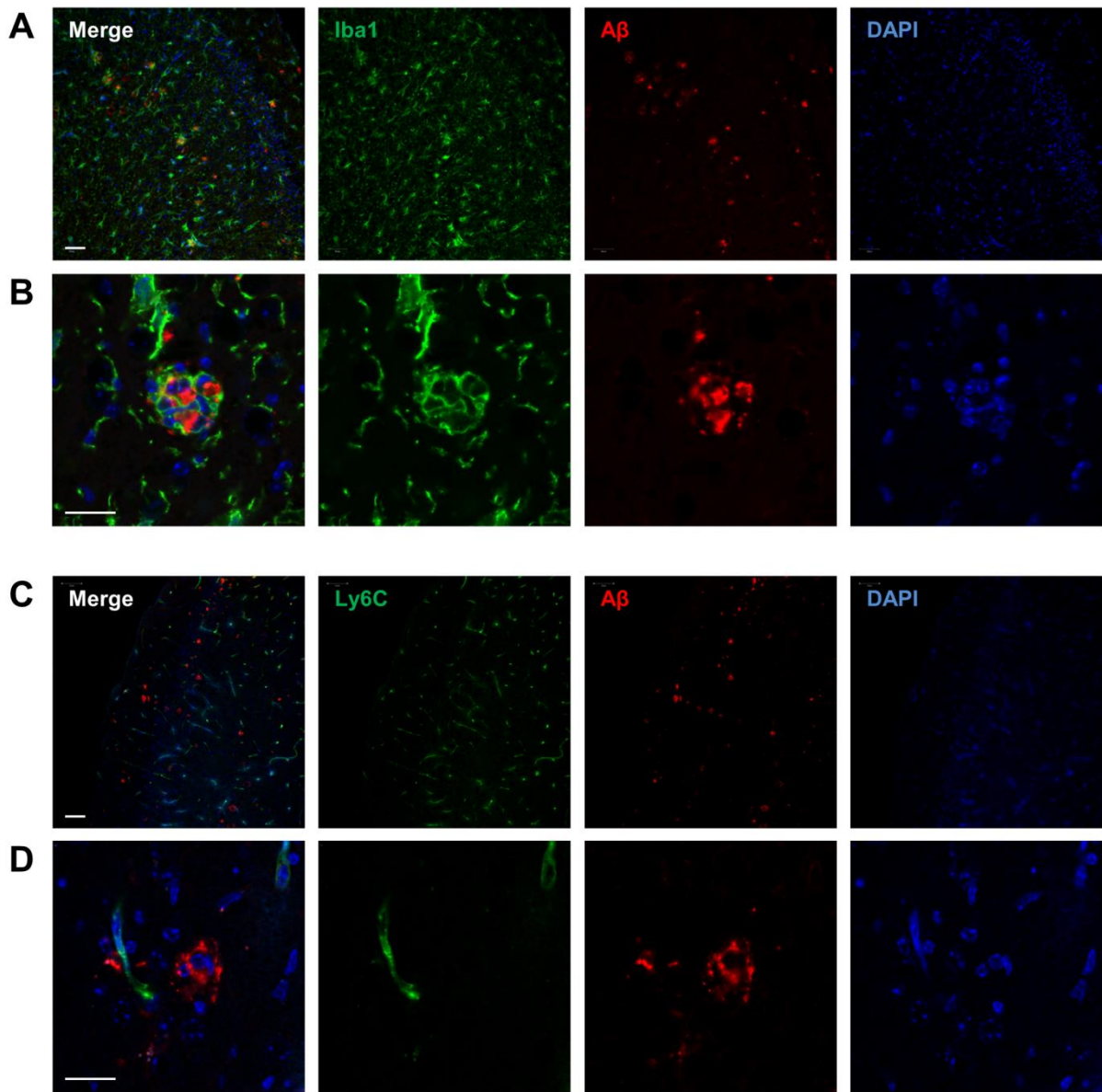


**Figure 3.23: Microglia but not Ly6C<sup>hi</sup> monocytes are located in the vicinity of Aβ plaques.**

Immunolabeled coronal sections from *T. gondii* infected 5xFAD mice.

(A, B) Co-labeling of Iba1 (microglia) and Aβ (plaques) reveals close interaction of microglia with plaques. (A) Low magnification (20x) overview of the cortex. Scale bar, 200 μm. (B) Representative cortical plaque surrounded by microglial processes. 63x magnification, scale bar, 20 μm.

(C, D) In sections co-labeled for Ly6C (Ly6C<sup>hi</sup> monocytes) and Aβ (plaques), Ly6C<sup>hi</sup> monocytes were not located in the direct vicinity of plaques. (C) Low magnification (20x) overview of the cortex. Scale bar, 200 μm. (D) Representative cortical plaque with a nearby Ly6C<sup>+</sup> blood vessel but no associated Ly6C<sup>hi</sup> monocytes. 63x magnification, scale bar, 20 μm.

## RESULTS

Taken together, our results reveal that Ly6C<sup>hi</sup>, Ly6C<sup>int</sup>, and Ly6C<sup>low</sup> mononuclear cells are highly capable of removing soluble A $\beta$  peptides. While Ly6C<sup>hi</sup> monocytes contribute significantly to this clearance, they cannot be found in the direct vicinity of established plaques and thus, may rather lower the general amount of A $\beta$  to prevent higher molecular weight A $\beta$  aggregates and plaque formation.

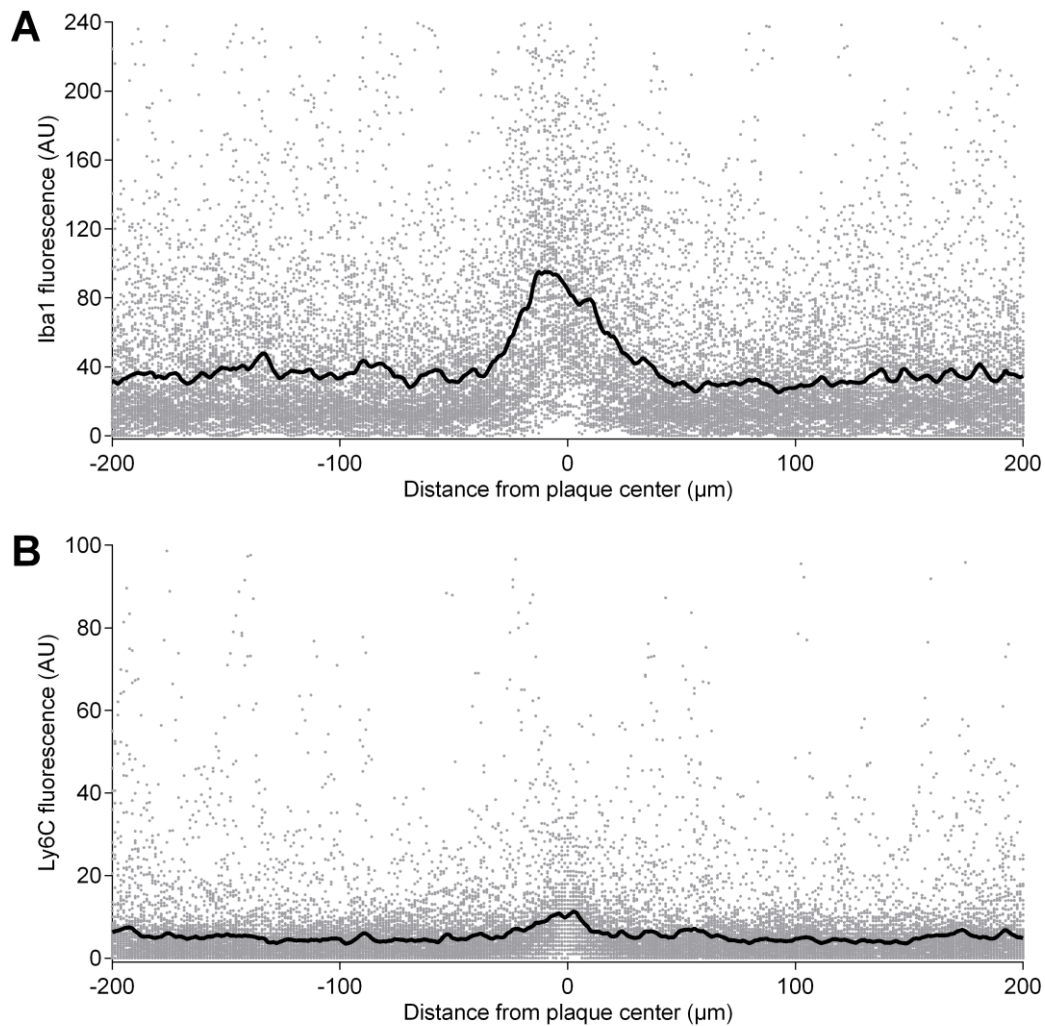


**Figure 3.24: Iba1 but not Ly6C reactivity is increased around A $\beta$  plaques**

(A, B) Immunolabeled coronal sections from *T. gondii* infected 5xFAD mice were analyzed to quantify the fluorescence intensity of (E) Iba1 and (F) Ly6C in the direct environment of plaques. The black line represents the average at a given distance. AU, arbitrary units.

### 3.2.6 *T. gondii* infection reduces A $\beta$ load in older animals

In the previously described experiments, mice were infected around the time point when first plaques become detectable in the brain (60 d). Additionally, we were interested whether in older animals the A $\beta$  burden can also be reduced by *T. gondii* infection. Therefore, we infected 7 months old 5xFAD mice and used ELISA to quantify A $\beta$ . After 6 weeks of infection, we found a significantly lower amount of A $\beta$  in the brains of *T. gondii* infected compared to non-infected 5xFAD mice (control 7529 $\pm$ 623 ng/ml, *T. gondii* 4641 $\pm$ 487 ng/ml,  $p < 0.001$ , Figure 3.25).

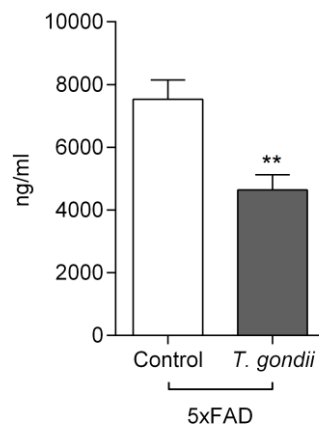


**Figure 3.25: Infection with *T. gondii* reduces total A $\beta$  burden in older animals.**

The amount of A $\beta_{42}$  in the brains of aged (7 months) non-infected and *T. gondii* infected 5xFAD mice was measured by ELISA on d44 post infection. The significance level ( $p$  value) determined by unpaired Student's  $t$  test is indicated. \*\* $p \leq 0.01$ .

## 4 Discussion

### 4.1 Role of monocytes in neurogenesis within the gut-brain-axis

In the first part of this study, we examined the interactions between antibiotic treatment, intestinal microbiota and adult hippocampal neurogenesis.

Treatment with antibiotics severely depleted the intestinal microbiota and was associated with reduced levels of proliferating cells in the hippocampus of mice. Reconstitution of the intestinal flora with probiotics rescued neurogenesis in antibiotic-treated mice. Similarly, a recent study conducted in a mouse model of stress has also found probiotics to increase neurogenesis levels (Ait-Belgnaoui et al. 2014). Like probiotics, voluntary exercise improved neurogenesis in antibiotic-treated mice to naïve SPF levels in our experiments. This is consistent with previous experimental setups where physical exercise is a widely used strategy known to promote neurogenesis in various disease models (Kempermann et al. 2010; van Praag et al. 1999; Wolf et al. 2011; Farioli-Vecchioli et al. 2014).

Interestingly, both treatment paradigms were accompanied by an increase of the Ly6C<sup>hi</sup> monocyte population in the brain. Previous findings indicate that CCR2<sup>+</sup> Ly6C<sup>hi</sup> monocytes entering the CNS are essential for recovery after spinal cord injury (Shechter et al. 2009) and potentially contribute to restrict cerebral amyloidosis (Naert & Rivest 2013). These results propose new beneficial roles in addition to the established pro-inflammatory one (Biswas et al. 2015; Hammond et al. 2014; Karlmark et al. 2012). With respect to neurogenesis, previous reports have linked cells of the adaptive immunity i. e. T cells to the maintenance of this homeostatic process (Ziv et al. 2006; Wolf et al. 2009).

Investigating the potential link between Ly6C<sup>hi</sup> monocytes and neurogenesis in more detail, we demonstrated that the lack of Ly6C<sup>hi</sup> monocytes, either by knockout of CCR2 or by antibody-induced depletion, led to decreased hippocampal neurogenesis levels. Moreover, substitution of antibiotic-treated mice with adoptively transferred Ly6C<sup>hi</sup> monocytes was also able to rescue neurogenesis.

Unexpectedly, the fecal transplant from naïve SPF into antibiotic-treated mice could not rescue neurogenesis and Ly6C<sup>hi</sup> monocyte numbers. Even though the SPF transplant seemed to promote a microbiome similar to that of naïve SPF mice, it cannot be excluded that the treatment induced fine-tuned robust changes as described for human subjects (Lozupone et al.

2012). Alternatively, these data suggest a (partial) direct and long-lasting effect of antibiotics on the host which is not mediated by the intestinal microbiota. Indeed, a recent study confirmed that at least two factors are responsible for antibiotic-induced changes in gene expression, depletion of microbiota and direct interaction with host tissues (Morgun et al. 2015). The authors argue that, as host mitochondria have retained many features of bacteria from which they descend, this similarity may actually facilitate the direct interaction between antibiotics and cell metabolism (Morgun et al. 2015). However, both adoptive transfer of Ly6C<sup>hi</sup> monocytes and voluntary exercise were able to increase neurogenesis in antibiotic-treatment mice, indicating that neurogenesis was not irreversibly impaired and that it is possible to overcome the potential direct effects of antibiotics using appropriate stimuli. From these results we concluded that not the lack of intestinal flora as such determines neurogenesis levels, but that there is a common regulator or messenger, mediating signals from the periphery to the brain and that this mediator is affected by antibiotic and probiotic treatment and exercise. Considering the results presented here as well as the finding that Ly6C<sup>hi</sup> monocytes can support neurosphere formation *in vitro* (data not included in this thesis), we suggest Ly6C<sup>hi</sup> monocytes as a potential mediator.

As Ly6C<sup>hi</sup> monocytes migrate via the bloodstream from the bone marrow to their destined location, we investigated their presence in both tissues. We revealed that antibiotic-induced depletion of microbiota reduces Ly6C<sup>hi</sup> monocyte numbers in the bone marrow. In line with our results, several studies have reported the substantial impact of microbiota on host immunity including their ability to regulate myeloid hematopoiesis in the bone marrow (Hill et al. 2012; Deshmukh et al. 2014). This effect is manifested in a reduced bone marrow-derived monocyte population in the spleen of germ-free mice (Khosravi et al. 2014).

Subsequently, antibiotic treatment also reduced the number of Ly6C<sup>hi</sup> monocytes in the blood. Four weeks after discontinuation of antibiotic treatment, both bone marrow and blood populations had recovered, but the reduced number of Ly6C<sup>hi</sup> monocytes in the brain was still evident. We presume that this is due to the slow turnover rate of peripheral immune cells in the brain as it has been previously described for leukocytes (Ousman & Kubes 2012).

We found no changes of the numbers of microglia, the brain's intrinsic immune cell population, upon any of the treatments. This finding is consistent with a recent study in germ-free mice (Erny et al. 2015). Despite unchanged cell numbers, Erny and colleagues describe alterations of morphology and phenotypic marker expression (Erny et al. 2015). However, it is unclear whether these modifications also occur upon antibiotic treatment as the absence of

microbiota during the entire ontogenesis (in germ-free mice) has more pronounced effects than short-term absence (due to antibiotic treatment), such as impaired brain and immune system development (Mazmanian et al. 2005; Abt et al. 2012; Diaz Heijtz et al. 2011; Cryan & Dinan 2012). As the study by Erny et al. investigated only microglia and missed the important contribution of myeloid-derived cells, a direct comparison of our results to this study is rather difficult. It is likely that some of the changes reported in germ-free mice could be attributed to alterations in the circulating immune cell composition and function.

This basic difference between the two models became further obvious when we quantified neurotrophic factors and did not find differences with respect to *BDNF* and *NGF* mRNA expression. In contrast, germ-free mice present with increased *BDNF* mRNA levels in the hippocampus (Neufeld et al. 2011) and decreased *BDNF* mRNA levels in the amygdala (Arentsen et al. 2015). Increased neurogenesis found in germ-free mice (Ogbonnaya et al. 2015) would correspond to the increased *BDNF* expression (Neufeld et al. 2011) as well as increased motor activity in this model (Diaz Heijtz et al. 2011). Another study reported reduced *BDNF* mRNA levels in the adult hippocampus after early depletion of intestinal microbiota from weaning onwards (Desbonnet et al. 2015). Thus, it becomes apparent that differences between our model and the germ-free model make it difficult to compare these studies.

CCR2<sup>+</sup> Ly6C<sup>hi</sup> monocytes were located mostly in the choroid plexus and only in rare cases in the hippocampus. The remote distance of Ly6C<sup>hi</sup> monocytes from the proliferating neuronal precursors indicates that it is probably soluble factors which mediate this interaction. We could not identify a concrete mechanism, but our results suggest that BDNF, NGF, TNF and IL-6 are not involved, even though they have all been shown to influence neurogenesis (Iosif et al. 2006; Scharfman et al. 2005; Rossi et al. 2006; Frielingsdorf et al. 2007; Islam et al. 2009). It also remains to be investigated whether this regulation has a direct effect on proliferating precursors or it indirectly modulates the neurogenic niche.

Taken together, our results demonstrate that antibiotic treatment results in a long lasting impairment of neurogenesis, which can be reversed by probiotics and exercise. Ly6C<sup>hi</sup> monocytes, a myeloid-derived innate immune cell population, critically contribute to this restoration. While we cannot completely rule out the contribution of other CNS resident cells, our analysis of Ly6C<sup>hi</sup> monocytes in different treatment paradigms in conjunction with the depletion and re-substitution experiments point toward their crucial involvement in maintenance of adult hippocampal neurogenesis. Among the multiple factors forming the gut-

immune-brain-axis, we highlight the synergy between intestinal flora and Ly6C<sup>hi</sup> monocytes as one potential route of communication. Finally, our results provide a rationale for probiotic supplementation and exercise to restore monocyte homeostasis and brain plasticity as countermeasure against the side effects of prolonged antibiotic treatment.

## **4.2 Role of monocytes in Alzheimer's disease**

In the second part of this study, we investigated the effect of the commonly persisting cerebral *Toxoplasma* infection and resulting CNS inflammation on A $\beta$  plaque formation in a murine model of AD. In the following, I will first discuss the etiologic connection between *T. gondii* and AD and how our results contribute to the understanding of this connection. Second, I will address the individual results and evaluate what we learned from this experimental setup with respect to a possible treatment of AD.

### **4.2.1 Etiologic connection between *T. gondii* and AD**

A $\beta$  and hyperphosphorylated tau form disease promoting aggregates in AD that trigger chronic cerebral inflammatory processes (Hickman et al. 2008; Meda et al. 1995). Further modulation of the chronic inflammation may occur following several infectious diseases, which are known to induce inflammatory cascades in the CNS. It is well established that certain pathogenic components modulate the course of disease in murine  $\beta$ -amyloidosis models (Kahn et al. 2012). Although the impact of particular infections during the pathogenesis of AD has been discussed, the underlying mechanisms are especially challenging to untangle (reviewed in Miklossy 2011). Periodontal infections have been found to increase the A $\beta$  load in vulnerable brain areas in non-AD humans (Kamer et al. 2015). The respiratory pathogen *Chlamydia pneumoniae* is more present in human AD patients (Balin et al. 1998) and is also able to induce A $\beta$  plaques in wildtype mice (Little et al. 2004). In general, previous studies have found chronic or latent infections to be associated with an increased risk for AD (reviewed in Miklossy 2011), although evidence regarding *T. gondii* specifically is inconclusive (Kusbeci et al. 2011; Perry et al. 2015). On the other hand, in a recent study using a mouse model of cerebral  $\beta$ -amyloidosis, *T. gondii* infection has been associated with a reduced risk of developing AD-like pathology (Jung et al. 2012). Our study provides further evidence for this notion, as we detected a significant reduction in the number and volume of  $\beta$ -amyloid plaques in *T. gondii* infected compared to non-infected 5xFAD mice.



Despite this observed reduction in plaque deposition, one should be cautious in concluding that *T. gondii* infection may protect against developing AD. In fact, while evidence regarding actual disease risk is sparse and conflicting (Kusbeci et al. 2011; Perry et al. 2015), latent toxoplasmosis in healthy individuals has recently been associated with subtle reductions of cognitive performance in various tasks (Gajewski et al. 2014; Shawn D. Gale et al. 2015; S D Gale et al. 2015). Directly translating this finding to the situation of human AD patients is rather difficult, considering the limitations of the applied experimental model. Low dose infection of mice with the parasite is a broadly used model to mimic human chronic *Toxoplasma* infection (Parlog et al. 2014; Möhle et al. 2014; Biswas et al. 2015; Nance et al. 2012; Z. T. Wang et al. 2015; Blanchard et al. 2015; Gulinello et al. 2010; Haroon et al. 2012; Hermes et al. 2008), although the immune cell recruitment in mice is most likely more pronounced than during latent chronic infection of humans. Considering that we propose the recruited immune cells as major mediators of the beneficial effect, it is unclear which effects are applicable to the human CNS.

#### **4.2.2 Insights regarding the treatment of AD**

As mentioned above, we measured decreased levels of A $\beta$  plaques in the brains of *T. gondii* infected 5xFAD mice and the remaining plaques were also smaller in volume. These findings are consistent with the aforementioned study by Jung and colleagues, where they further described an improved performance in behavioral tests compared to non-infected transgenic mice (Jung et al. 2012).

We performed a more detailed investigation of the A $\beta$  load and detected that the general reduction of A $\beta$  plaques was paralleled by a decrease in small soluble A $\beta$  species. Because higher levels of soluble A $\beta$  has previously been linked to decreased cognitive performance (Zhang et al. 2011; Lesné et al. 2008), this finding suggests that our experimental setup at least partially protects from cognitive decline.

Before studying the direct contribution of immune cells, we outlined the immune response in the brain. We measured increased levels of *IFN- $\gamma$* , *TNF*, *IL-1 $\beta$* , *IL-6*, *IL-10* and *TGF- $\beta$*  mRNA in *T. gondii* infected wildtype and 5xFAD mice compared to respective controls. IFN- $\gamma$  is the key cytokine controlling *T. gondii* infection (Wang et al. 2004; Wang et al. 2005), but also TNF, IL-1 $\beta$  and IL-6 carry out important anti-parasitic effector activities (Jebbari et al. 1998; Schlüter et al. 2003; Hunter et al. 1995). Increased IL-10 and TGF- $\beta$  have been described to counterbalance the inflammation and thus, prevent extensive tissue damage in chronic *T. gondii* infection (Wilson et al. 2005; Cekanaviciute et al. 2014). Interestingly, in addition to

its involvement in the immune reaction against *T. gondii*, IL-6 has been found to induce phagocytic markers and therefore reduce A $\beta$  deposition (Chakrabarty et al. 2010). Overall, the significant changes in cytokine mRNA expression are attributed to the infection and not the mouse genotype. Despite the broad changes in inflammatory gene expression, APP expression remained unaltered in *T. gondii* infected 5xFAD mice compared to non-infected controls and cannot account for the reduced plaque burden.

Curiously, in the study by Jung and colleagues, the authors did not measure elevated IFN- $\gamma$  levels in *T. gondii* infected Tg2576 mice despite using the same parasite strain as we did and an even higher infection dose (Jung et al. 2012). With respect to the experimental setup, the main difference between their study and ours is the mouse model. Due to only one genetic mutation, Tg2576 mice start to develop plaques only at the age of 9 months (Chin 2011), while the 5xFAD mice used by us already show plaque deposition starting from the age of 2 months (Chin 2011; Fröhlich et al. 2013). This faster progression allows for shorter experiment times, but both transgenic models are based on the C57BL/6 background (Chin 2011) and thus, show a high susceptibility to the infection with *T. gondii* compared to other mouse strains like Balb/c (Dupont et al. 2012).

Consequently, our histopathological evaluation revealed substantial changes in both cortical and subcortical brain regions of infected mice, indicating the infiltration by immune cells (monocytes and lymphocytes) and the pronounced activation of resident microglia and astrocytes. These observations point toward a functional role for resident and recruited immune cells in reducing the A $\beta$  burden.

Controlling the infection with *T. gondii* requires the collaboration of innate and adaptive immunity (Dupont et al. 2012). Even though there are inflammatory diseases of the CNS which involve adaptive immune cells, such as multiple sclerosis, the inflammation observed in AD seems to be restricted to innate immune cells (Heppner et al. 2015). Thus, we focused our further analysis on the contribution of the innate compartment.

The detailed analysis of infiltrating immune cells confirmed the strong recruitment of innate immune cells, particularly CD45<sup>hi</sup> CD11b<sup>hi</sup> myeloid cells, to the brains of *T. gondii* infected 5xFAD mice, similar to that seen in wildtype mice. It has been described previously by our group that in mice chronically infected with *T. gondii*, Ly6C<sup>hi</sup> monocytes migrate to the CNS and further differentiate into Ly6C<sup>int</sup> mononuclear cells and Ly6C<sup>low</sup> macrophages in order to carry out specific tasks in host defense, such as cytokine production and Fc receptor mediated cellular phagocytosis (Biswas et al. 2015; Möhle et al. 2014).

We analyzed the contribution of these myeloid-derived mononuclear cell subsets in the process of accumulating A $\beta$  plaques that, according to the widely accepted view on AD pathophysiology, ultimately promote neurodegeneration.

*Ex vivo* phagocytosis assay most likely by an antibody-independent mechanism revealed that all recruited mononuclear subpopulations were able to take up significantly more A $\beta_{42}$  than microglia from non-infected or activated microglia from *T. gondii* infected 5xFAD mice. We found that Ly6C<sup>hi</sup> monocytes displayed an even higher uptake compared to Ly6C<sup>low</sup> cells. Comparing the ability to take up A $\beta_{42}$  with the ability to take up latex spheres as previously published (Biswas et al. 2015), we noted a difference with respect to the Ly6C<sup>hi</sup> and Ly6C<sup>int</sup> subsets. While their uptake of latex spheres is very low (Biswas et al. 2015), they displayed a prominent uptake of A $\beta_{42}$ . Even though our results are against the general view that Ly6C<sup>low</sup> cells are the most macrophage-like subset, other publications have attributed phagocytic activity to Ly6C<sup>+</sup> monocytes against parasites (Sponaas et al. 2009; Sheel & Engwerda 2012). Thus, we conclude that uptake of latex beads and A $\beta_{42}$  is mediated by different mechanisms with diverse appearance in Ly6C<sup>hi</sup> monocytes and Ly6C<sup>low</sup> macrophages.

While neuroinflammation has been conventionally reported to be detrimental and associated with several neurological diseases (London et al. 1996; Akiyama et al. 2000; Lyman et al. 2013), emerging research promotes a more differentiated view on the roles of recruited immune cells in homeostatic and repair mechanisms (Shechter et al. 2009; Ziv et al. 2006; Frenkel et al. 2005; Pahnke et al. 2013; Fröhlich et al. 2013). Consistent with this concept, there are a growing number of reports indicating the beneficial effect of recruited immune cells in AD and vascular amyloidosis (Simard et al. 2006; Naert & Rivest 2012b; El Khoury et al. 2007; Hawkes & McLaurin 2009; Michaud et al. 2013; Koronyo et al. 2015).

Performing the *ex vivo* phagocytosis assay with cells obtained from both wildtype and 5xFAD mice, we also observed that the relative contributions were independent of the genotype, despite absolute values being different. As these differences were most likely caused by the different quantification methods, we conclude that wildtype cells are potent A $\beta$  clearing cells as well. Importantly, this finding suggests that cells probably do not have to be pre-exposed to A $\beta$  to efficiently phagocytose A $\beta$  in a possible treatment strategy. It is somehow challenging that human macrophages were found to be ineffective at A $\beta$  phagocytosis when derived from AD patients (Fiala et al. 2005). Nevertheless, modulating the route of entry may provide a tool to skew recruited monocytes towards an inflammation resolving phenotype (Schwartz & Baruch 2014) and the capacity of these manipulated monocytes to remove A $\beta$  remains to be

investigated, as two studies have found that the replacement of brain resident microglia with peripheral myeloid cells does not reduce the A $\beta$  burden (Prokop et al. 2015; Varvel et al. 2015). Both studies used a similar approach to replace microglia with peripheral cells, i. e. depletion of brain resident CD11b-expressing cells during a 10 to 14 days intracerebral ganciclovir treatment of CD11b-HSVTK (herpes simplex virus thymidine kinase) transgenic mice (Prokop et al. 2015; Varvel et al. 2015). This treatment leads to a one-time replacement with bone marrow-derived myeloid cells, as opposed to the continuous influx observed in our model of chronic cerebral *T. gondii* infection. Additionally, Prokop and colleagues point out the lack of an activating stimulus in their model, which would be able to induce the uptake of A $\beta$  by myeloid cells (Prokop et al. 2015). Even though this lack of stimulation is resolved in our experimental model, finding appropriate stimuli to manipulate the cells is a complex task, as we have to keep in mind that beneficial and detrimental effects of monocytes and macrophages can occur at the same time (Gensel et al. 2009).

The increased amount of A $\beta_{42}$  detected following CCR2<sup>hi</sup> Ly6C<sup>hi</sup> monocyte ablation in infected 5xFAD mice points to a causal role of these cells to A $\beta$  clearance. Our findings are supported by a report from Naert and Rivest, who have linked the lack of Ly6C<sup>hi</sup> (CX3CR1<sup>low</sup> CCR2<sup>+</sup> Gr1<sup>+</sup>) monocytes to cognitive decline in APP<sub>Swe</sub>/PS1 mice (Naert & Rivest 2012a). This hypothesis is further strengthened by two recent studies where myeloid cell recruitment to the CNS was correlated with A $\beta$  plaque reduction (Koronyo et al. 2015; Hohsfield & Humpel 2015). In a very recently published study, Baruch and colleagues proposed a novel treatment strategy to target AD via programmed death-1 (PD-1) inhibition and thereby increasing the recruitment of Ly6C<sup>hi</sup> monocytes to the CNS in an IFN- $\gamma$  dependent manner (Baruch et al. 2016). The proposed mechanisms included enhanced cellular uptake and degradation. Furthermore, Savage et al. detected phagocytic cells directly associated with plaques, and the CD45<sup>hi</sup> status of these cells suggested their myeloid origin (Savage et al. 2015). Only short-term recruitment of monocytes did not alter plaque deposition as seen in a mouse model of traumatic brain injury (Collins et al. 2015).

Having confirmed Ly6C<sup>hi</sup> monocytes as key contributors to A $\beta$  removal in our model, we were interested if they migrate into the parenchyma to “attack” A $\beta$  plaques like previous reports have shown (Mildner et al. 2011; Simard et al. 2006; Hohsfield & Humpel 2015). However, CCR2<sup>+</sup> Ly6C<sup>+</sup> monocytes were not located in the vicinity of plaques in our experiments. Therefore, we propose that the low plaque burden in the applied experimental model is due to Ly6C<sup>hi</sup> monocytes’ increased capacity to remove soluble A $\beta$  rather than due to direct removal of established plaques. In addition, monocyte-derived Ly6C<sup>low</sup> macrophages

upregulate F4/80 and Iba1, and can be located adjacent to the plaques, similarly to resident microglia.

It has to be carefully investigated, at which stages of disease the recruitment of monocytes and subsequent removal of A $\beta$  is beneficial and can delay the onset of disease, and at which stages the cascade triggered by A $\beta$  is already on its way and additional cell recruitment potentially worsens neuroinflammation (Musiek & Holtzman 2015). Our data from old animals provides evidence that the ability of freshly recruited immune cells to remove A $\beta$  persists at later stages of experimental amyloidosis.

Searching for a mechanism mediating A $\beta$  uptake, we analyzed the expression of cell surface markers related to phagocytosis on CD11b<sup>hi</sup> Ly6G<sup>-</sup> myeloid-derived cells. The measurements revealed intermediate levels of TREM2, CD36 and SCARA1 on Ly6C<sup>hi</sup> monocytes and high levels on Ly6C<sup>low</sup> monocyte-derived macrophages. Recent reports of a correlation between genetic TREM2 mutation and AD (Jonsson et al. 2013; Guerreiro et al. 2013), along with experiments pointing out the anti-inflammatory and phagocytosis-enhancing role of TREM2, have drawn the attention towards this molecule (Jones et al. 2014; Jiang et al. 2013; Cantoni et al. 2015; Y. Wang et al. 2015). We detected that monocyte-derived Ly6C<sup>low</sup> macrophages expressed high levels of TREM2, in contrast to Ly6C<sup>hi</sup> monocytes. This result underlines that, besides TREM2, other factors may determine the capacity of immune cells such as monocytes to phagocytose A $\beta$ . Several studies have suggested that CD36 expression is associated with A $\beta$  uptake (Yamanaka et al. 2012; Koenigsnecht & Landreth 2004; Hickman et al. 2008), consistent with the CD36 expression of Ly6C<sup>low</sup> monocyte-derived macrophages. Moreover, the lower expression of CD36 detected on Ly6C<sup>hi</sup> monocytes may be beneficial because of less harmful pro-inflammatory CD36-A $\beta$  interaction (Kagan & Horng 2013; Frenkel et al. 2013; Moore et al. 2002; Wilkinson & El Khoury 2012). Frenkel and colleagues had shown that SCARA1 (and not CD36) mediates phagocytosis of A $\beta$  (Frenkel et al. 2013). However, similar to TREM2 and CD36, SCARA1 expression was not a reliable predictor of the A $\beta$  phagocytic capacity of each myeloid-derived mononuclear cell subset in our model.

Recent research highlights the importance of proteolytic A $\beta$  degradation. Several enzymes are known to digest A $\beta$ , including MMP9 and IDE, but the contribution of each enzyme is crucial. Removal of only one can result in significantly increased cerebral A $\beta$  levels (Saido & Leissring 2012), and overexpression leads to decreased A $\beta$  loads (Leissring et al. 2003; Hoshino et al. 2011; Saido & Leissring 2012). We found both MMP9 and IDE upregulated significantly upon *T. gondii* infection in 5xFAD mice.

MMP9 is one of several matrix metalloproteinases that have been implicated in A $\beta$  degradation and administration of an MMP inhibitor resulted in increased A $\beta$  loads (Saido & Leissring 2012). Activation of MMPs has to be regarded carefully as well, as a recent study has shown that A $\beta$  increases the permeability of the BCSFB by activation of MMPs (Brkic et al. 2015). Even though Brkic and colleagues found the biggest changes for MMP3 expression, the contribution of other MMPs cannot be ruled out. IDE has several substrates and exists as a cytosolic, membranous, and secreted variant (Wang et al. 2006), which can be ubiquitously found in human tissue including immune cells like granulocytes (Weirich et al. 2008). It hydrolytically cleaves A $\beta$  (Mukherjee et al. 2000), and the significantly increased expression of *IDE*, particularly in conjunction with the simultaneously increased *MMP9* expression, therefore most likely promoted the enhanced degradation of A $\beta$  in *T. gondii* infected 5xFAD mice, when compared to non-infected controls. Upregulation of *IDE* may be a compensatory mechanism, since insulin has been shown to stimulate the growth of *T. gondii* *in vitro* (Zhu et al. 2006), and increased A $\beta$  degradation could be a beneficial secondary effect. An interesting, yet unanswered question is whether IDE family members expressed by *T. gondii* itself (Laliberté & Carruthers 2011) could also contribute to A $\beta$  degradation. Their substrates are, however, not currently known, although structural analysis suggests that *T. gondii* IDEs may be different from other family members (Hajagos et al. 2012).

In addition, intracellular control of protein homeostasis is mediated by the ubiquitin-proteasome system (UPS), whereby proteasomes represent the proteolytically active part. Dysfunction of the UPS has been shown to be an early event in AD, suggesting that proteasomes may be unable to properly degrade ubiquitin-tagged proteins (Dantuma & Bott 2014). Immunoproteasomes are specific proteasome isoforms that have incorporated immunosubunits instead of the conventional proteases. Data not included in this thesis (Möhle et al. 2016) suggest a possible involvement of the immunoproteasome in A $\beta$  degradation particularly by monocytes. The exact engagement of the UPS in the mentioned processes still requires detailed investigation in forthcoming experiments.

Taken together, our results demonstrate that mononuclear cell recruitment to the brain upon chronic *T. gondii* infection leads to reduced plaque burden by promoting phagocytosis of soluble A $\beta_{42}$  and enhanced proteolytic degradation. This aspect is especially critical in a situation where resident microglia are dysfunctional and fail to control amyloid plaque deposition (Hickman et al. 2008; Orre et al. 2014). Chronic *T. gondii* infection acts as a strong immunological stimulus, possibly even overcoming the impaired phagocytic capacities of monocytes/macrophages as observed in AD patients (Fiala et al. 2005). In the light of a future

treatment option, a recent study by Neal and Knoll presented data from mice showing that infection with *T. gondii* protects from bacterial infection with *Listeria monocytogenes* by recruitment of Ly6C<sup>hi</sup> monocytes. Further experiments revealed that only application of a component of *T. gondii* is sufficient to mediate the resistance (Neal & Knoll 2014). This method of recruiting monocytes may be interesting to consider, as our results suggest a promising candidate mechanism for the protective effect, namely increased phagocytosis and degradation of A $\beta$ .

### 4.3 Conclusions

With two distinct experimental setups I could demonstrate that Ly6C<sup>hi</sup> monocytes significantly contribute to brain homeostasis, in addition to their well-established roles in inflammatory and infectious conditions. I have presented evidence that they link changes in neurogenesis to an altered gut flora and physical exercise, and that they are also highly potent A $\beta$  removing cells. As discussed above, these findings add to an increasing body of work which focusses on the beneficial effects of monocytes and possible therapeutic applications. Although the experiments presented in this thesis were conducted exclusively in mouse models, the results open the door for subsequent studies with human subjects.

While my thesis has focused on one particular subset of innate immune cells, the immune system is extremely complex and new types of immune cells are still being discovered e. g. certain ILCs have emerged only in the past years. Thus, it is very likely that future research will discover more diverse roles for other immune cell types.

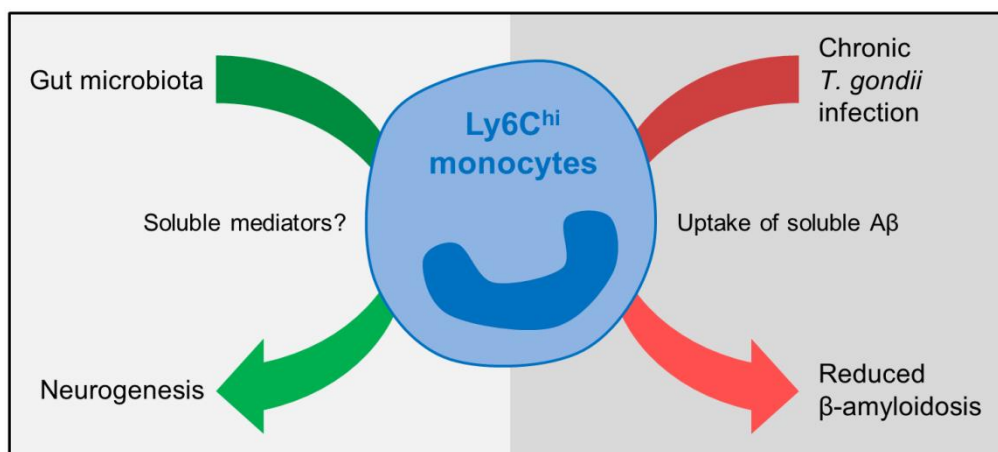


Figure 4.1: Graphical summary

## References

- Abbott, N.J., Rönnebeck, L. & Hansson, E., 2006. Astrocyte-endothelial interactions at the blood-brain barrier. *Nature reviews. Neuroscience*, 7(1), pp.41–53.
- Abt, M.C. et al., 2012. Commensal bacteria calibrate the activation threshold of innate antiviral immunity. *Immunity*, 37(1), pp.158–70.
- Aguzzi, A., Barres, B.A. & Bennett, M.L., 2013. Microglia: scapegoat, saboteur, or something else? *Science (New York, N.Y.)*, 339(6116), pp.156–61.
- Ait-Belgnaoui, A. et al., 2014. Probiotic gut effect prevents the chronic psychological stress-induced brain activity abnormality in mice. *Neurogastroenterology and motility: the official journal of the European Gastrointestinal Motility Society*, 26(4), pp.510–20.
- Ajami, B. et al., 2007. Local self-renewal can sustain CNS microglia maintenance and function throughout adult life. *Nature neuroscience*, 10(12), pp.1538–1543.
- Akiyama, H. et al., 2000. Inflammation and Alzheimer's disease. *Neurobiology of aging*, 21(3), pp.383–421.
- Akiyama, H. et al., 1996. The amino-terminally truncated forms of amyloid  $\beta$ -protein in brain macrophages in the ischemic lesions of Alzheimer's disease patients. *Neuroscience Letters*, 219(2), pp.115–118.
- Altman, J. & Das, G.D., 1967. Postnatal neurogenesis in the guinea-pig. *Nature*, 214(5093), pp.1098–1101.
- Alzheimer, A., Förstl, H. & Levy, R., 1991. On certain peculiar diseases of old age. *History of psychiatry*, 2(5 Pt 1), pp.71–101.
- Arango Duque, G. & Descoteaux, A., 2014. Macrophage cytokines: involvement in immunity and infectious diseases. *Frontiers in immunology*, 5(October), p.491.
- Arck, P.C. et al., 2008. The alchemy of immune privilege explored from a neuroimmunological perspective. *Current opinion in pharmacology*, 8(4), pp.480–9.
- Arentsen, T. et al., 2015. Host microbiota modulates development of social preference in mice. *Microbial ecology in health and disease*, 26, p.29719.
- Arnold, L. et al., 2007. Inflammatory monocytes recruited after skeletal muscle injury switch into antiinflammatory macrophages to support myogenesis. *The Journal of experimental medicine*, 204(5), pp.1057–69.
- Auffray, C. et al., 2007. Monitoring of blood vessels and tissues by a population of monocytes with patrolling behavior. *Science (New York, N.Y.)*, 317(5838), pp.666–70.
- Auffray, C., Sieweke, M.H. & Geissmann, F., 2009. Blood monocytes: development, heterogeneity, and relationship with dendritic cells. *Annual review of immunology*, 27, pp.669–692.
- Balin, B.J. et al., 1998. Identification and localization of Chlamydia pneumoniae in the Alzheimer's brain. *Medical microbiology and immunology*, 187(1), pp.23–42.
- Baruch, K. et al., 2016. PD-1 immune checkpoint blockade reduces pathology and improves memory in mouse models of Alzheimer's disease. *Nature medicine*, (October 2015), pp.1–5.
- Bekris, L.M. et al., 2010. Genetics of Alzheimer disease. *Journal of geriatric psychiatry and neurology*, 23(4), pp.213–27.
- Berer, K. et al., 2011. Commensal microbiota and myelin autoantigen cooperate to trigger autoimmune demyelination. *Nature*, 479(7374), pp.538–41.
- Bereswill, S. et al., 2014. The impact of Toll-like-receptor-9 on intestinal microbiota composition and extra-intestinal sequelae in experimental Toxoplasma gondii induced ileitis. *Gut pathogens*, 6, p.19.
- Biswas, A. et al., 2015. Ly6Chigh Monocytes Control Cerebral Toxoplasmosis. *Journal of immunology (Baltimore, Md. : 1950)*, 194(7), pp.3223–3235.
- Blanchard, N., Dunay, I.R. & Schlüter, D., 2015. Persistence of Toxoplasma gondii in the central nervous system: a fine-tuned balance between the parasite, the brain and the immune system. *Parasite immunology*, 37(3), pp.150–8.
- Boissonneault, V. et al., 2009. Powerful beneficial effects of macrophage colony-stimulating



- factor on beta-amyloid deposition and cognitive impairment in Alzheimer's disease. *Brain: a journal of neurology*, 132(Pt 4), pp.1078–1092.
- Braak, H. & Braak, E., 1991. Neuropathological staging of Alzheimer-related changes. *Acta neuropathologica*, 82(4), pp.239–59.
- Brkic, M. et al., 2015. Amyloid  $\beta$  Oligomers Disrupt Blood-CSF Barrier Integrity by Activating Matrix Metalloproteinases. *The Journal of neuroscience: the official journal of the Society for Neuroscience*, 35(37), pp.12766–78.
- Bruce-Keller, A.J. et al., 2015. Obese-type gut microbiota induce neurobehavioral changes in the absence of obesity. *Biological psychiatry*, 77(7), pp.607–15.
- Butovsky, O. et al., 2006. Microglia activated by IL-4 or IFN-gamma differentially induce neurogenesis and oligodendrogenesis from adult stem/progenitor cells. *Molecular and cellular neurosciences*, 31(1), pp.149–60.
- Cadwell, K., 2015. Expanding the role of the virome: commensalism in the gut. *Journal of virology*, 89(4), pp.1951–3.
- Cantoni, C. et al., 2015. TREM2 regulates microglial cell activation in response to demyelination in vivo. *Acta Neuropathologica*, 129, pp.429–447.
- Cekanaviciute, E. et al., 2014. Astrocytic TGF- $\beta$  Signaling Limits Inflammation and Reduces Neuronal Damage during Central Nervous System Toxoplasma Infection. *Journal of immunology (Baltimore, Md. : 1950)*, 193(1), pp.139–49.
- Chakrabarty, P. et al., 2010. Massive gliosis induced by interleukin-6 suppresses A $\beta$  deposition in vivo: evidence against inflammation as a driving force for amyloid deposition. *FASEB journal: official publication of the Federation of American Societies for Experimental Biology*, 24(2), pp.548–59.
- Chin, J., 2011. Selecting a Mouse Model of Alzheimer's Disease. E. D. Roberson, ed. *Methods in Molecular Biology*, 670.
- Chua, C.L.L. et al., 2013. Monocytes and macrophages in malaria: protection or pathology? *Trends in parasitology*, 29(1), pp.26–34.
- Clark, R.T. et al., 2011. T-cell production of matrix metalloproteinases and inhibition of parasite clearance by TIMP-1 during chronic Toxoplasma infection in the brain. *ASN neuro*, 3(1), p.e00049.
- Collins, J.M. et al., 2015. The effect of focal brain injury on beta-amyloid plaque deposition, inflammation and synapses in the APP/PS1 mouse model of Alzheimer's disease. *Experimental neurology*, 267, pp.219–29.
- Courret, N. et al., 2006. CD11c- and CD11b-expressing mouse leukocytes transport single Toxoplasma gondii tachyzoites to the brain. *Blood*, 107(1), pp.309–16.
- Crouzet, L. et al., 2013. The hypersensitivity to colonic distension of IBS patients can be transferred to rats through their fecal microbiota. *Neurogastroenterology and motility: the official journal of the European Gastrointestinal Motility Society*, 25(4), pp.e272–82.
- Croxford, J.L. & Yamamura, T., 2005. Cannabinoids and the immune system: potential for the treatment of inflammatory diseases? *Journal of neuroimmunology*, 166(1-2), pp.3–18.
- Cryan, J.F. & Dinan, T.G., 2012. Mind-altering microorganisms: the impact of the gut microbiota on brain and behaviour. *Nature reviews. Neuroscience*, 13(10), pp.701–12.
- Dantuma, N.P. & Bott, L.C., 2014. The ubiquitin-proteasome system in neurodegenerative diseases: precipitating factor, yet part of the solution. *Frontiers in molecular neuroscience*, 7(July), p.70.
- Davies, L.C. et al., 2013. Tissue-resident macrophages. *Nature immunology*, 14(10), pp.986–95.
- Delves, P.J. & Roitt, I.M., 2000. The immune system. First of two parts. *The New England journal of medicine*, 343(1), pp.37–49.
- Deng, W., Aimone, J.B. & Gage, F.H., 2010. New neurons and new memories: how does adult hippocampal neurogenesis affect learning and memory? *Nature reviews. Neuroscience*, 11(5), pp.339–350.
- Desbonnet, L. et al., 2015. Gut microbiota depletion from early adolescence in mice: Implications for brain and behaviour. *Brain, behavior, and immunity*, 48, pp.165–73.
- Deshmukh, H.S. et al., 2014. The microbiota regulates neutrophil homeostasis and host resistance to Escherichia coli K1 sepsis in neonatal mice. *Nature medicine*, 20(5), pp.524–30.
- Diaz Heijtz, R. et al., 2011. Normal gut microbiota modulates brain development and behavior. *Proceedings of the National Academy of*

## REFERENCES

- Sciences of the United States of America*, 108(7), pp.3047–52.
- Dicksved, J. et al., 2014. Susceptibility to *Campylobacter* Infection Is Associated with the Species Composition of the Human Fecal Microbiota. *mBio*, 5(5), pp.e01212–14–e01212–14.
- Diefenbach, A., Colonna, M. & Koyasu, S., 2014. Development, differentiation, and diversity of innate lymphoid cells. *Immunity*, 41(3), pp.354–65.
- Dunay, I.R. et al., 2008. Gr1(+) inflammatory monocytes are required for mucosal resistance to the pathogen *Toxoplasma gondii*. *Immunity*, 29(2), pp.306–17.
- Dunay, I.R., Fuchs, A. & Sibley, L.D., 2010. Inflammatory monocytes but not neutrophils are necessary to control infection with *Toxoplasma gondii* in mice. *Infection and immunity*, 78(4), pp.1564–70.
- Dupont, C.D., Christian, D.A. & Hunter, C.A., 2012. Immune response and immunopathology during toxoplasmosis. *Seminars in immunopathology*.
- Eckburg, P.B. et al., 2005. Diversity of the human intestinal microbial flora. *Science (New York, N.Y.)*, 308(5728), pp.1635–8.
- Ekdahl, C.T. et al., 2003. Inflammation is detrimental for neurogenesis in adult brain. *Proceedings of the National Academy of Sciences of the United States of America*, 100(23), pp.13632–13637.
- Eriksson, P.S. et al., 1998. Neurogenesis in the adult human hippocampus. *Nature medicine*, 4(11), pp.1313–7.
- Erny, D. et al., 2015. Host microbiota constantly control maturation and function of microglia in the CNS. *Nature neuroscience*, 18(7), pp.965–977.
- Fanselow, M.S. & Dong, H.-W., 2010. Are the dorsal and ventral hippocampus functionally distinct structures? *Neuron*, 65(1), pp.7–19.
- Farina, C., Aloisi, F. & Meinl, E., 2007. Astrocytes are active players in cerebral innate immunity. *Trends in Immunology*, 28(3), pp.138–145.
- Farioli-Vecchioli, S. et al., 2014. Running rescues defective adult neurogenesis by shortening the length of the cell cycle of neural stem and progenitor cells. *Stem cells (Dayton, Ohio)*, 32(7), pp.1968–82.
- Fiala, M. et al., 2005. Ineffective phagocytosis of amyloid-beta by macrophages of Alzheimer's disease patients. *Journal of Alzheimer's disease : JAD*, 7(3), pp.221–32; discussion 255–62.
- Fischer, H.G., Bonifas, U. & Reichmann, G., 2000. Phenotype and functions of brain dendritic cells emerging during chronic infection of mice with *Toxoplasma gondii*. *Journal of immunology (Baltimore, Md. : 1950)*, 164(9), pp.4826–34.
- Flannagan, R.S., Jaumouillé, V. & Grinstein, S., 2012. The Cell Biology of Phagocytosis. *Annual Review of Pathology: Mechanisms of Disease*, 7(1), pp.61–98.
- Förstl, H. & Kurz, A., 1999. Clinical features of Alzheimer's disease. *European archives of psychiatry and clinical neuroscience*, 249(6), pp.288–290.
- Frenkel, D. et al., 2005. Neuroprotection by IL-10-producing MOG CD4+ T cells following ischemic stroke. *Journal of the neurological sciences*, 233(1-2), pp.125–32.
- Frenkel, D. et al., 2013. Scara1 deficiency impairs clearance of soluble amyloid- $\beta$  by mononuclear phagocytes and accelerates Alzheimer's-like disease progression. *Nature communications*, 4, p.2030.
- Frielingsdorf, H. et al., 2007. Nerve growth factor promotes survival of new neurons in the adult hippocampus. *Neurobiology of disease*, 26(1), pp.47–55.
- Fröhlich, C. et al., 2013. Genomic background-related activation of microglia and reduced  $\beta$ -amyloidosis in a mouse model of Alzheimer's disease. *European journal of microbiology & immunology*, 3(1), pp.21–27.
- Fukami, S. et al., 2002. Abeta-degrading endopeptidase, neprilysin, in mouse brain: synaptic and axonal localization inversely correlating with Abeta pathology. *Neuroscience research*, 43(1), pp.39–56.
- Gaddi, P.J. & Yap, G.S., 2007. Cytokine regulation of immunopathology in toxoplasmosis. *Immunology and cell biology*, 85(2), pp.155–9.
- Gajewski, P.D. et al., 2014. *Toxoplasma gondii* impairs memory in infected seniors. *Brain, behavior, and immunity*, 36, pp.193–9.
- Gale, S.D. et al., 2015. Association between latent toxoplasmosis and cognition in adults: a cross-sectional study. *Parasitology*, 142(4), pp.557–65.
- Gale, S.D. et al., 2015. Infectious Disease Burden and Cognitive Function in Young to Middle-Aged Adults. *Brain, behavior, and immunity*.

## REFERENCES

- Gavazzi, G. & Krause, K.-H., 2002. Ageing and infection. *The Lancet Infectious Diseases*, 2(11), pp.659–66.
- Geissmann, F. et al., 2010. Development of monocytes, macrophages, and dendritic cells. *Science (New York, N.Y.)*, 327(5966), pp.656–661.
- Geissmann, F., Jung, S. & Littman, D.R., 2003. Blood monocytes consist of two principal subsets with distinct migratory properties. *Immunity*, 19(1), pp.71–82.
- Gensel, J.C. et al., 2009. Macrophages promote axon regeneration with concurrent neurotoxicity. *The Journal of neuroscience : the official journal of the Society for Neuroscience*, 29(12), pp.3956–3968.
- Getts, D.R. et al., 2008. Ly6c+ “inflammatory monocytes” are microglial precursors recruited in a pathogenic manner in West Nile virus encephalitis. *The Journal of experimental medicine*, 205(10), pp.2319–37.
- Ginhoux, F. et al., 2010. Fate mapping analysis reveals that adult microglia derive from primitive macrophages. *Science (New York, N.Y.)*, 330(6005), pp.841–845.
- Gordon, S., 2002. Pattern recognition receptors: Doubling up for the innate immune response. *Cell*, 111(7), pp.927–930.
- Gordon, S. & Taylor, P.R., 2005. Monocyte and macrophage heterogeneity. *Nature reviews. Immunology*, 5(12), pp.953–64.
- Grathwohl, S.A. et al., 2009. Formation and maintenance of Alzheimer’s disease beta-amyloid plaques in the absence of microglia. *Nature neuroscience*, 12(11), pp.1361–3.
- Guarner, F. & Malagelada, J.-R., 2003. Gut flora in health and disease. *Lancet*, 361(9356), pp.512–9.
- Guerreiro, R. et al., 2013. TREM2 variants in Alzheimer’s disease. *The New England journal of medicine*, 368(2), pp.117–27.
- Gulinello, M. et al., 2010. Acquired infection with *Toxoplasma gondii* in adult mice results in sensorimotor deficits but normal cognitive behavior despite widespread brain pathology. *Microbes and infection / Institut Pasteur*, 12(7), pp.528–37.
- Haag, L.-M. et al., 2012. Intestinal microbiota shifts towards elevated commensal *Escherichia coli* loads abrogate colonization resistance against *Campylobacter jejuni* in mice. *PloS one*, 7(5), p.e35988.
- Haass, C. et al., 2012. Trafficking and proteolytic processing of APP. *Cold Spring Harbor perspectives in medicine*, 2(5), p.a006270.
- Hajagos, B.E. et al., 2012. Molecular dissection of novel trafficking and processing of the *Toxoplasma gondii* rhoptry metalloprotease toxolysin-1. *Traffic (Copenhagen, Denmark)*, 13(2), pp.292–304.
- Hammond, M.D. et al., 2014.  $\alpha 4$  integrin is a regulator of leukocyte recruitment after experimental intracerebral hemorrhage. *Stroke; a journal of cerebral circulation*, 45(8), pp.2485–7.
- Hanisch, U.K., 2002. Microglia as a source and target of cytokines. *Glia*, 40(2), pp.140–155.
- Hardy, J. & Selkoe, D.J., 2002. The amyloid hypothesis of Alzheimer’s disease: progress and problems on the road to therapeutics. *Science (New York, N.Y.)*, 297(5580), pp.353–6.
- Hardy, J.A. & Higgins, G.A., 1992. Alzheimer’s disease: the amyloid cascade hypothesis. *Science (New York, N.Y.)*, 256(5054), pp.184–185.
- Haroon, F. et al., 2012. *Toxoplasma gondii* actively inhibits neuronal function in chronically infected mice. *PloS one*, 7(4), p.e35516.
- Hawkes, C.A. & McLaurin, J., 2009. Selective targeting of perivascular macrophages for clearance of beta-amyloid in cerebral amyloid angiopathy. *Proceedings of the National Academy of Sciences of the United States of America*, 106(4), pp.1261–6.
- Heimesaat, M.M. et al., 2006. Gram-Negative Bacteria Aggravate Murine Small Intestinal Th1-Type Immunopathology following Oral Infection with *Toxoplasma gondii*. *The Journal of Immunology*, 177(12), pp.8785–8795.
- Heneka, M.T. et al., 2015. Neuroinflammation in Alzheimer’s disease. *The Lancet Neurology*, 14(4), pp.388–405.
- Heppner, F.L., Ransohoff, R.M. & Becher, B., 2015. Immune attack: the role of inflammation in Alzheimer disease. *Nature Reviews Neuroscience*, 16(6), pp.358–372.
- Hermes, G. et al., 2008. Neurological and behavioral abnormalities, ventricular dilatation, altered cellular functions, inflammation, and neuronal injury in brains of mice due to common, persistent, parasitic infection. *Journal of neuroinflammation*, 5, p.48.
- Hickman, S.E., Allison, E.K. & El Khoury, J., 2008. Microglial dysfunction and defective

## REFERENCES

- beta-amyloid clearance pathways in aging Alzheimer's disease mice. *The Journal of neuroscience: the official journal of the Society for Neuroscience*, 28(33), pp.8354–60.
- Hill, D.A. et al., 2012. Commensal bacteria-derived signals regulate basophil hematopoiesis and allergic inflammation. *Nature medicine*, 18(4), pp.538–46.
- Hofrichter, J. et al., 2013. Reduced Alzheimer's disease pathology by St. John's Wort treatment is independent of hyperforin and facilitated by ABCC1 and microglia activation in mice. *Current Alzheimer research*, 10(10), pp.1057–69.
- Hohsfield, L.A. & Humpel, C., 2015. Intravenous Infusion of Monocytes Isolated from 2-Week-Old Mice Enhances Clearance of Beta-Amyloid Plaques in an Alzheimer Mouse Model. *Plos One*, 10(4), p.e0121930.
- Holmes, C., 2013. Review: systemic inflammation and Alzheimer's disease. *Neuropathology and applied neurobiology*, 39(1), pp.51–68.
- Holmes, C. et al., 2003. Systemic infection, interleukin 1beta, and cognitive decline in Alzheimer's disease. *Journal of neurology, neurosurgery, and psychiatry*, 74(6), pp.788–9.
- Hooper, L. V, Littman, D.R. & Macpherson, A.J., 2012. Interactions between the microbiota and the immune system. *Science (New York, N.Y.)*, 336(6086), pp.1268–73.
- Hoshino, T. et al., 2011. Suppression of Alzheimer's disease-related phenotypes by expression of heat shock protein 70 in mice. *The Journal of neuroscience: the official journal of the Society for Neuroscience*, 31(14), pp.5225–34.
- Hunter, C.A., Chizzonite, R. & Remington, J.S., 1995. IL-1 beta is required for IL-12 to induce production of IFN-gamma by NK cells. A role for IL-1 beta in the T cell-independent mechanism of resistance against intracellular pathogens. *Journal of immunology (Baltimore, Md. : 1950)*, 155(9), pp.4347–54.
- Ichinohe, T. et al., 2011. Microbiota regulates immune defense against respiratory tract influenza A virus infection. *Proceedings of the National Academy of Sciences of the United States of America*, 108(13), pp.5354–9.
- Iosif, R.E. et al., 2006. Tumor necrosis factor receptor 1 is a negative regulator of progenitor proliferation in adult hippocampal neurogenesis. *The Journal of neuroscience: the official journal of the Society for Neuroscience*, 26(38), pp.9703–12.
- Islam, O. et al., 2009. Interleukin-6 and neural stem cells: more than gliogenesis. *Molecular biology of the cell*, 20(1), pp.188–99.
- Itagaki, S. et al., 1989. Relationship of microglia and astrocytes to amyloid deposits of Alzheimer disease. *Journal of neuroimmunology*, 24(3), pp.173–82.
- Iwata, N. et al., 2001. Metabolic regulation of brain Abeta by neprilysin. *Science (New York, N.Y.)*, 292(5521), pp.1550–1552.
- Jebbari, H. et al., 1998. A protective role for IL-6 during early infection with *Toxoplasma gondii*. *Parasite immunology*, 20(5), pp.231–9.
- Jiang, T. et al., 2013. TREM2 in Alzheimer's disease. *Molecular neurobiology*, 48(1), pp.180–5.
- John, B. et al., 2011. Analysis of behavior and trafficking of dendritic cells within the brain during toxoplasmic encephalitis. *PLoS pathogens*, 7(9), p.e1002246.
- Jones, B.M. et al., 2014. Regulating amyloidogenesis through the natural triggering receptor expressed in myeloid/microglial cells 2 (TREM2). *Frontiers in cellular neuroscience*, 8(March), p.94.
- Jones, J.L. et al., 2001. *Toxoplasma gondii* infection in the United States: seroprevalence and risk factors. *American journal of epidemiology*, 154(4), pp.357–65.
- Jonsson, T. et al., 2013. Variant of TREM2 associated with the risk of Alzheimer's disease. *The New England journal of medicine*, 368(2), pp.107–16.
- Jung, B.-K. et al., 2012. *Toxoplasma gondii* infection in the brain inhibits neuronal degeneration and learning and memory impairments in a murine model of Alzheimer's disease. *PloS one*, 7(3), p.e33312.
- Jutila, M.A. et al., 1988. Ly-6C is a monocyte/macrophage and endothelial cell differentiation antigen regulated by interferon-gamma. *European journal of immunology*, 18(11), pp.1819–26.
- Kagan, J.C. & Horng, T., 2013. NLRP3 inflammasome activation: CD36 serves double duty. *Nature immunology*, 14(8), pp.772–4.

## REFERENCES

- Kahn, M.S. et al., 2012. Prolonged elevation in hippocampal A $\beta$  and cognitive deficits following repeated endotoxin exposure in the mouse. *Behavioural brain research*, 229(1), pp.176–84.
- Kamer, A.R. et al., 2015. Periodontal disease associates with higher brain amyloid load in normal elderly. *Neurobiology of aging*, 36(2), pp.627–33.
- Karlmarm, K.R. et al., 2009. Hepatic recruitment of the inflammatory Gr1+ monocyte subset upon liver injury promotes hepatic fibrosis. *Hepatology (Baltimore, Md.)*, 50(1), pp.261–74.
- Karlmarm, K.R. et al., 2010. The fractalkine receptor CX3CR1 protects against liver fibrosis by controlling differentiation and survival of infiltrating hepatic monocytes. *Hepatology (Baltimore, Md.)*, 52(5), pp.1769–82.
- Karlmarm, K.R., Tacke, F. & Dunay, I.R., 2012. Monocytes in health and disease — Minireview. *European Journal of Microbiology and Immunology*, 2(2), pp.97–102.
- Kempermann, G. et al., 2010. Why and how physical activity promotes experience-induced brain plasticity. *Frontiers in neuroscience*, 4(December), p.189.
- Kempermann, G. & Gage, F.H., 2000. Neurogenesis in the adult hippocampus. *Novartis Foundation symposium*, 231, pp.220–35; discussion 235–41, 302–6.
- Kempermann, G., Kuhn, H.G. & Gage, F.H., 1997. More hippocampal neurons in adult mice living in an enriched environment. *Nature*, 386(6624), pp.493–5.
- Kettenmann, H. et al., 2011. Physiology of microglia. *Physiological reviews*, 91(2), pp.461–553.
- Khosravi, A. et al., 2014. Gut microbiota promote hematopoiesis to control bacterial infection. *Cell host & microbe*, 15(3), pp.374–81.
- El Khoury, J. et al., 2007. Ccr2 deficiency impairs microglial accumulation and accelerates progression of Alzheimer-like disease. *Nature medicine*, 13(4), pp.432–8.
- El Khoury, J.B. et al., 2003. CD36 mediates the innate host response to beta-amyloid. *The Journal of experimental medicine*, 197(12), pp.1657–1666.
- Kipnis, J. et al., 2004. T cell deficiency leads to cognitive dysfunction: implications for therapeutic vaccination for schizophrenia and other psychiatric conditions. *Proceedings of the National Academy of Sciences of the United States of America*, 101(21), pp.8180–5.
- Kleinberger, G. et al., 2014. TREM2 mutations implicated in neurodegeneration impair cell surface transport and phagocytosis. *Science translational medicine*, 6(243), p.243ra86.
- Koenigsknecht, J. & Landreth, G., 2004. Microglial phagocytosis of fibrillar beta-amyloid through a beta1 integrin-dependent mechanism. *The Journal of neuroscience: the official journal of the Society for Neuroscience*, 24(44), pp.9838–46.
- Kohman, R.A. & Rhodes, J.S., 2013. Neurogenesis, inflammation and behavior. *Brain, behavior, and immunity*, 27(1), pp.22–32.
- Kolaczowska, E. & Kubes, P., 2013. Neutrophil recruitment and function in health and inflammation. *Nature reviews. Immunology*, 13(3), pp.159–75.
- Kornack, D.R. & Rakic, P., 1999. Continuation of neurogenesis in the hippocampus of the adult macaque monkey. *Proceedings of the National Academy of Sciences of the United States of America*, 96(10), pp.5768–73.
- Koronyo, Y. et al., 2015. Therapeutic effects of glatiramer acetate and grafted CD115+ monocytes in a mouse model of Alzheimer's disease. *Brain: a journal of neurology*, 138(Pt 8), pp.2399–422.
- Krabbe, G. et al., 2013. Functional impairment of microglia coincides with Beta-amyloid deposition in mice with Alzheimer-like pathology. *PloS one*, 8(4), p.e60921.
- Krohn, M. et al., 2011. Cerebral amyloid- $\beta$  proteostasis is regulated by the membrane transport protein ABCC1 in mice. *The Journal of clinical investigation*, 121(10), pp.3924–31.
- Kusbeci, O.Y. et al., 2011. Could *Toxoplasma gondii* have any role in Alzheimer disease? *Alzheimer disease and associated disorders*, 25(1), pp.1–3.
- Laliberté, J. & Carruthers, V.B., 2011. *Toxoplasma gondii* toxolysin 4 is an extensively processed putative metalloproteinase secreted from micronemes. *Molecular and biochemical parasitology*, 177(1), pp.49–56.
- Lawson, L.J. et al., 1990. Heterogeneity in the distribution and morphology of microglia in the normal adult mouse brain. *Neuroscience*, 39(1), pp.151–170.
- Leissring, M.A. et al., 2003. Enhanced proteolysis

## REFERENCES

- of beta-amyloid in APP transgenic mice prevents plaque formation, secondary pathology, and premature death. *Neuron*, 40(6), pp.1087–93.
- Lesné, S., Kotilinek, L. & Ashe, K.H., 2008. Plaque-bearing mice with reduced levels of oligomeric amyloid-beta assemblies have intact memory function. *Neuroscience*, 151(3), pp.745–9.
- Ley, R. et al., 2006. Microbial ecology: human gut microbes associated with obesity. *Nature*, 444(7122), pp.1022–3.
- Lim, G.P. et al., 2000. Ibuprofen suppresses plaque pathology and inflammation in a mouse model for Alzheimer's disease. *The Journal of neuroscience: the official journal of the Society for Neuroscience*, 20(15), pp.5709–5714.
- Lin, S.L. et al., 2009. Bone marrow Ly6Chigh monocytes are selectively recruited to injured kidney and differentiate into functionally distinct populations. *Journal of immunology (Baltimore, Md. : 1950)*, 183(10), pp.6733–6743.
- Little, C.S. et al., 2004. Chlamydia pneumoniae induces Alzheimer-like amyloid plaques in brains of BALB/c mice. *Neurobiology of aging*, 25(4), pp.419–29.
- Liu, A. & Niswander, L.A., 2005. Bone morphogenetic protein signalling and vertebrate nervous system development. *Nature reviews. Neuroscience*, 6(12), pp.945–54.
- Lleó, A., Greenberg, S.M. & Growdon, J.H., 2006. Current pharmacotherapy for Alzheimer's disease. *Annual review of medicine*, 57, pp.513–33.
- London, J.A., Biegel, D. & Pachter, J.S., 1996. Neurocytopathic effects of beta-amyloid-stimulated monocytes: a potential mechanism for central nervous system damage in Alzheimer disease. *Proceedings of the National Academy of Sciences of the United States of America*, 93(9), pp.4147–52.
- Louveau, A. et al., 2015. Structural and functional features of central nervous system lymphatic vessels. *Nature*, 523(7560), pp.337–341.
- Lozupone, C.A. et al., 2012. Diversity, stability and resilience of the human gut microbiota. *Nature*, 489(7415), pp.220–30.
- Lue, L.-F., Schmitz, C. & Walker, D.G., 2014. What happens to microglial TREM2 in Alzheimer's disease: Immunoregulatory turned into immunopathogenic? *Neuroscience*, 302, pp.138–150.
- Lyman, M. et al., 2013. Neuroinflammation: The role and consequences. *Neuroscience research*, pp.1–12.
- Masters, C.L. & Selkoe, D.J., 2012. Biochemistry of amyloid  $\beta$ -protein and amyloid deposits in Alzheimer disease. *Cold Spring Harbor perspectives in medicine*, 2(6), p.a006262.
- Mawuenyega, K.G. et al., 2010. Decreased clearance of CNS beta-amyloid in Alzheimer's disease. *Science (New York, N.Y.)*, 330(6012), p.1774.
- Mayer, E.A., 2011. Gut feelings: the emerging biology of gut-brain communication. *Nature reviews. Neuroscience*, 12(8), pp.453–66.
- Mayer-Barber, K.D. et al., 2011. Innate and adaptive interferons suppress IL-1 $\alpha$  and IL-1 $\beta$  production by distinct pulmonary myeloid subsets during Mycobacterium tuberculosis infection. *Immunity*, 35(6), pp.1023–34.
- Mazmanian, S.K. et al., 2005. An immunomodulatory molecule of symbiotic bacteria directs maturation of the host immune system. *Cell*, 122(1), pp.107–118.
- Meda, L. et al., 1995. Activation of microglial cells by beta-amyloid protein and interferon-gamma. *Nature*, 374(6523), pp.647–650.
- Merad, M. et al., 2013. The dendritic cell lineage: ontogeny and function of dendritic cells and their subsets in the steady state and the inflamed setting. *Annual review of immunology*, 31, pp.563–604.
- Michaud, J.-P. et al., 2013. Real-time in vivo imaging reveals the ability of monocytes to clear vascular amyloid beta. *Cell reports*, 5(3), pp.646–53.
- Miklossy, J., 2011. Emerging roles of pathogens in Alzheimer disease. *Expert reviews in molecular medicine*, 13(September), p.e30.
- Mildner, A. et al., 2011. Distinct and Non-Redundant Roles of Microglia and Myeloid Subsets in Mouse Models of Alzheimer's Disease. *Journal of Neuroscience*, 31(31), pp.11159–11171.
- Ming, G. & Song, H., 2005. Adult neurogenesis in the mammalian central nervous system. *Annual review of neuroscience*, 28, pp.223–250.
- Ming, G.L. & Song, H., 2011. Adult Neurogenesis in the Mammalian Brain: Significant Answers and Significant Questions. *Neuron*, 70(4), pp.687–702.
- Möhle, L. et al., 2014. Spinal cord pathology in

## REFERENCES

- chronic experimental *Toxoplasma gondii* infection. *European journal of microbiology & immunology*, 4(1), pp.65–75.
- Monje, M.L., Toda, H. & Palmer, T.D., 2003. Inflammatory blockade restores adult hippocampal neurogenesis. *Science (New York, N.Y.)*, 302(5651), pp.1760–1765.
- Moore, K.J. et al., 2002. A CD36-initiated signaling cascade mediates inflammatory effects of beta-amyloid. *The Journal of biological chemistry*, 277(49), pp.47373–9.
- Morgun, A. et al., 2015. Uncovering effects of antibiotics on the host and microbiota using transkingdom gene networks. *Gut*, 64(11), pp.1732–43.
- Mukherjee, A. et al., 2000. Insulysin hydrolyzes amyloid beta peptides to products that are neither neurotoxic nor deposit on amyloid plaques. *The Journal of neuroscience: the official journal of the Society for Neuroscience*, 20(23), pp.8745–8749.
- Mullen, R.J., Buck, C.R. & Smith, A.M., 1992. NeuN, a neuronal specific nuclear protein in vertebrates. *Development (Cambridge, England)*, 116(1), pp.201–211.
- Munoz, M., Liesenfeld, O. & Heimesaat, M.M., 2011. Immunology of *Toxoplasma gondii*. *Immunological reviews*, 240(1), pp.269–85.
- Musiek, E.S. & Holtzman, D.M., 2015. Three dimensions of the amyloid hypothesis: time, space and “wingmen.” *Nat Neurosci*, 18(6), pp.800–806.
- Mustroph, M.L. et al., 2012. Aerobic exercise is the critical variable in an enriched environment that increases hippocampal neurogenesis and water maze learning in male C57BL/6J mice. *Neuroscience*, 219, pp.62–71.
- Naert, G. & Rivest, S., 2013. A deficiency in CCR2<sup>+</sup> monocytes: the hidden side of Alzheimer’s disease. *Journal of molecular cell biology*, 5(5), pp.284–93.
- Naert, G. & Rivest, S., 2012a. Age-related changes in synaptic markers and monocyte subsets link the cognitive decline of APP(Swe)/PS1 mice. *Frontiers in cellular neuroscience*, 6(November), p.51.
- Naert, G. & Rivest, S., 2012b. Hematopoietic CC-chemokine receptor 2 (CCR2) competent cells are protective for the cognitive impairments and amyloid pathology in a transgenic mouse model of Alzheimer’s disease. *Molecular medicine (Cambridge, Mass.)*, 18(1), pp.297–313.
- Nance, J.P. et al., 2012. Chitinase dependent control of protozoan cyst burden in the brain. *PLoS pathogens*, 8(11), p.e1002990.
- Naseribafrouei, A. et al., 2014. Correlation between the human fecal microbiota and depression. *Neurogastroenterology and motility: the official journal of the European Gastrointestinal Motility Society*, 26(8), pp.1155–62.
- Neal, L.M. & Knoll, L.J., 2014. *Toxoplasma gondii* profilin promotes recruitment of Ly6Chi CCR2<sup>+</sup> inflammatory monocytes that can confer resistance to bacterial infection. *PLoS pathogens*, 10(6), p.e1004203.
- Nedergaard, M., 2013. Garbage truck of the brain. *Science (New York, N.Y.)*, 340(6140), pp.1529–30.
- Nergiz-Unal, R. et al., 2011. CD36 as a multiple-ligand signaling receptor in atherosclerosis. *Cardiovascular & hematological agents in medicinal chemistry*, 9(1), pp.42–55.
- Neufeld, K.M. et al., 2011. Reduced anxiety-like behavior and central neurochemical change in germ-free mice. *Neurogastroenterology and motility: the official journal of the European Gastrointestinal Motility Society*, 23(3), pp.255–64, e119.
- Niederhorn, J.Y., 2006. See no evil, hear no evil, do no evil: the lessons of immune privilege. *Nature immunology*, 7(4), pp.354–9.
- Van Nostrand, W.E. et al., 1992. Decreased levels of soluble amyloid beta-protein precursor in cerebrospinal fluid of live Alzheimer disease patients. *Proceedings of the National Academy of Sciences of the United States of America*, 89(7), pp.2551–2555.
- Oakley, H. et al., 2006. Intraneuronal beta-amyloid aggregates, neurodegeneration, and neuron loss in transgenic mice with five familial Alzheimer’s disease mutations: potential factors in amyloid plaque formation. *The Journal of neuroscience: the official journal of the Society for Neuroscience*, 26(40), pp.10129–40.
- Ogbonnaya, E.S. et al., 2015. Adult Hippocampal Neurogenesis Is Regulated by the Microbiome. *Biological psychiatry*, 78(4), pp.e7–9.
- Orre, M. et al., 2014. Isolation of glia from Alzheimer’s mice reveals inflammation and dysfunction. *Neurobiology of aging*, 35(12), pp.2746–60.
- Ousman, S.S. & Kubes, P., 2012. Immune surveillance in the central nervous system. *Nature neuroscience*, 15(8), pp.1096–101.

## REFERENCES

- Pahnke, J. et al., 2013. Impaired mitochondrial energy production and ABC transporter function-A crucial interconnection in dementing proteopathies of the brain. *Mechanisms of ageing and development*, 134(10), pp.506–15.
- Pahnke, J., Langer, O. & Krohn, M., 2014. Alzheimer's and ABC transporters - new opportunities for diagnostics and treatment. *Neurobiology of disease*, pp.1–7.
- Paolicelli, R.C. et al., 2011. Synaptic pruning by microglia is necessary for normal brain development. *Science (New York, N.Y.)*, 333(6048), pp.1456–1458.
- Park, Y.M., 2014. CD36, a scavenger receptor implicated in atherosclerosis. *Experimental & molecular medicine*, 46(6), p.e99.
- Parkin, J. & Cohen, B., 2001. An overview of the immune system. *Lancet*, 357(9270), pp.1777–89.
- Parlog, A. et al., 2014. Chronic murine toxoplasmosis is defined by subtle changes in neuronal connectivity. *Disease models & mechanisms*, 7(4), pp.459–69.
- Parracho, H.M.R.T. et al., 2005. Differences between the gut microflora of children with autistic spectrum disorders and that of healthy children. *Journal of medical microbiology*, 54(Pt 10), pp.987–91.
- Paton, J.A. & Nottebohm, F.N., 1984. Neurons generated in the adult brain are recruited into functional circuits. *Science (New York, N.Y.)*, 225(4666), pp.1046–1048.
- Perry, C.E. et al., 2015. Seroprevalence and Serointensity of Latent *Toxoplasma gondii* in a Sample of Elderly Adults With and Without Alzheimer Disease. *Alzheimer disease and associated disorders*, 00(00), pp.1–4.
- Perry, V.H., Cunningham, C. & Holmes, C., 2007. Systemic infections and inflammation affect chronic neurodegeneration. *Nature reviews. Immunology*, 7(2), pp.161–167.
- Perry, V.H., Nicoll, J.A.R. & Holmes, C., 2010. Microglia in neurodegenerative disease. *Nature reviews. Neurology*, 6(4), pp.193–201.
- Poon, I.K.H. et al., 2014. Apoptotic cell clearance: basic biology and therapeutic potential. *Nature Reviews Immunology*, 14(3), pp.166–180.
- Potgieter, M. et al., 2015. The dormant blood microbiome in chronic, inflammatory diseases. *FEMS microbiology reviews*, 39(4), pp.567–91.
- van Praag, H., Kempermann, G. & Gage, F.H., 1999. Running increases cell proliferation and neurogenesis in the adult mouse dentate gyrus. *Nature neuroscience*, 2(3), pp.266–70.
- Prokop, S. et al., 2015. Impact of peripheral myeloid cells on amyloid- $\beta$  pathology in Alzheimer's disease-like mice. *The Journal of experimental medicine*, 212(11), pp.1811–8.
- Prokop, S., Miller, K.R. & Heppner, F.L., 2013. Microglia actions in Alzheimer's disease. *Acta neuropathologica*, 2, pp.461–477.
- Purves, D. et al., 2004. *Neuroscience Third Edition*,
- Ransohoff, R.M. & Brown, M.A., 2012. Innate immunity in the central nervous system. *The Journal of clinical investigation*, 122(4), pp.1164–71.
- Ransohoff, R.M. & Engelhardt, B., 2012. The anatomical and cellular basis of immune surveillance in the central nervous system. *Nature Reviews Immunology*, 12(9), pp.623–635.
- Reitz, C., Brayne, C. & Mayeux, R., 2011. Epidemiology of Alzheimer disease. *Nature reviews. Neurology*, 7(3), pp.137–52.
- Rossi, C. et al., 2006. Brain-derived neurotrophic factor (BDNF) is required for the enhancement of hippocampal neurogenesis following environmental enrichment. *The European journal of neuroscience*, 24(7), pp.1850–6.
- Round, J.L. & Mazmanian, S.K., 2009. The gut microbiota shapes intestinal immune responses during health and disease. *Nature reviews. Immunology*, 9(5), pp.313–323.
- Rubio-Perez, J.M. & Morillas-Ruiz, J.M., 2012. A review: inflammatory process in Alzheimer's disease, role of cytokines. *TheScientificWorldJournal*, 2012, p.756357.
- Saido, T. & Leissring, M.A., 2012. Proteolytic degradation of amyloid  $\beta$ -protein. *Cold Spring Harbor perspectives in medicine*, 2(6), p.a006379.
- Saido, T.C. & Iwata, N., 2006. Metabolism of amyloid beta peptide and pathogenesis of Alzheimer's disease. Towards presymptomatic diagnosis, prevention and therapy. *Neuroscience research*, 54(4), pp.235–53.
- Saijo, K. et al., 2009. A Nurr1/CoREST Pathway in Microglia and Astrocytes Protects Dopaminergic Neurons from Inflammation-Induced Death. *Cell*, 137(1), pp.47–59.



## REFERENCES

- Saijo, K. & Glass, C.K., 2011. Microglial cell origin and phenotypes in health and disease. *Nature reviews. Immunology*, 11(11), pp.775–87.
- Savage, J.C. et al., 2015. Nuclear receptors license phagocytosis by trem2+ myeloid cells in mouse models of Alzheimer’s disease. *The Journal of neuroscience : the official journal of the Society for Neuroscience*, 35(16), pp.6532–43.
- Scharfman, H. et al., 2005. Increased neurogenesis and the ectopic granule cells after intrahippocampal BDNF infusion in adult rats. *Experimental neurology*, 192(2), pp.348–56.
- Scheffler, K. et al., 2011. Determination of spatial and temporal distribution of microglia by 230nm-high-resolution, high-throughput automated analysis reveals different amyloid plaque populations in an APP/PS1 mouse model of Alzheimer’s disease. *Current Alzheimer research*, 8(7), pp.781–8.
- Scheffler, K. et al., 2012. Mitochondrial DNA polymorphisms specifically modify cerebral  $\beta$ -amyloid proteostasis. *Acta neuropathologica*, 124(2), pp.199–208.
- Schlüter, D. et al., 2003. Both lymphotoxin-alpha and TNF are crucial for control of *Toxoplasma gondii* in the central nervous system. *Journal of immunology (Baltimore, Md. : 1950)*, 170(12), pp.6172–82.
- Schlüter, D. et al., 1995. Different subsets of T cells in conjunction with natural killer cells, macrophages, and activated microglia participate in the intracerebral immune response to *Toxoplasma gondii* in athymic nude and immunocompetent rats. *The American journal of pathology*, 146(4), pp.999–1007.
- Schmidt, A. & Pahnke, J., 2012. Efficient near-infrared in vivo imaging of amyloid- $\beta$  deposits in Alzheimer’s disease mouse models. *Journal of Alzheimer’s disease : JAD*, 30(3), pp.651–64.
- Schumacher, T. et al., 2012. ABC transporters B1, C1 and G2 differentially regulate neuroregeneration in mice. *PloS one*, 7(4), p.e35613.
- Schwartz, M. et al., 2013. How do immune cells support and shape the brain in health, disease, and aging? *The Journal of Neuroscience*, 33(45), pp.17587–17596.
- Schwartz, M. & Baruch, K., 2014. The resolution of neuroinflammation in neurodegeneration: leukocyte recruitment via the choroid plexus. *The EMBO journal*, 33(1), pp.7–22.
- Serbina, N. V et al., 2003. TNF/iNOS-producing dendritic cells mediate innate immune defense against bacterial infection. *Immunity*, 19(1), pp.59–70.
- Serbina, N. V & Pamer, E.G., 2006. Monocyte emigration from bone marrow during bacterial infection requires signals mediated by chemokine receptor CCR2. *Nature immunology*, 7(3), pp.311–7.
- Shantsila, E. et al., 2012. The effects of exercise and diurnal variation on monocyte subsets and monocyte-platelet aggregates. *European journal of clinical investigation*, 42(8), pp.832–9.
- Shechter, R. et al., 2009. Infiltrating blood-derived macrophages are vital cells playing an anti-inflammatory role in recovery from spinal cord injury in mice. *PLoS medicine*, 6(7), p.e1000113.
- Shechter, R., London, A. & Schwartz, M., 2013. Orchestrated leukocyte recruitment to immune-privileged sites: absolute barriers versus educational gates. *Nature reviews. Immunology*, 13(3), pp.206–18.
- Shechter, R. & Schwartz, M., 2013. Harnessing monocyte-derived macrophages to control central nervous system pathologies: no longer “if” but “how”. *The Journal of pathology*, 229(2), pp.332–46.
- Sheel, M. & Engwerda, C.R., 2012. The diverse roles of monocytes in inflammation caused by protozoan parasitic diseases. *Trends in parasitology*, 28(10), pp.408–16.
- Shishido, S.N. et al., 2012. Humoral innate immune response and disease. *Clinical Immunology*, 144(2), pp.142–158.
- Sierra, A. et al., 2010. Microglia shape adult hippocampal neurogenesis through apoptosis-coupled phagocytosis. *Cell stem cell*, 7(4), pp.483–95.
- Simard, A.R. et al., 2006. Bone marrow-derived microglia play a critical role in restricting senile plaque formation in Alzheimer’s disease. *Neuron*, 49(4), pp.489–502.
- Sonnenberg, G.F. & Artis, D., 2015. Innate lymphoid cells in the initiation, regulation and resolution of inflammation. *Nature medicine*, 21(7), pp.698–708.
- Spalding, K.L. et al., 2013. Dynamics of hippocampal neurogenesis in adult humans. *Cell*, 153(6), pp.1219–27.
- Sponaas, A.M. et al., 2009. Migrating monocytes

## REFERENCES

- recruited to the spleen play an important role in control of blood stage malaria. *Blood*, 114(27), pp.5522–5531.
- Stewart, C.R. et al., 2010. CD36 ligands promote sterile inflammation through assembly of a Toll-like receptor 4 and 6 heterodimer. *Nature immunology*, 11(2), pp.155–161.
- Streit, W.J., 2005. Microglia and neuroprotection: Implications for Alzheimer's disease. In *Brain Research Reviews*. pp. 234–239.
- Tacke, F. & Zimmermann, H.W., 2014. Macrophage heterogeneity in liver injury and fibrosis. *Journal of hepatology*, 60(5), pp.1090–1096.
- Teipel, S.J. et al., 2011. Development of Alzheimer-disease neuroimaging-biomarkers using mouse models with amyloid-precursor protein-transgene expression. *Progress in neurobiology*, 95(4), pp.547–556.
- Tilg, H. & Kaser, A., 2011. Gut microbiome, obesity, and metabolic dysfunction. *The Journal of clinical investigation*, 121(6), pp.2126–32.
- Turnbaugh, P.J. et al., 2006. An obesity-associated gut microbiome with increased capacity for energy harvest. *Nature*, 444(7122), pp.1027–31.
- Underhill, D.M. & Goodridge, H.S., 2012. Information processing during phagocytosis. *Nature Reviews Immunology*, 12(7), pp.492–502.
- Underhill, D.M. & Iliev, I.D., 2014. The mycobiota: interactions between commensal fungi and the host immune system. *Nature reviews. Immunology*, 14(6), pp.405–16.
- Varvel, N.H. et al., 2015. Replacement of brain-resident myeloid cells does not alter cerebral amyloid- $\beta$  deposition in mouse models of Alzheimer's disease. *The Journal of experimental medicine*, 212(11), pp.1803–9.
- Voehringer, D., 2013. Protective and pathological roles of mast cells and basophils. *Nature reviews. Immunology*, 13(5), pp.362–75.
- Wang, D.-S., Dickson, D.W. & Malter, J.S., 2006. beta-Amyloid degradation and Alzheimer's disease. *Journal of biomedicine & biotechnology*, 2006(3), p.58406.
- Wang, J.Z. et al., 2012. Abnormal hyperphosphorylation of tau: Sites, regulation, and molecular mechanism of neurofibrillary degeneration. *Advances in Alzheimer's Disease*, 3, pp.123–139.
- Wang, X. et al., 2004. Gamma interferon production, but not perforin-mediated cytolytic activity, of T cells is required for prevention of toxoplasmic encephalitis in BALB/c mice genetically resistant to the disease. *Infection and immunity*, 72(8), pp.4432–8.
- Wang, X. et al., 2005. Importance of CD8(+)Vbeta8(+) T cells in IFN-gamma-mediated prevention of toxoplasmic encephalitis in genetically resistant BALB/c mice. *Journal of interferon & cytokine research: the official journal of the International Society for Interferon and Cytokine Research*, 25(6), pp.338–44.
- Wang, X. et al., 2014. Resolution of inflammation is altered in Alzheimer's disease. *Alzheimer's and Dementia*, 11, pp.40–50.
- Wang, Y. et al., 2015. TREM2 Lipid Sensing Sustains the Microglial Response in an Alzheimer's Disease Model. *Cell*, pp.1–11.
- Wang, Z.T. et al., 2015. Reassessment of the role of aromatic amino acid hydroxylases and the effect of infection by *Toxoplasma gondii* on host dopamine. *Infection and immunity*, 83(3), pp.1039–47.
- Weintraub, S., Wicklund, A.H. & Salmon, D.P., 2012. The neuropsychological profile of Alzheimer disease. *Cold Spring Harbor perspectives in medicine*, 2(4), p.a006171.
- Weirich, G. et al., 2008. Immunohistochemical evidence of ubiquitous distribution of the metalloendoprotease insulin-degrading enzyme (IDE; insulysin) in human non-malignant tissues and tumor cell lines. *Biological Chemistry*, 389(November), pp.1441–1445.
- Whitelaw, D.M., 1966. The intravascular lifespan of monocytes. *Blood*, 28(3), pp.455–64.
- Wilkinson, K. & El Khoury, J., 2012. Microglial scavenger receptors and their roles in the pathogenesis of Alzheimer's disease. *International journal of Alzheimer's disease*, 2012, p.489456.
- Wilson, E.H. et al., 2005. A critical role for IL-10 in limiting inflammation during toxoplasmic encephalitis. *Journal of neuroimmunology*, 165(1-2), pp.63–74.
- Wisniewski, H.M., Barcikowska, M. & Kida, E., 1991. Phagocytosis of beta/A4 amyloid fibrils of the neuritic neocortical plaques. *Acta neuropathologica*, 81(5), pp.588–90.
- Wolf, S.A. et al., 2009. CD4-positive T lymphocytes provide a neuroimmunological link in the control of adult hippocampal

## REFERENCES

---

- neurogenesis. *Journal of immunology (Baltimore, Md. : 1950)*, 182(7), pp.3979–84.
- Wolf, S.A., Melnik, A. & Kempermann, G., 2011. Physical exercise increases adult neurogenesis and telomerase activity, and improves behavioral deficits in a mouse model of schizophrenia. *Brain, behavior, and immunity*, 25(5), pp.971–80.
- Wu, G.D., Bushmanc, F.D. & Lewis, J.D., 2013. Diet, the human gut microbiota, and IBD. *Anaerobe*, 24, pp.117–20.
- Yamanaka, M. et al., 2012. PPAR $\gamma$ /RXR $\alpha$ -induced and CD36-mediated microglial amyloid- $\beta$  phagocytosis results in cognitive improvement in amyloid precursor protein/presenilin 1 mice. *The Journal of neuroscience*, 32(48), pp.17321–31.
- Yan, P. et al., 2006. Matrix metalloproteinase-9 degrades amyloid- $\beta$  fibrils in vitro and compact plaques in situ. *Journal of Biological Chemistry*, 281(34), pp.24566–24574.
- Yan, Q. et al., 2003. Anti-inflammatory drug therapy alters beta-amyloid processing and deposition in an animal model of Alzheimer's disease. *The Journal of neuroscience: the official journal of the Society for Neuroscience*, 23(20), pp.7504–7509.
- Yfanti, C. et al., 2008. Expression of metalloprotease insulin-degrading enzyme insulysin in normal and malignant human tissues. *International Journal of Molecular Medicine*, 22, pp.421–431.
- Yin, K.-J. et al., 2006. Matrix metalloproteinases expressed by astrocytes mediate extracellular amyloid-beta peptide catabolism. *The Journal of neuroscience: the official journal of the Society for Neuroscience*, 26(43), pp.10939–10948.
- Yona, S. et al., 2013. Fate mapping reveals origins and dynamics of monocytes and tissue macrophages under homeostasis. *Immunity*, 38(1), pp.79–91.
- Yu, Y. & Ye, R.D., 2015. Microglial A $\beta$  receptors in Alzheimer's disease. *Cellular and molecular neurobiology*, 35(1), pp.71–83.
- Zhang, W. et al., 2011. Soluble A $\beta$  levels correlate with cognitive deficits in the 12-month-old APP<sup>swe</sup>/PS1<sup>dE9</sup> mouse model of Alzheimer's disease. *Behavioural brain research*, 222(2), pp.342–50.
- Zhu, S. et al., 2006. Stimulative effects of insulin on Toxoplasma gondii replication in 3T3-L1 cells. *Cell biology international*, 30(2), pp.149–53.
- Zigmond, E. et al., 2012. Ly6C(hi) Monocytes in the Inflamed Colon Give Rise to Proinflammatory Effector Cells and Migratory Antigen-Presenting Cells. *Immunity*, 80, pp.1–15.
- Ziv, Y. et al., 2006. Immune cells contribute to the maintenance of neurogenesis and spatial learning abilities in adulthood. *Nature neuroscience*, 9(2), pp.268–75.

## **Selbstständigkeitserklärung**

Hiermit erkläre ich, dass ich die von mir eingereichte Dissertation zum Thema

**“The Role of Ly6C<sup>hi</sup> Monocytes in Brain Homeostasis and Neurodegeneration”**

selbstständig verfasst, nicht schon als Dissertation verwendet habe und die benutzten Hilfsmittel und Quellen vollständig angegeben wurden.

Weiterhin erkläre ich, dass ich weder diese noch eine andere Arbeit zur Erlangung des akademischen Grades *doctor rerum naturalium* (Dr. rer. nat.) an anderen Einrichtungen eingereicht habe.

Magdeburg, den 22.02.2016

Luisa Möhle

# Curriculum Vitae

## Personal data

---

|             |                                      |
|-------------|--------------------------------------|
| Name        | Luisa Möhle<br>luisamoehle@gmail.com |
| Birth date  | 27.11.1986                           |
| Birth place | Stuttgart, Germany                   |
| Nationality | German                               |

## Education

---

|             |   |
|-------------|---|
| 2013 – 2016 | Doctoral studies (Dr. rer. nat.), Otto-von-Guericke-University Magdeburg, Faculty of Natural Sciences |
| 2007 – 2013 | Studies of biology (Diploma), Albert-Ludwig-University Freiburg im Breisgau                           |

## Work experience

---

|             |   |
|-------------|---|
| 2013 – 2016 | Doctoral studies, Institute of Medical Microbiology, University Hospital, Magdeburg |
| 2012 – 2013 | Diploma thesis, Institute of Medical Microbiology, University Hospital, Magdeburg   |